Synchrotron Radiation Photoemission or Photoelectron Spectroscopy

Lecturer: 皮敦文，國家同步輻射研究中心
Email: pi@nsrrc.org.tw
Mobile: 0972 156 674

Historical Timeline

- First spectrophotometer: 1850s
- First **I**nfar**R**ed: 1880s
- First crystallography: 1912
- First **N**uclear **M**agnetic **R**esonance: 1938
- First **E**lectron **P**aramagnetic **R**esonance: 1944
- First **P**hoto **E**mission **S**pectroscopy: 1957
- During the mid 1960's Dr. Siegbahn developed the PES technique, who was awarded the 1981 Nobel Prize in Physics for the development of the PES technique

Why a hundred years delayed?

- Development of electron kinetic energy analyzers
- Development of excitation sources
- Development of electron detectors
- Development of UHV technology

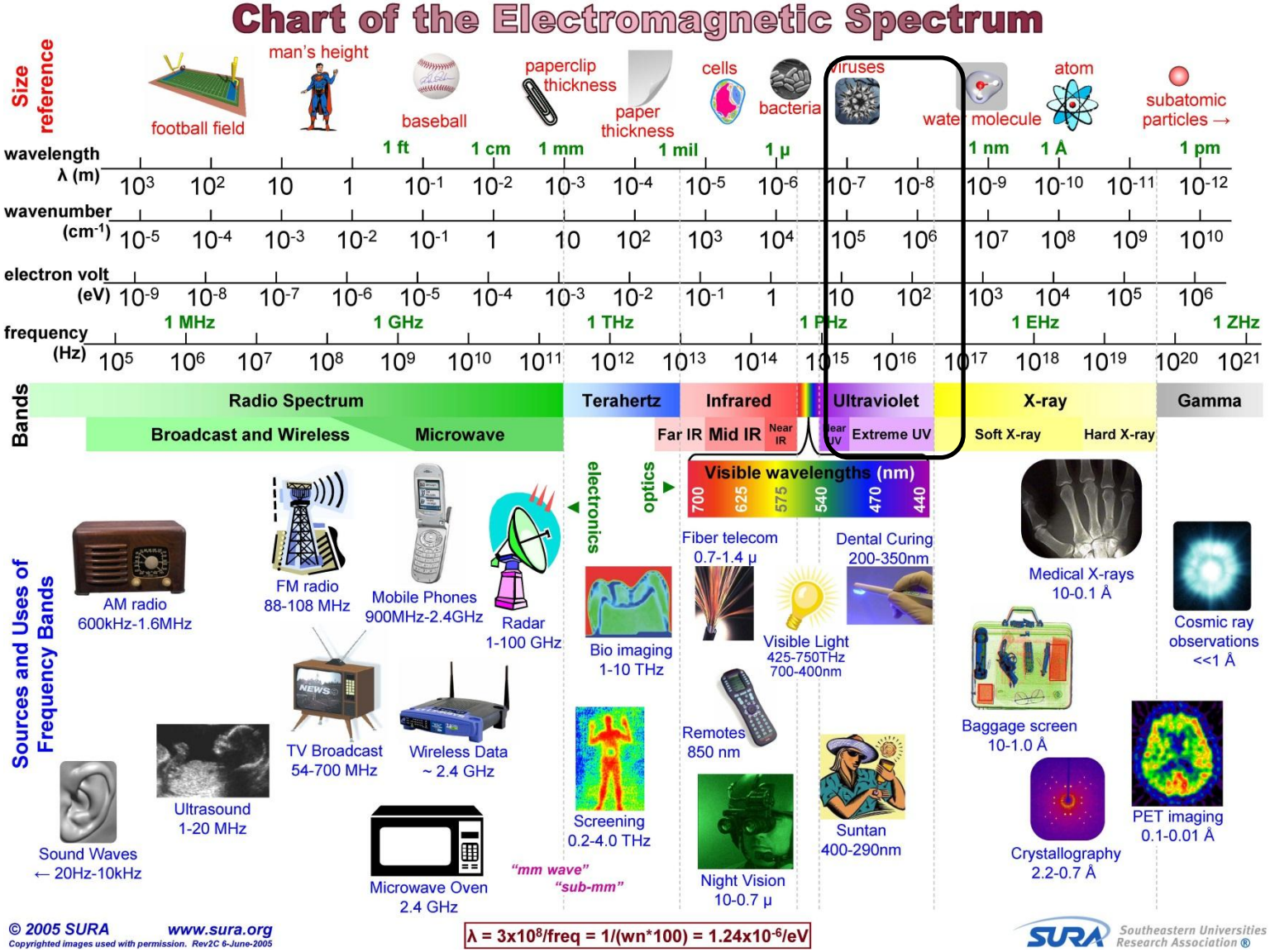

First Ionization Energies:	cesium	3.89 eV (319 nm)
	ferrocene	7.90 eV (157 nm)
	water	12.61 eV (98 nm)

可探測到的物體

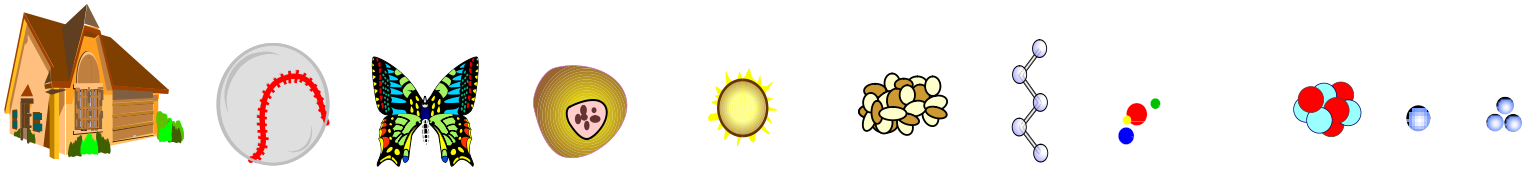

建築物　棒球　昆蟲　細胞　病毒　蛋白質　分子　原子　原子核質子夸克？

10^{3}　10^{1}　10^{-1}　10^{-3}　10^{-5}　10^{-7}　10^{-9}　10^{-11}　10^{-13}　10^{-15}　波長(米)

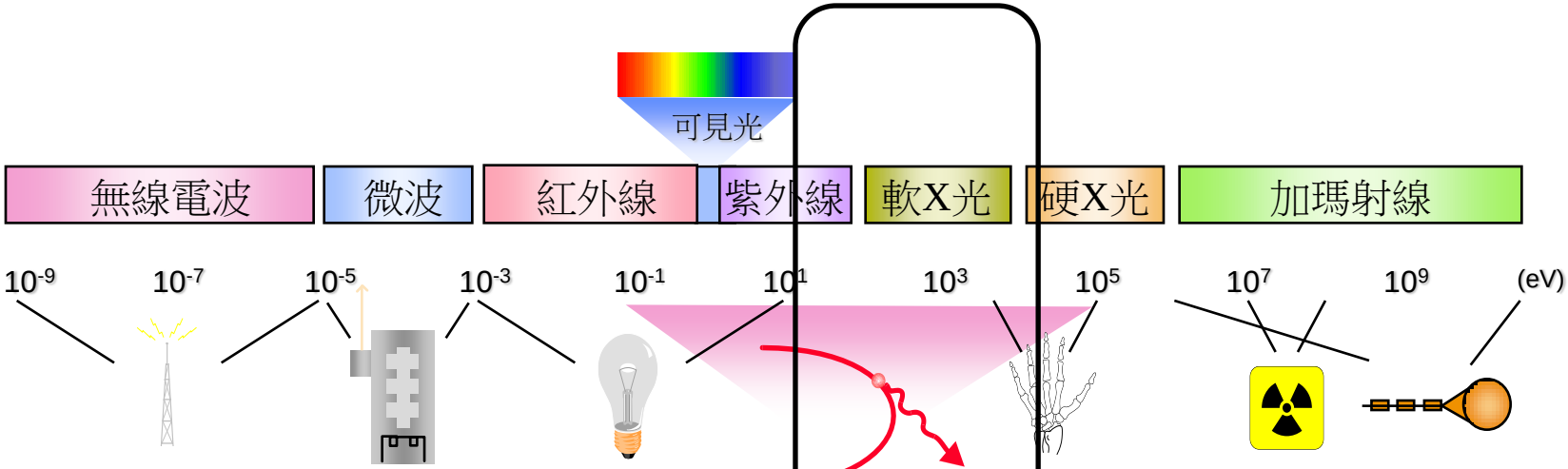

輻　射　源

General Overview of Spectroscopy

- Spectroscopy uses interaction of electromagnetic radiation with matter to learn the physical properties about the matter.
- If electromagnetic radiation is in resonance with the energy spacing between different states (electronic, vibrational, rotational, etc) of matter, radiation will be absorbed, and transitions will occur.
- The radiation that is transmitted through the sample is measured, and spectrum can be reported as either transmittance or absorbance of radiation.
- However, photoelectron spectroscopy is entirely different!

Photoelectron Spectroscopy *vs*. Other Spectroscopies

Others Spectroscopies

- Photon must be in resonance with transition energy
- Measure absorbance or transmittance of photons

Photoelectron Spectroscopy

- Photon just needs enough energy to eject electron
- Measure kinetic energy of ejected electrons
- Monochromatic photon source

Photoelectric Effect

Ionization occurs when matter interacts with light of sufficient energy (Heinrich Hertz, 1886)
(Albert Einstein, Ann. Phys. Leipzig 1905, 17, 132-148.)

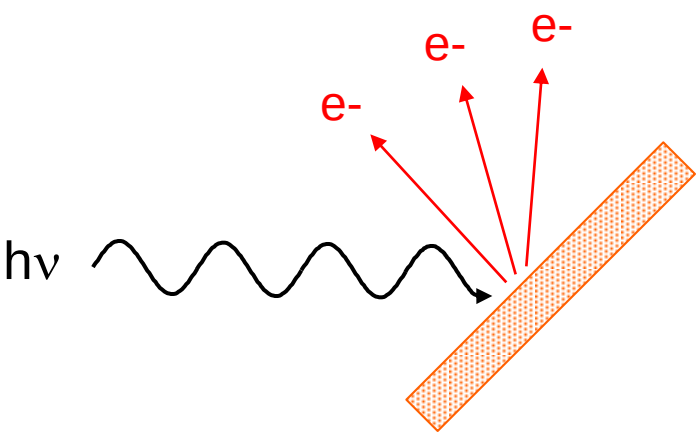

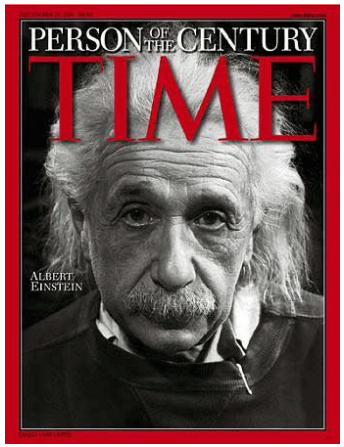

electron kinetic energy (KE) = hν - electron binding energy (BE)

Physical Basis

- Photoelectron spectroscopy is based on a single photon in/electron out process, and the energy of a photon is given by the Einstein relation: $E=h\nu-\phi$.
- Photoelectron spectroscopy uses monochromatic sources of radiation, where the photon is absorbed by an atom in a molecule or solid, leading to ionization and emission of a core (inner shell) or an valence (outer shell) electron.
- The kinetic energy distribution of the emitted photoelectrons (i.e. the number of emitted photoelectrons as a function of their kinetic energy) can be measured using any electron energy analyzer and a photoelectron spectrum can thus be recorded.

Kai Seigbahn: Development of X-ray Photoelectron Spectroscopy

C. Nordling E. Sokolowski and K. Siegbahn, *Phys. Rev.* **1957**, *105*, 1676.

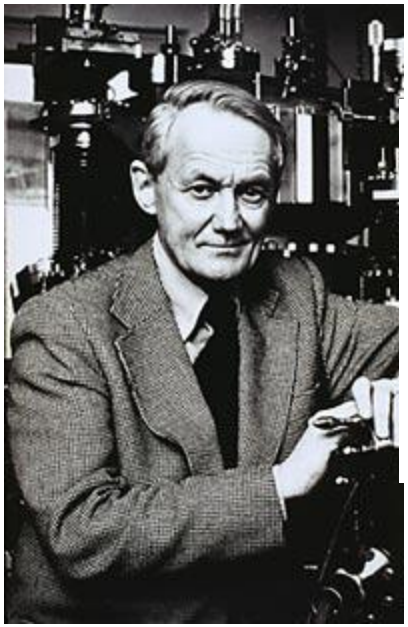

Precision Method for Obtaining Absolute Values of Atomic Binding Energies

CARL NORDLING, EVELYN SOKOLOWSKI, AND KAI SIEGBAHN
Department of Physics, University of Uppsala, Uppsala, Sweden
(Received January 10, 1957)

WE have recently developed a precision method of investigating atomic binding energies, which we believe will find application in a variety of problems in atomic and solid state physics. In principle, the method

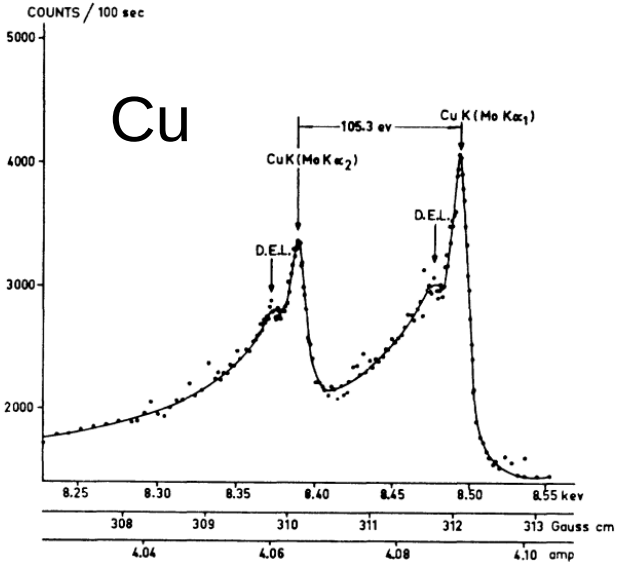

FIG. 1. Lines resulting from photoelectrons expelled from Cu by Mo $K\alpha_1$ and Mo $K\alpha_2$ x-radiation. The satellites marked D.E.L. are interpreted as due to electrons which have suffered a discrete energy loss when scattered in the source.

Nobel Prize in Physics 1981
(His father, Manne Siegbahn, won the Nobel Prize in Physics in 1924 for the discovery and research of X-ray spectroscopy)

Electron Spectroscopy for Chemical Analysis (ESCA)

S. Hagström, C. Nordling and K. Siegbahn, *Phys. Lett.* **1964**, *9*, 235.

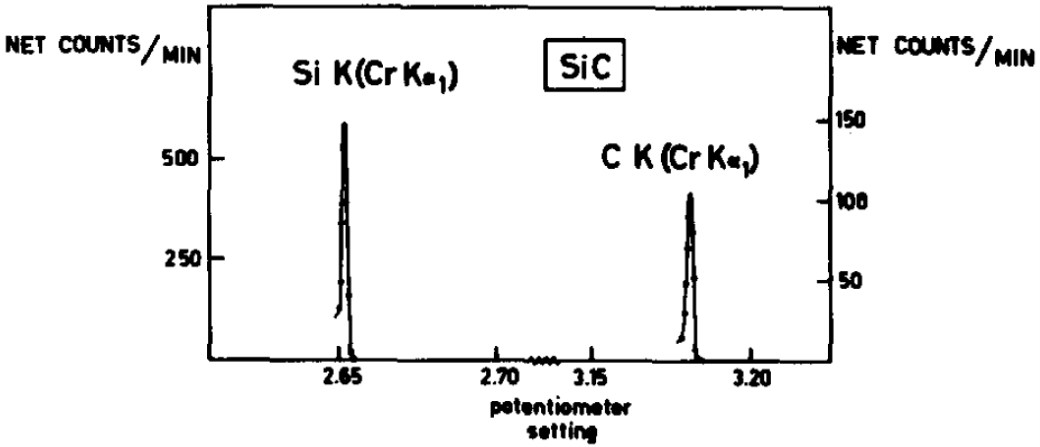

Fig. 1. Photo electron spectrum from silicon carbide, SiC. K photo-electrons are expelled from silicon and carbon atoms by $CrK\alpha_1$ X-radiation. From the *positions* of the lines a qualitative analysis of the elements can be made. A quantitative analysis is obtained from the *intensities* of the photo electron lines and gives a silicon-carbon ratio of 100 : 95.

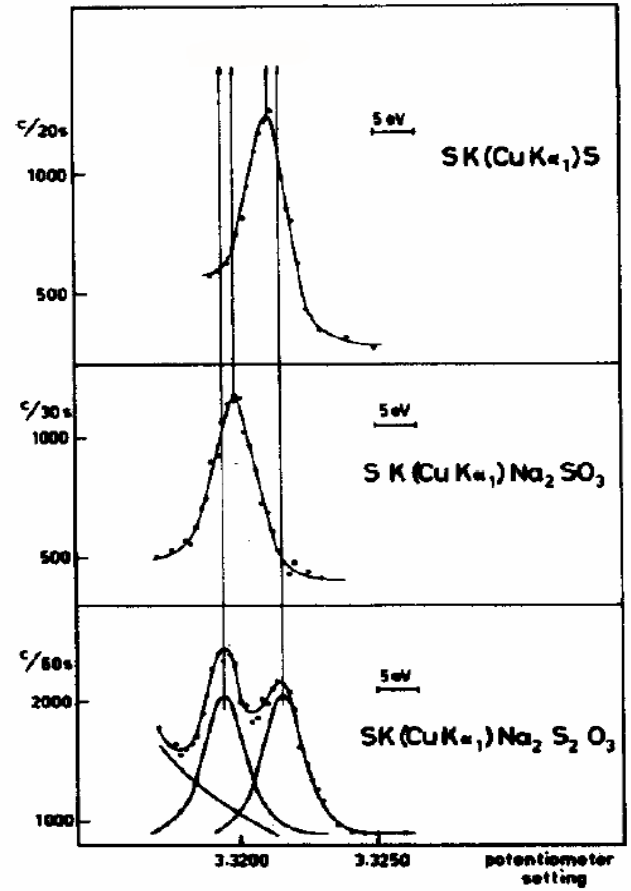

Qualitative Element Analysis

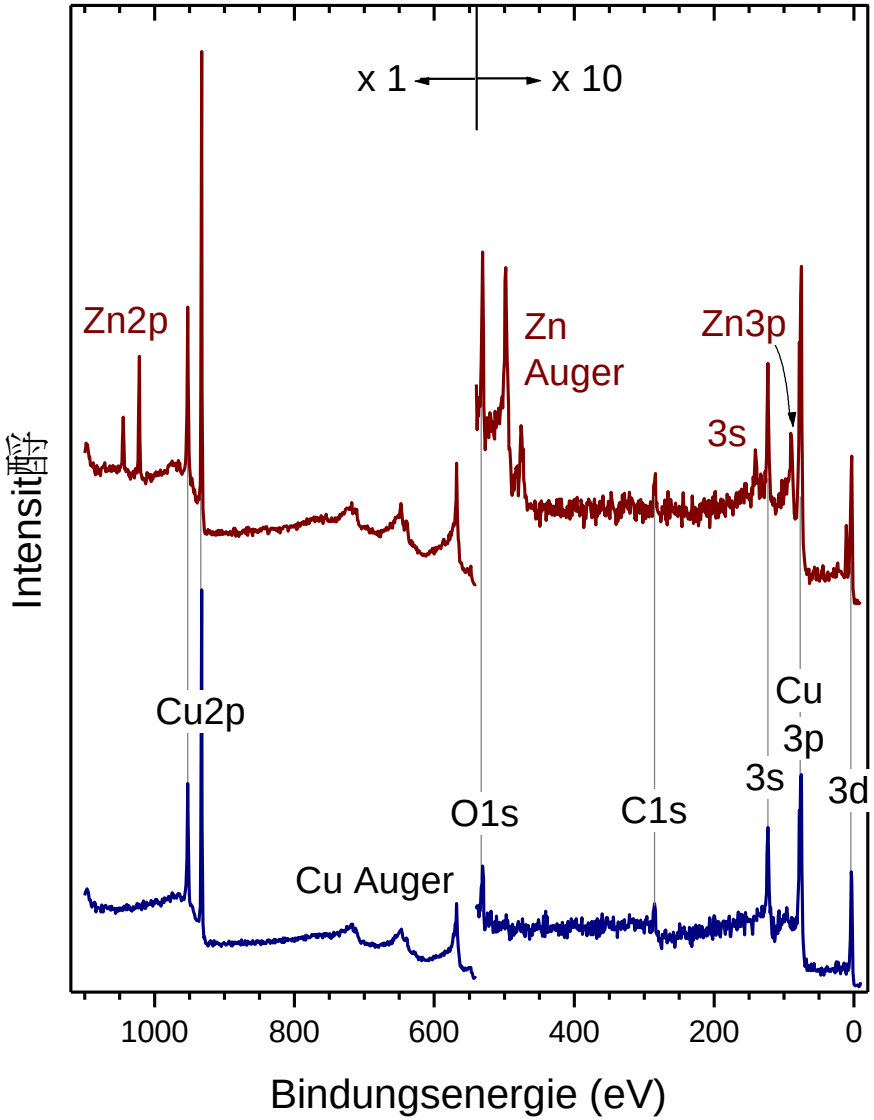

pigment of mummy artwork

Egyptian Mummy
2nd Century AD
World Heritage Museum
University of Illinois

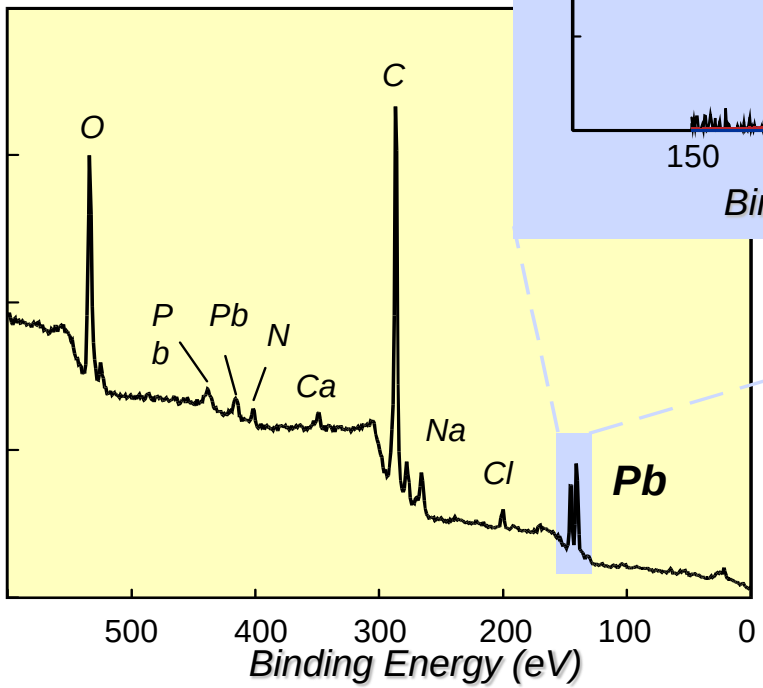

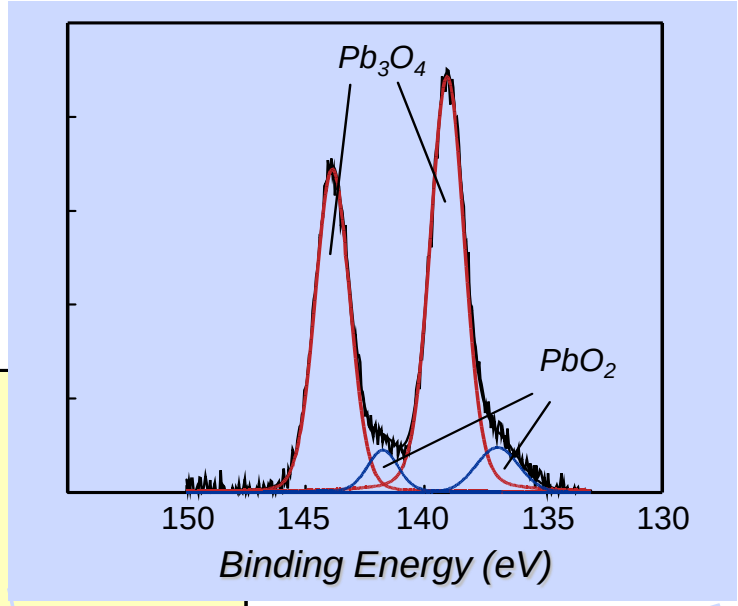

XPS analysis showed that the pigment used on the mummy wrapping was Pb_3O_4 rather than Fe_2O_3

basic equation:

$KE = h\nu - BE - \phi$

KE: Kinetic Energy measured in the analyzer

$h\nu$: photon energy from a source

ϕ: spectrometer work function

BE: Binding Energy, the unknown variable

Energy Levels

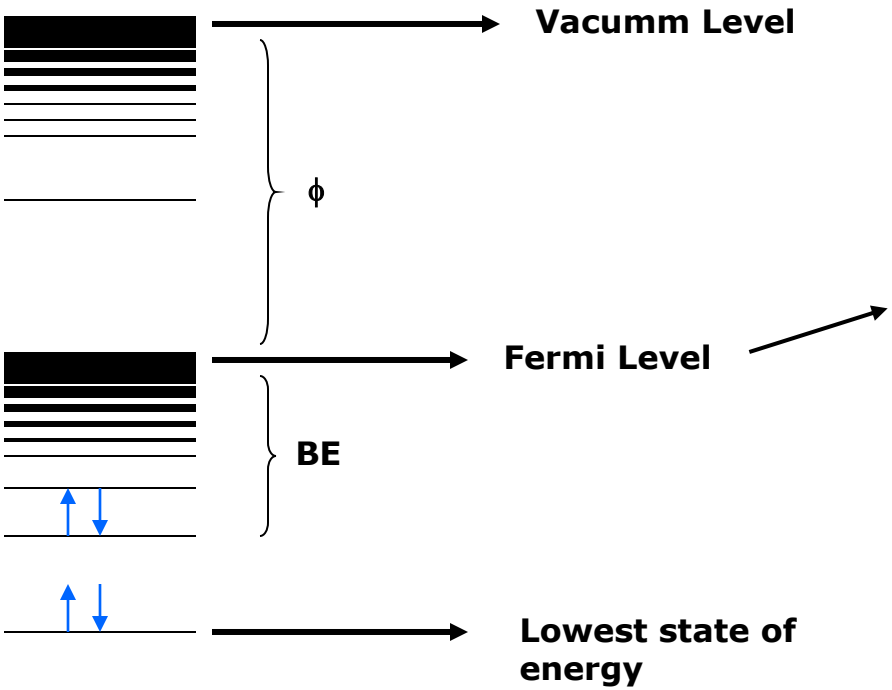

At absolute 0 Kelvin the electrons fill from the lowest energy states up. When the electrons occupy up to this level the neutral solid is in its “ground state.”

Binding energies

Table 4.2. Binding energies of some elements

Z	El	$1s_{1/2}$ K	$2s_{1/2}$ L_1	$2p_{1/2}$ L_2	$2p_{3/2}$ L_3	$3s_{1/2}$ M_1	$3p_{1/2}$ M_2	$3p_{1/2}$ M_3	$3d_{3/2}$ M_4	$3d_{5/2}$ M_5
1	H	14								
2	He	25								
3	Li	55								
4	Be	111								
5	B	188		5						
6	C	284		6						
7	N	399		9						
8	O	532	24	7						
9	F	686	31	9						
10	Ne	867	45	18						
11	Na	1072	63	31		1				
12	Mg	1305	89	52		2				
13	Ml	1560	118	74	73	1				
14	Si	1839	149	100	99	8				
15	P	2149	189	136	135	16	10			
16	S	2472	229	165	164	16	8			
17	Cl	2823	270	202	200	18	7			
18	Ar	3202	320	247	245	25	12			
19	K	3608	377	297	294	34	18			
20	Ca	4038	438	350	347	44	26		5	
21	Sc	4493	500	407	402	54	32		7	
22	Ti	4965	564	461	455	59	34		3	
23	V	5465	628	520	513	66	38		2	
24	Cr	5989	695	584	757	74	43		2	
25	Mn	6539	769	652	641	84	49		4	
26	Fe	7114	846	723	710	95	56		6	
27	Co	7709	926	794	779	101	60		3	
28	Ni	8333	1008	872	855	112	68		4	
29	Cu	8979	1096	951	932	120	74		2	
30	Zn	9659	1194	1044	1021	137	90		9	
31	Ga	10367	1299	1144	1117	160	106		20	
42	Mo	20000	2866	2625	2520	505	410	393	208	205
46	Pd	24350	36304	3330	3173	670	559	531	340	335
48	Ag	25514	3806	3523	3351	718	602	571	373	367
73	Ta*	67416	11681	11136	11544	*566	*464	*403	*24	*22
79	Au*	80724	14352	13733	14208	*763	*643	*547	*88	*84

* 4s, 4p et 4f levels indicated, respectively

Photoemission

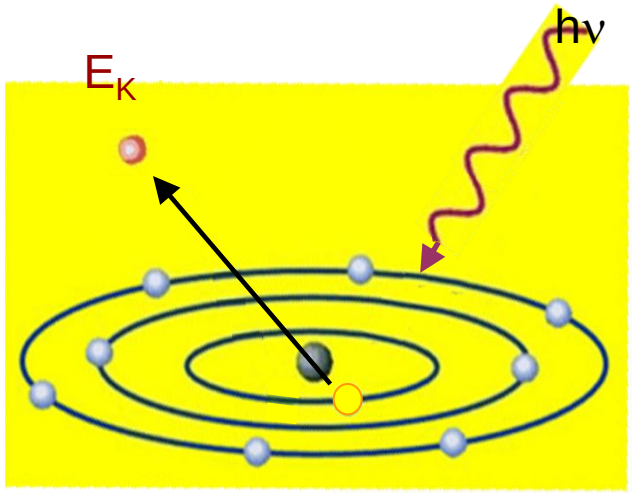

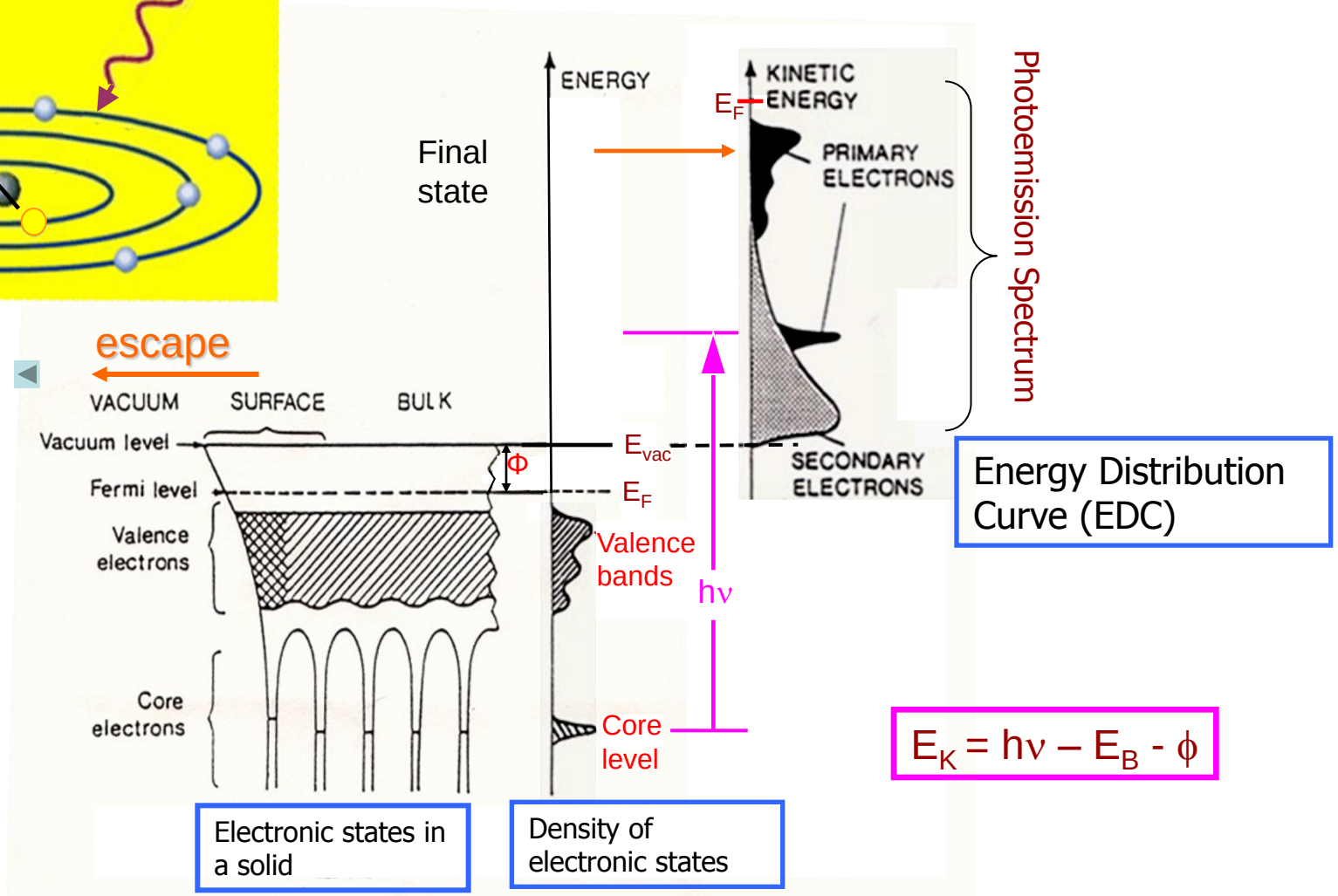

$$E_K = h\nu - E_B - \phi$$

Energy diagrams of photoelectron spectroscopy

Energetic photons on the Surface

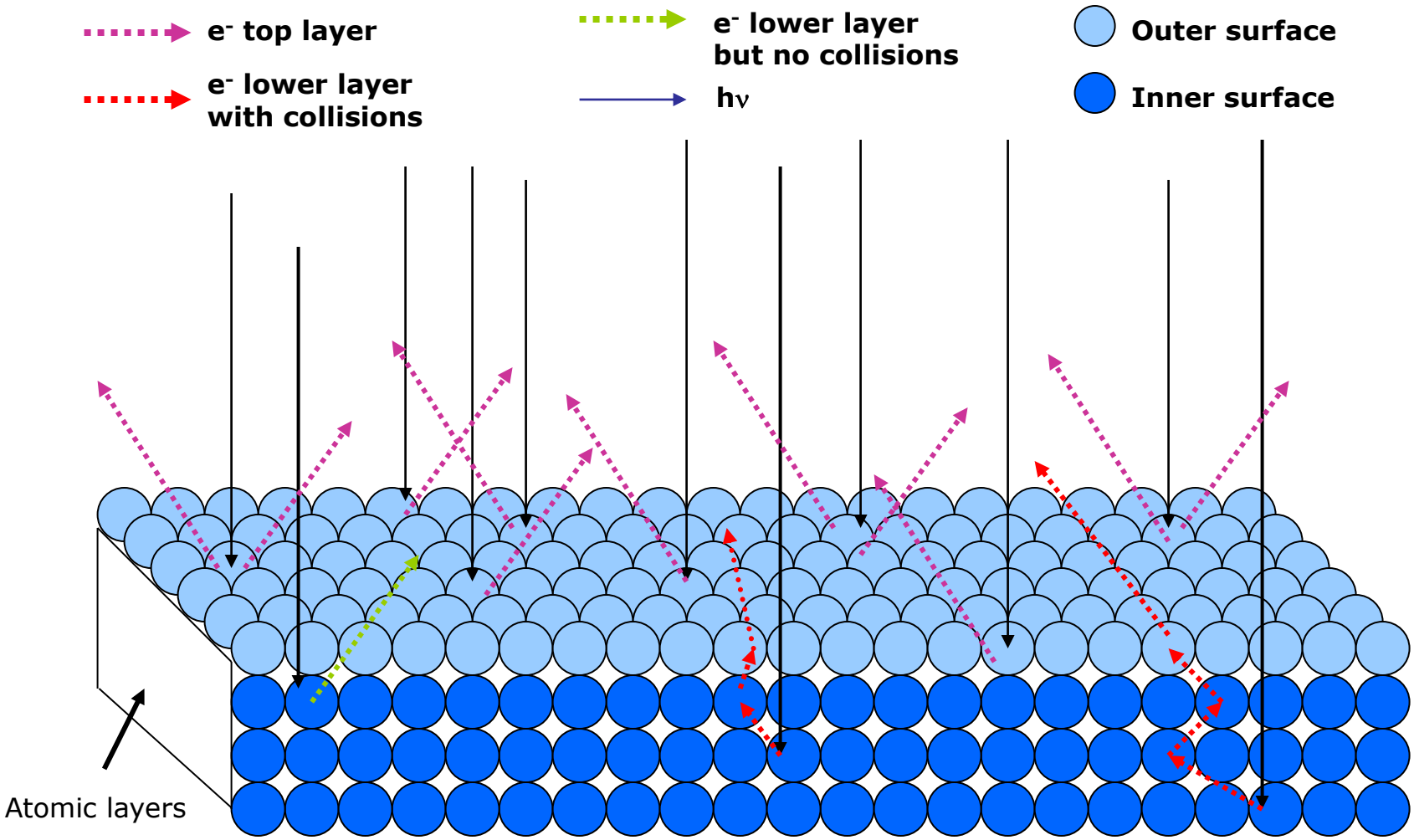

The Sudden Approximation

Assumes the remaining orbitals (often called the passive orbitals) are the same in the final state as they were in the initial state (also called the *frozen-orbital approximation*). Under this assumption, the photoelectron spectroscopy measures the negative Hartree-Fock orbital energy:

Koopman's Binding Energy

$$E_{B,K} \cong -\varepsilon_{B,K}$$

Actual binding energy will represent the readjustment of the N-1 charges to minimize energy, a relaxation process:

$$E_B = E_f^{\ N-1} - E_i^{\ N}$$

Fermi Level Referencing

Free electrons (those giving rise to conductivity) find an equal potential which is constant throughout the material.

Fermi-Dirac Statistics:

$$f(E) = \frac{1}{\exp[(E-E_f)/kT] + 1}$$

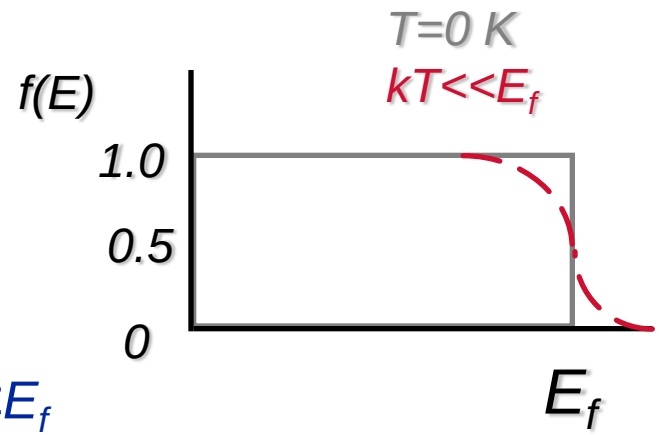

1. At $T=0$ K: $f(E)=1$ for $E<E_f$
   $f(E)=0$ for $E>E_f$

2. At $kT<<E_f$ (at RT, $kT=25$ meV)
   $f(E)=0.5$ for $E=E_f$

Fermi Level Referencing

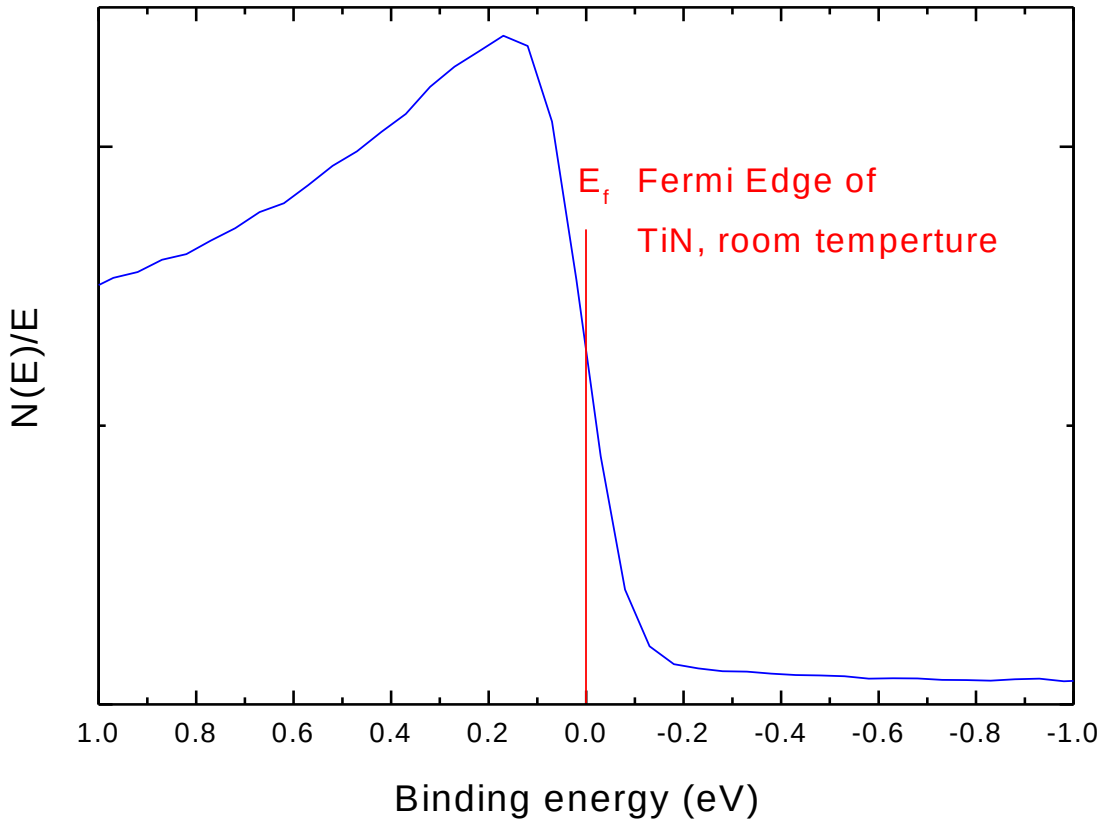

Spin-orbit Coupling

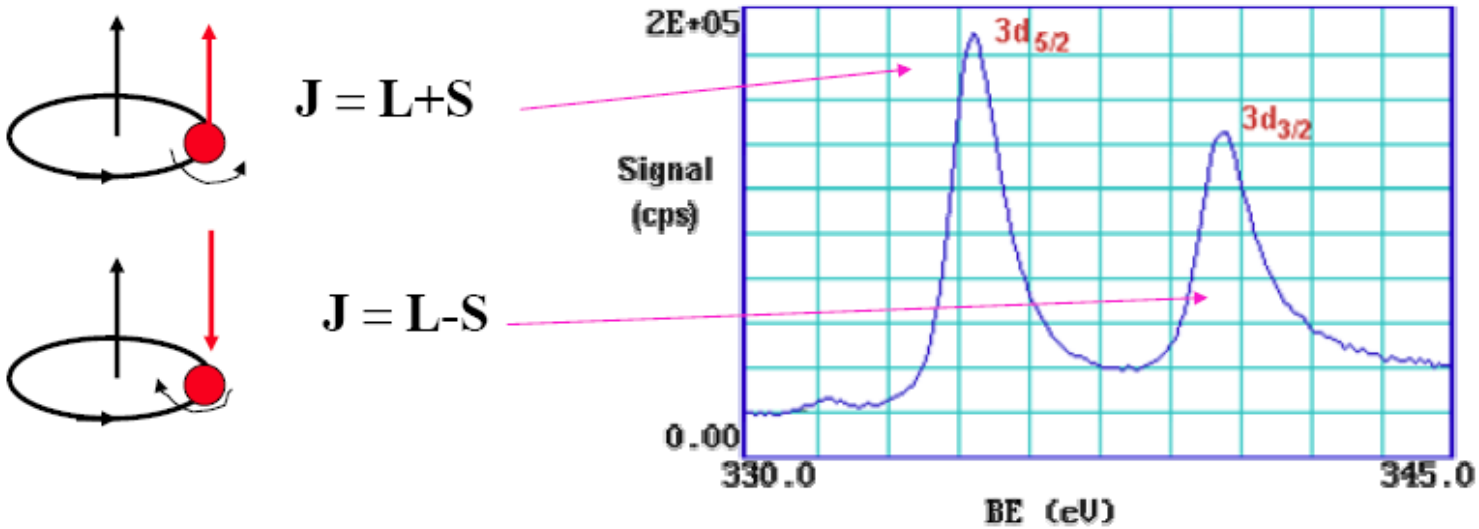

Pd: $(3d)^{10} + h\nu \rightarrow (3d)^{9} + e$

$L = 2$, $S = ½$, $J = L+S, \ldots, L-S = 5/2, 3/2$

$^2D_{5/2}$ $g_J = 2x\{5/2\}+1 = 6$

$^2D_{3/2}$ $g_J = 2x\{3/2\}+1 = 4$

-p,d and f orbitals splitted into two peaks in XPS spectra

-BE (J=L-S) >BE(J=L+S)

-Splitting↑ as Z ↑, n ↑

Electronic Effects: Spin-Orbit Coupling

s orbital

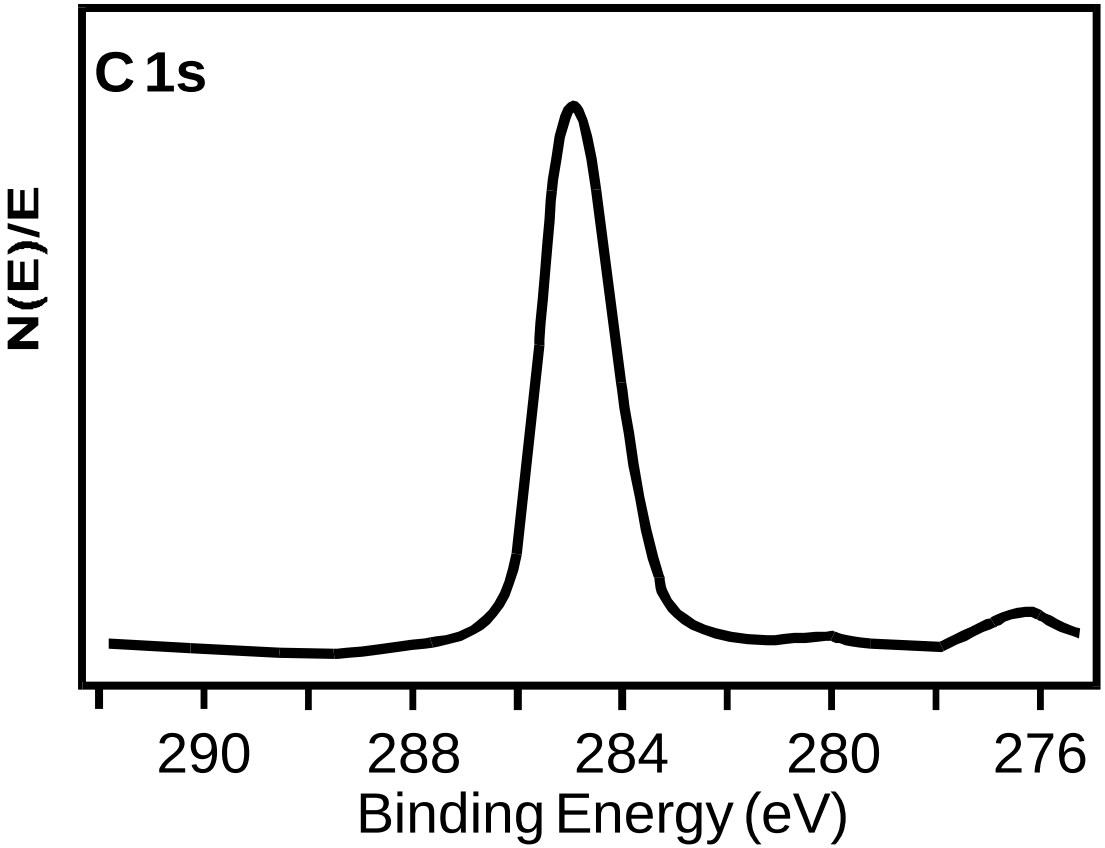

Orbital=s

l=0

s=+/-1/2

ls=1/2

Electronic Effects: Spin-Orbit Coupling

p orbital

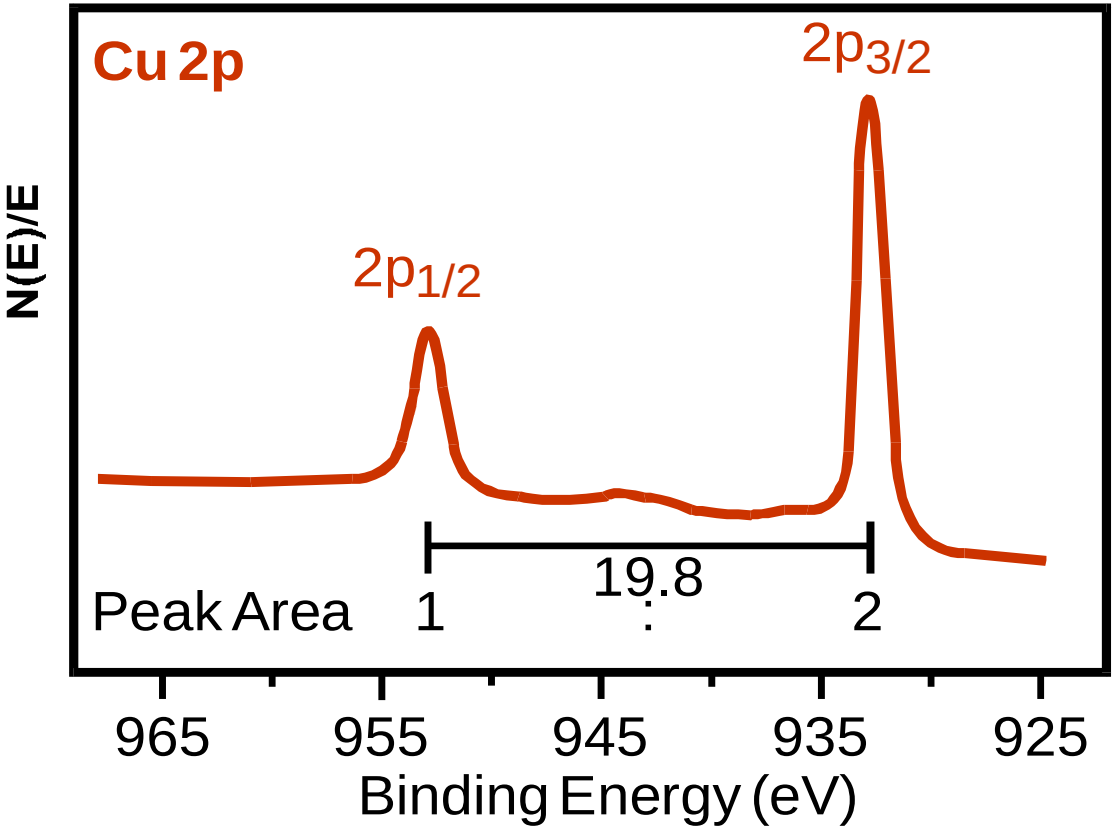

Orbital=p

l=1

s=+/-1/2

ls=1/2,3/2

Electronic Effects: Spin-Orbit Coupling

d orbital

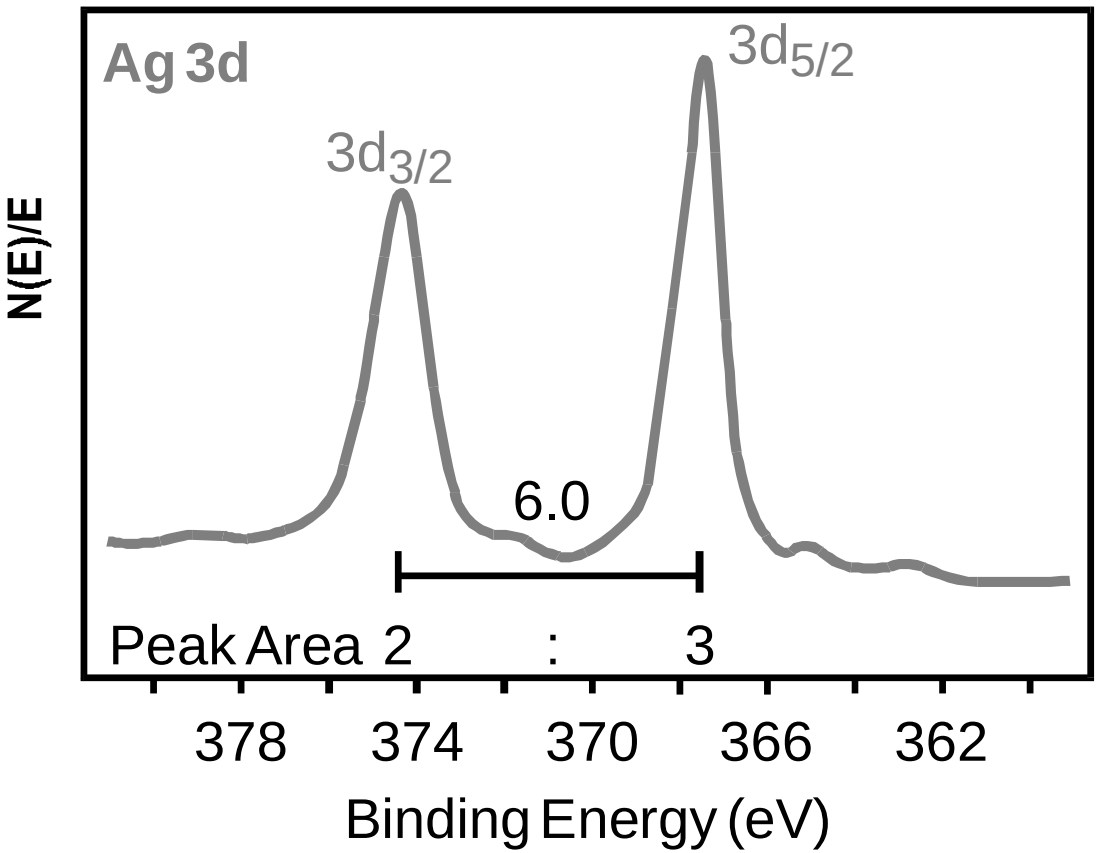

Orbital=d

l=2

s=+/-1/2

ls=3/2,5/2

Electronic Effects: Spin-Orbit Coupling

f orbital

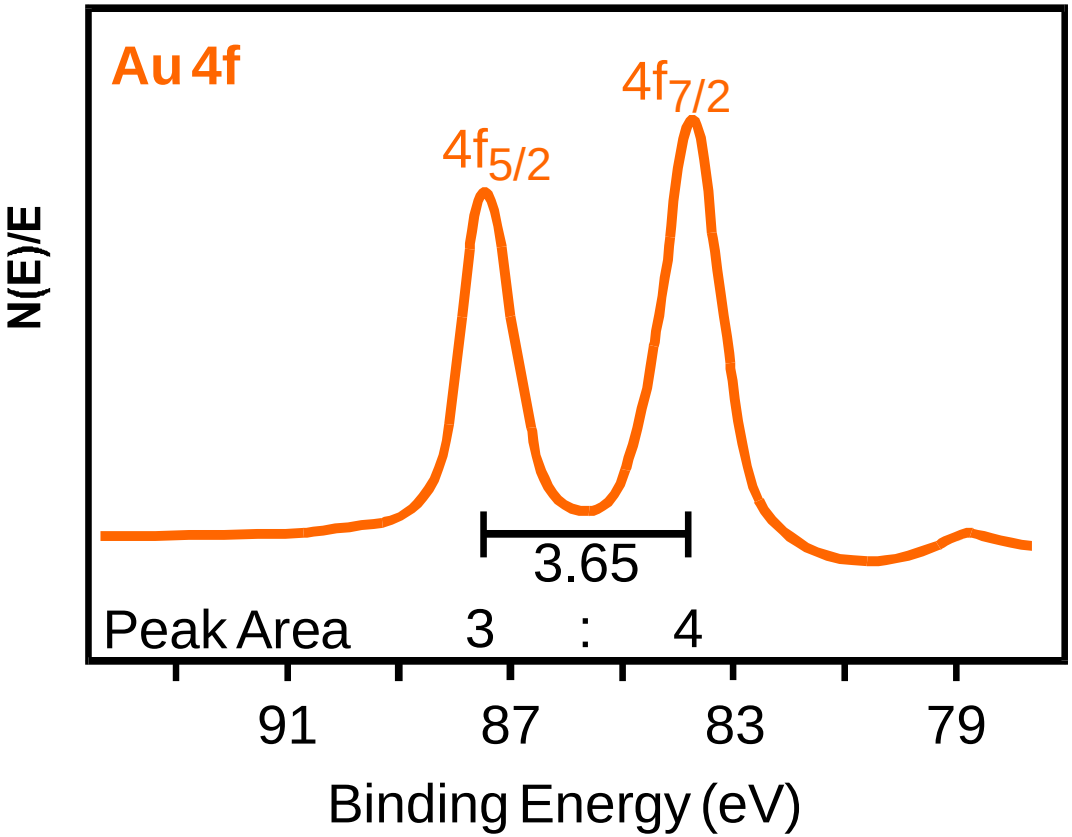

Orbital=f

l=3

s=+/-1/2

ls=5/2,7/2

Example of Chemical Shift

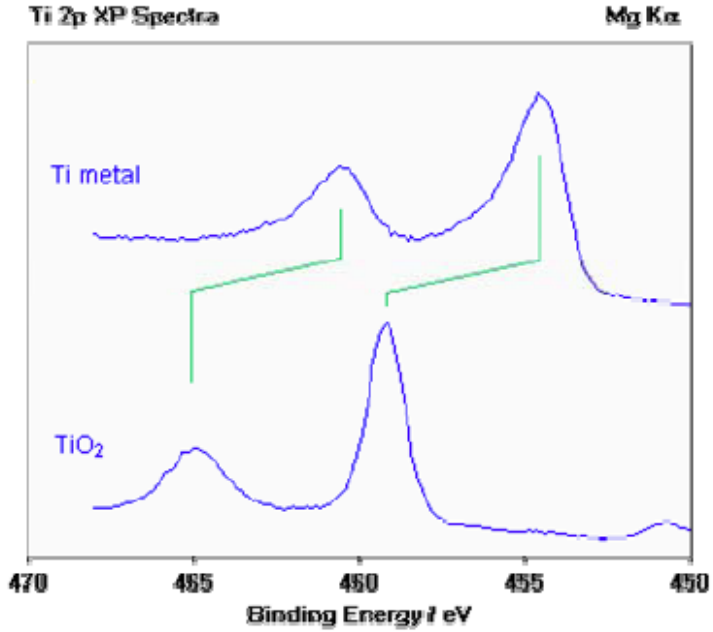

- The chemical shift: ~4.6 eV
- Metals: an asymmetric line shape (Doniach-Sunjic)
- Insulating oxides: more symmetric peak

Chemical Shifts- Electronegativity Effects

Functional Group		***Binding Energy (eV)***
hydrocarbon	C-H, C-C	285.0
amine	C-N	286.0
alcohol, ether	C-O-H, C-O-C	286.5
Cl bound to C	C-Cl	286.5
F bound to C	C-F	287.8
carbonyl	C=O	288.0

Chemical Shifts: Sensitivity to Atomic Valence

In metals, the spectrum of a given core level is often affected by the metals‘ valency

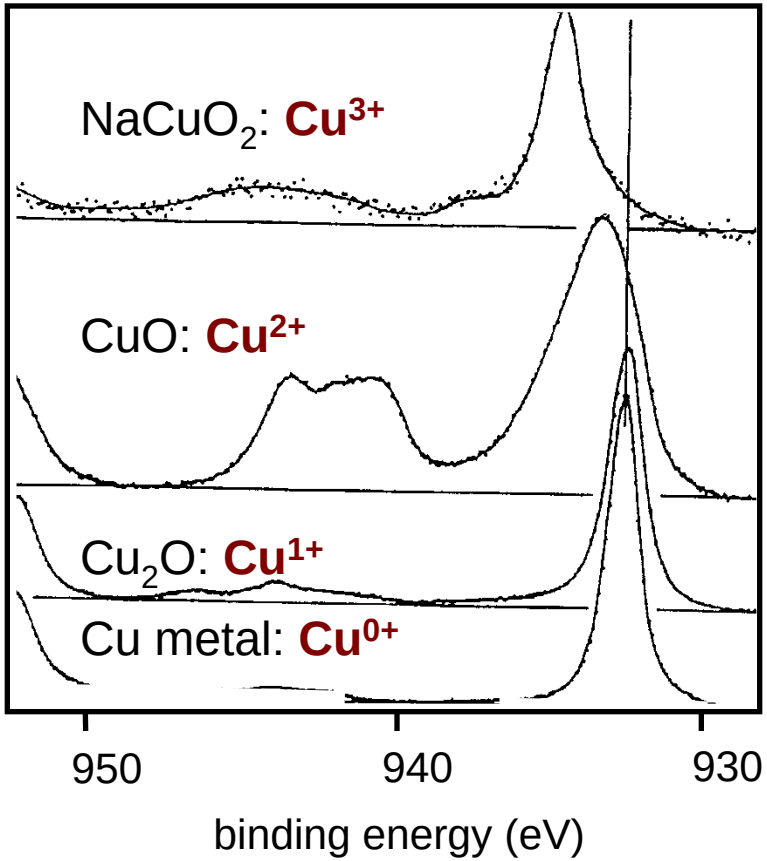

Example:
Valence effects in Cu compounds

- for higher valency, main peak shifts to higher binding energy
- occurence of additional "satellite" peaks on high binding energy side ("shake-up satellites")

Final State Effects: Multiplet Splitting

Following photoelectron emission, the remaining unpaired electron may couple with other unpaired electrons in the atom, resulting in an ion with several possible final state configurations with as many different energies. This produces a line which is split asymmetrically into several components

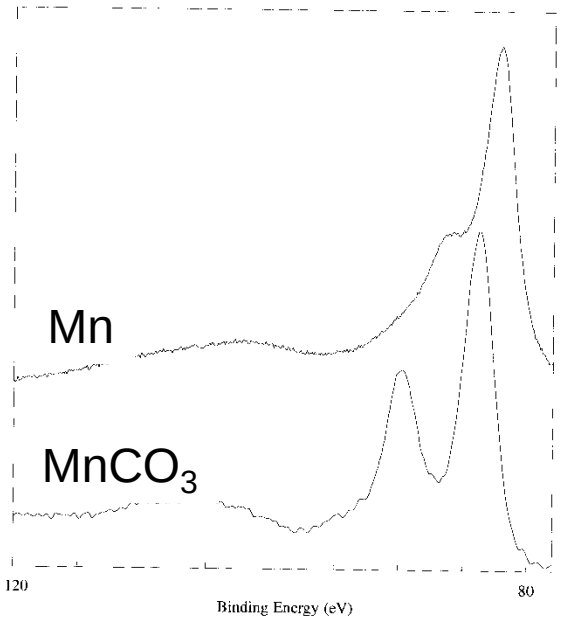

Figure 10. Multiplet splitting of the Mn 3s.

Electron Scattering Effects: Plasmon Loss Peak in metal

Metal

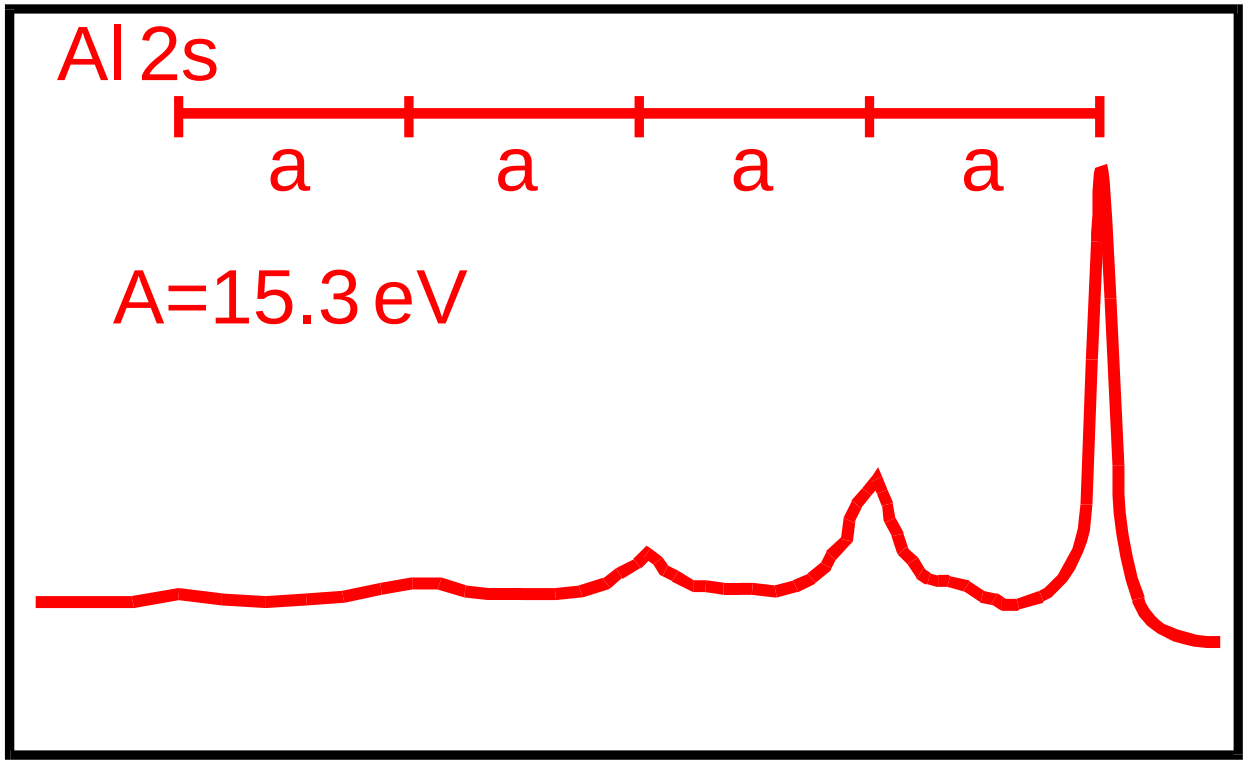

Electron Scattering Effects: Plasmon Loss Peak in insulator

Insulating Material

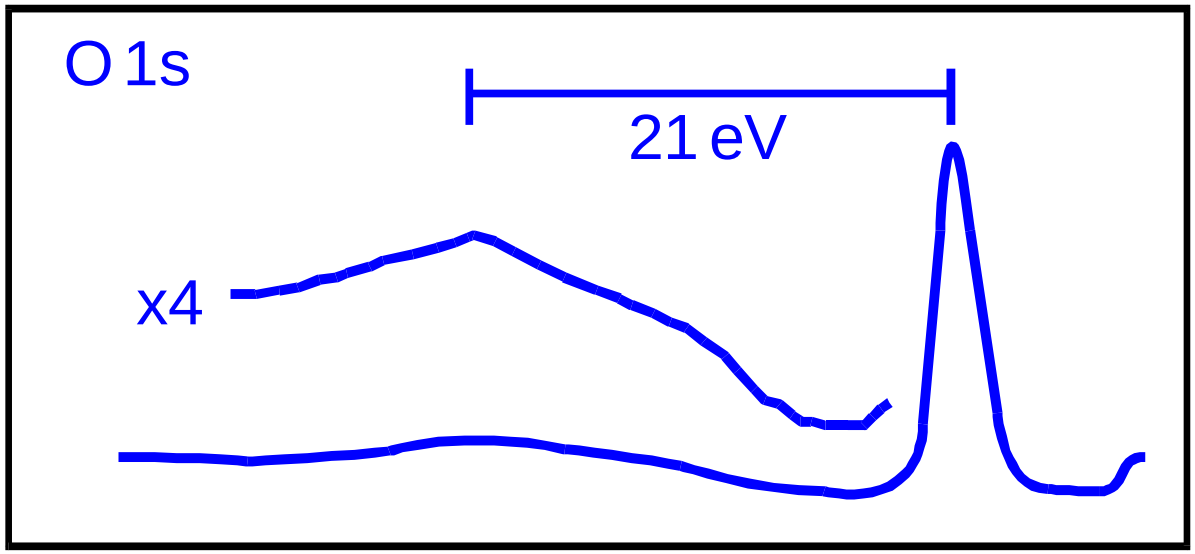

Light Source

x-Ray Tube + Monochom. by Bragg-Reflection or Grating

- **Al-K $\alpha_{1,2}$** **1486 ± 0.9 eV** Transition $2p_{3(1)/2} \rightarrow 1s$
- **Mg-K α** **1254 eV ± 0.7 eV**
- **Zr-M ξ** **151.4 ± 0.8 eV** Transition $4p_{3/2} \rightarrow 3d_{5/2}$

Beam Lines, Synchrotron-Radiation

- **Wide spectral Range of 10 ... 10^5 eV ± < 1%**

Noblegas Discharge Lamp

- **He I** **21.2 eV ± 0.01eV** $He\,(^1P_1) \rightarrow He(^1S_0) + \hbar\,\omega(21{,}2\ eV)$
- **He II** **40.8 eV ± 0.01 eV**

HHG from a Ti:Sapphire-fs-Laser

- **21st Order** **32.55 eV ± 0.1eV**

高亮度的第三代同步輻射光源

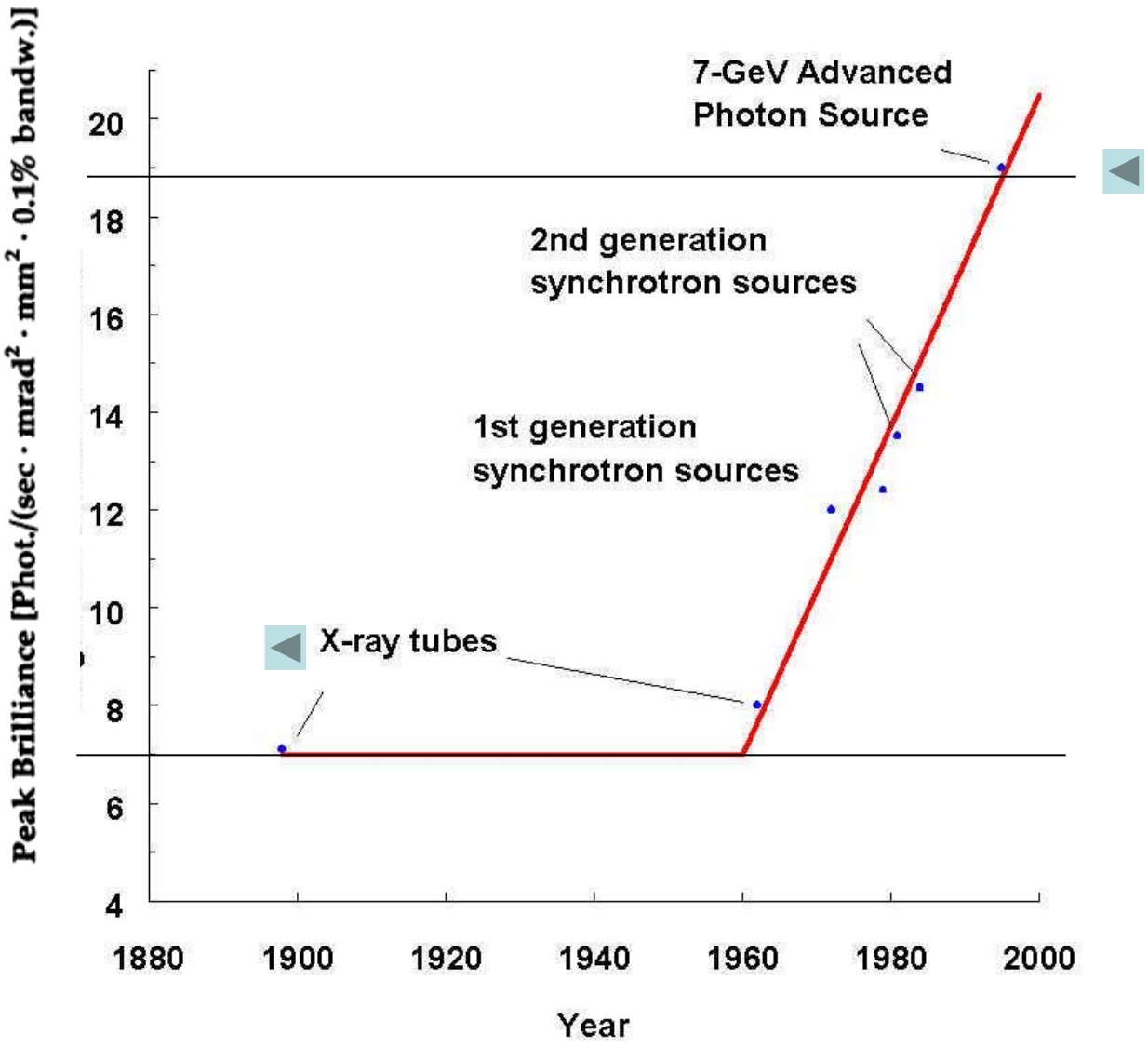

國家同步輻射研究中心鳥瞰圖

Storage Ring

Bending magnet radiation

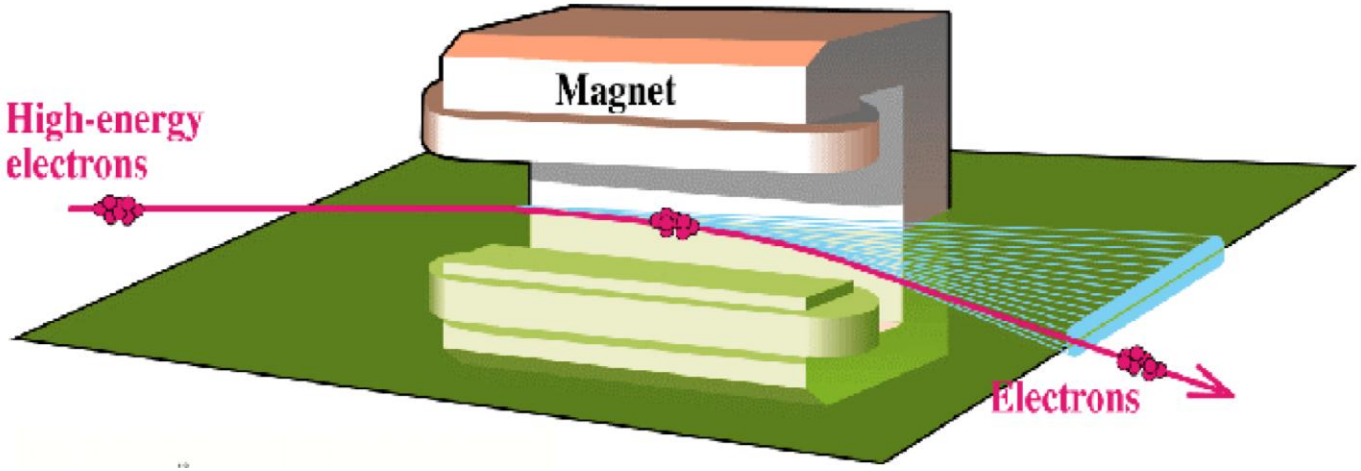

Spectrum emitted by SR

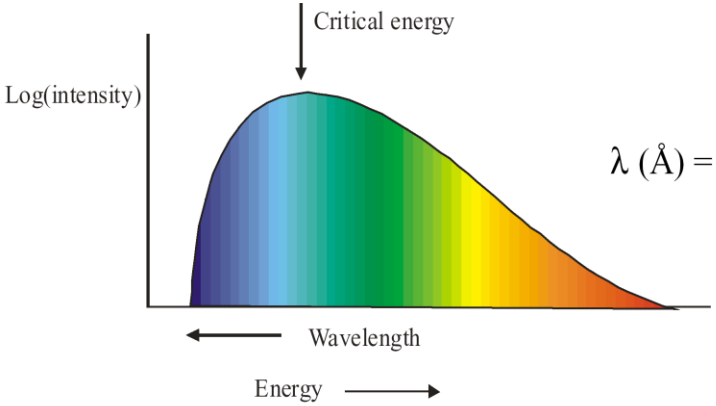

λ (Å) = 12.4/E (keV)

Insertion devices - undulator

- 3rd generation undulator is much more than "***hundreds of thousands***" times brighter than a conventional source

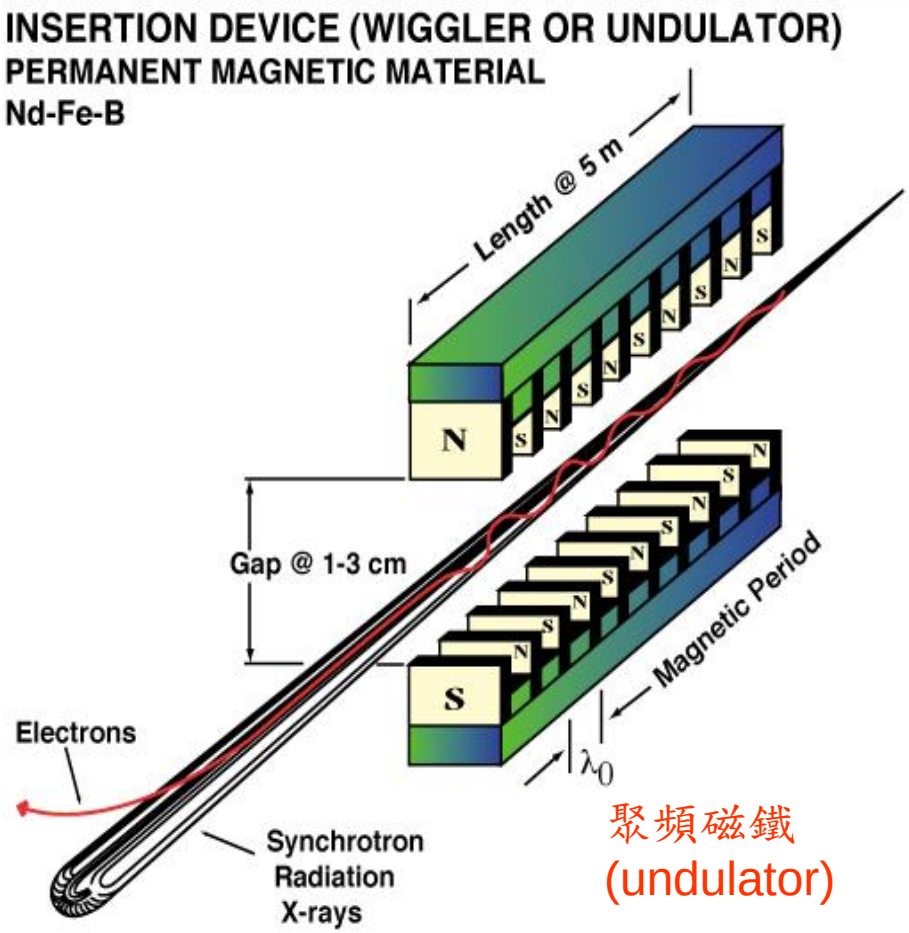

聚頻磁鐵
(undulator)

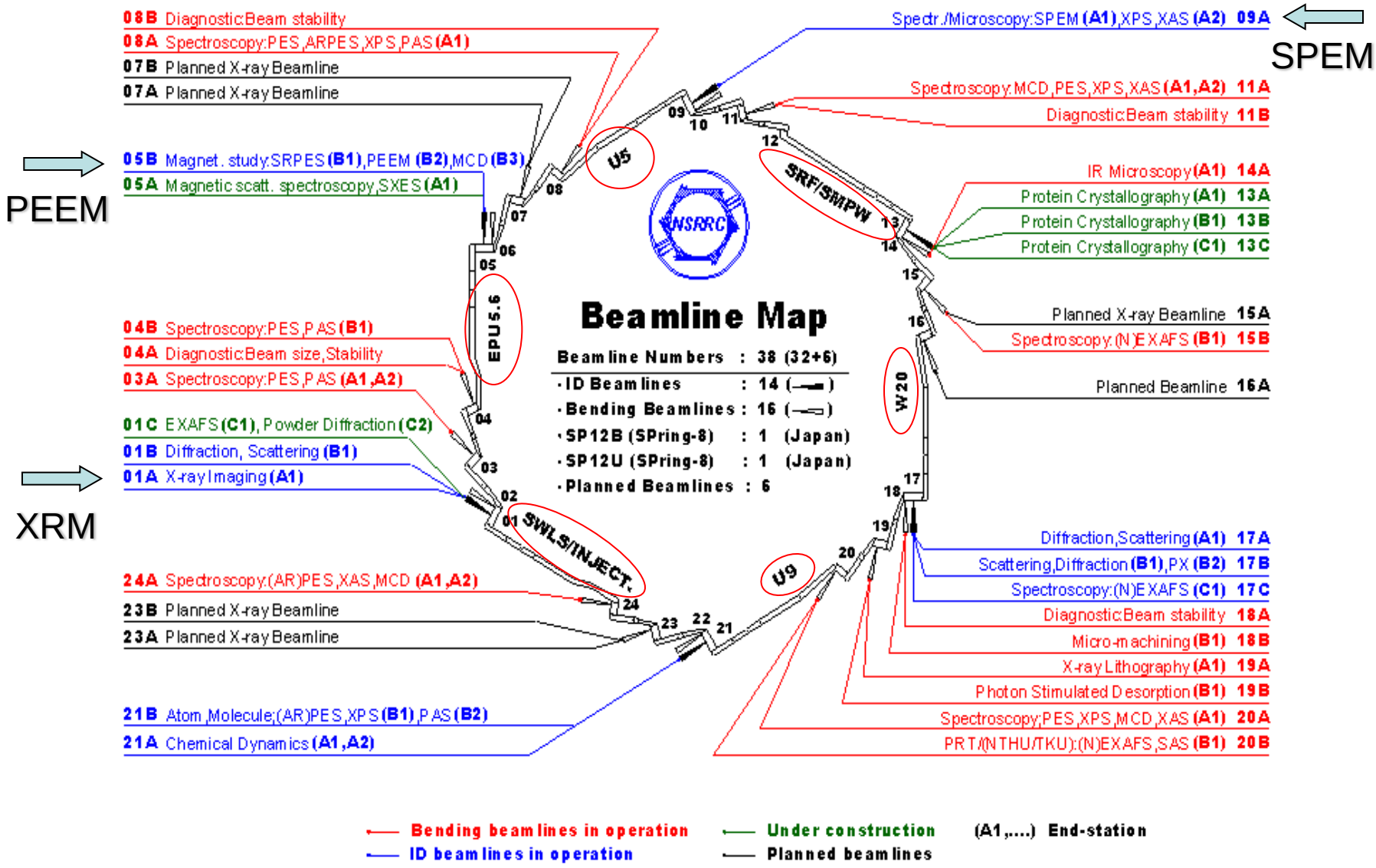
Beamline Map
Beamline Numbers : 38 (32+6)
· ID Beamlines : 14
· Bending Beamlines : 16
· SP12B (SPring-8) : 1 (Japan)
· SP12U (SPring-8) : 1 (Japan)
· Planned Beamlines : 6
NSRRC
SWLS/INJECT.
EPU5.6
U5
SRF/SMPW
W20
U9
08B Diagnostic:Beam stability
08A Spectroscopy:PES,ARPES,XPS,PAS (A1)
07B Planned X-ray Beamline
07A Planned X-ray Beamline
05B Magnet. study:SRPES (B1),PEEM (B2),MCD (B3)
05A Magnetic scatt. spectroscopy,SXES (A1)
04B Spectroscopy:PES,PAS (B1)
04A Diagnostic:Beam size,Stability
03A Spectroscopy:PES,PAS (A1,A2)
01C EXAFS (C1), Powder Diffraction (C2)
01B Diffraction, Scattering (B1)
01A X-ray Imaging (A1)
24A Spectroscopy:(AR)PES,XAS,MCD (A1,A2)
23B Planned X-ray Beamline
23A Planned X-ray Beamline
21B Atom,Molecule;(AR)PES,XPS (B1),PAS (B2)
21A Chemical Dynamics (A1,A2)
Spectr./Microscopy:SPEM (A1),XPS,XAS (A2) 09A
Spectroscopy:MCD,PES,XPS,XAS (A1,A2) 11A
Diagnostic:Beam stability 11B
IR Microscopy (A1) 14A
Protein Crystallography (A1) 13A
Protein Crystallography (B1) 13B
Protein Crystallography (C1) 13C
Planned X-ray Beamline 15A
Spectroscopy:(N)EXAFS (B1) 15B
Planned Beamline 16A
Diffraction,Scattering (A1) 17A
Scattering,Diffraction (B1),PX (B2) 17B
Spectroscopy:(N)EXAFS (C1) 17C
Diagnostic:Beam stability 18A
Micro-machining (B1) 18B
X-ray Lithography (A1) 19A
Photon Stimulated Desorption (B1) 19B
Spectroscopy:PES,XPS,MCD,XAS (A1) 20A
PRT/(NTHU/TKU):(N)EXAFS,SAS (B1) 20B
SPEM
PEEM
XRM
Bending beamlines in operation
ID beamlines in operation
Under construction
Planned beamlines
(A1,....) End-station

同步輻射研究中心加速器配置圖

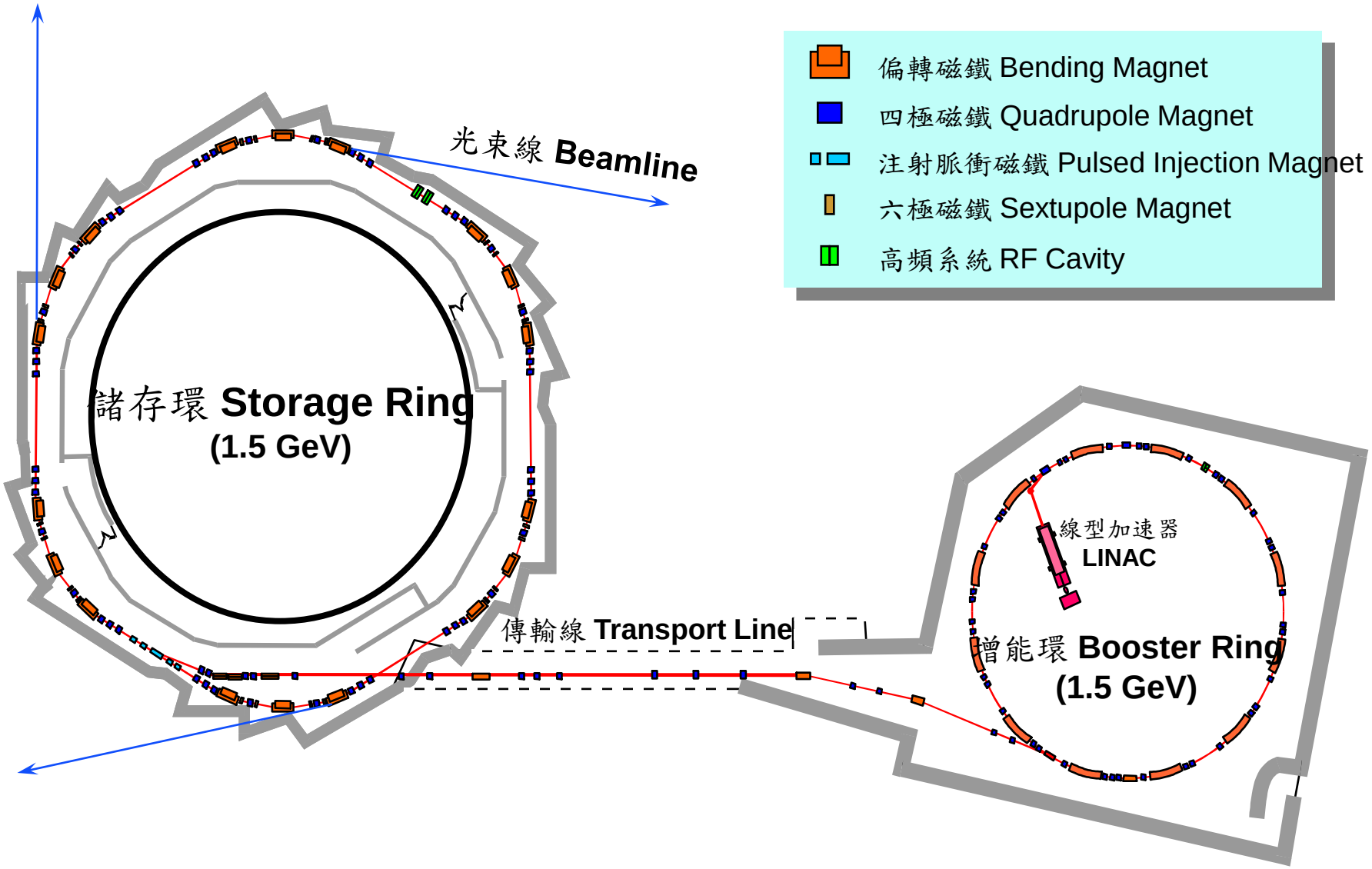

國家同步輻射研究中心儲存環館實驗區

Photoelectron analyzer

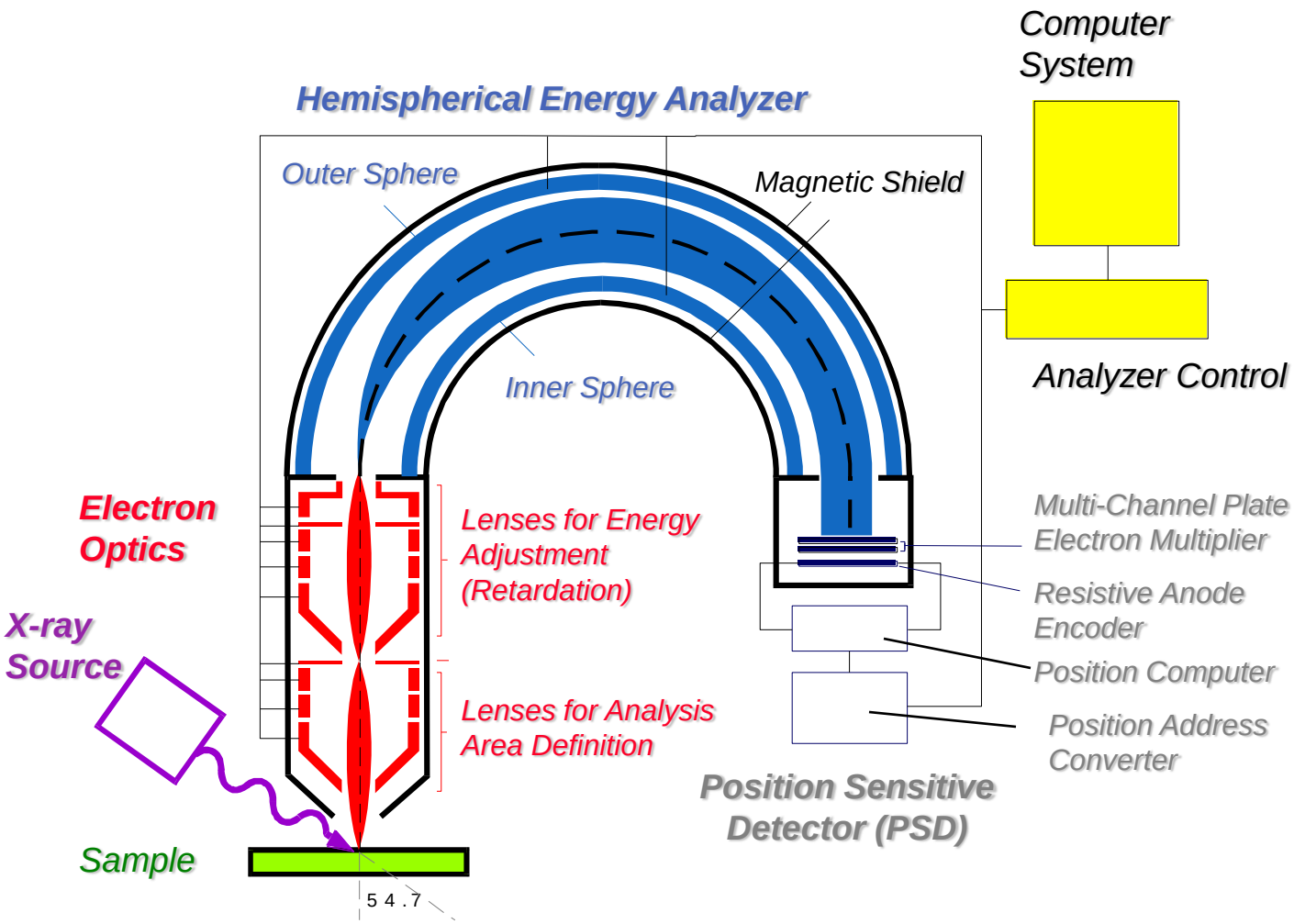

Detector

- Electron multiplier
  Channeltron
  -single channle detection
- Multichannel plate
  - multichannel detection
  - 2D-imaging

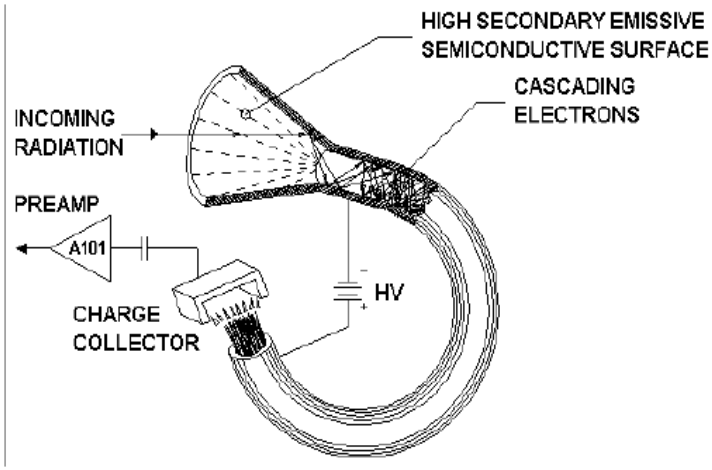

Typical gain : 10^3~10^6
bias voltage: 1-5kV

$1e = 1.6 \times 10^{-19}$ C

$1.6 \times 10^{-19} \times 10^6 = 1.6 \times 10^{-13} = 0.16$ pA

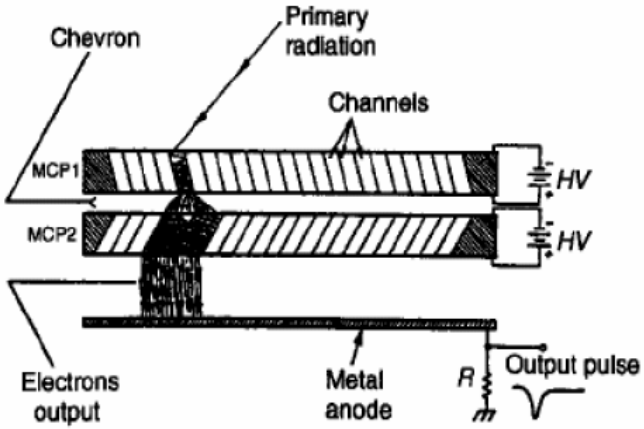

Photoelectron Spectroscopy

hv= 90 ~ 1500 eV

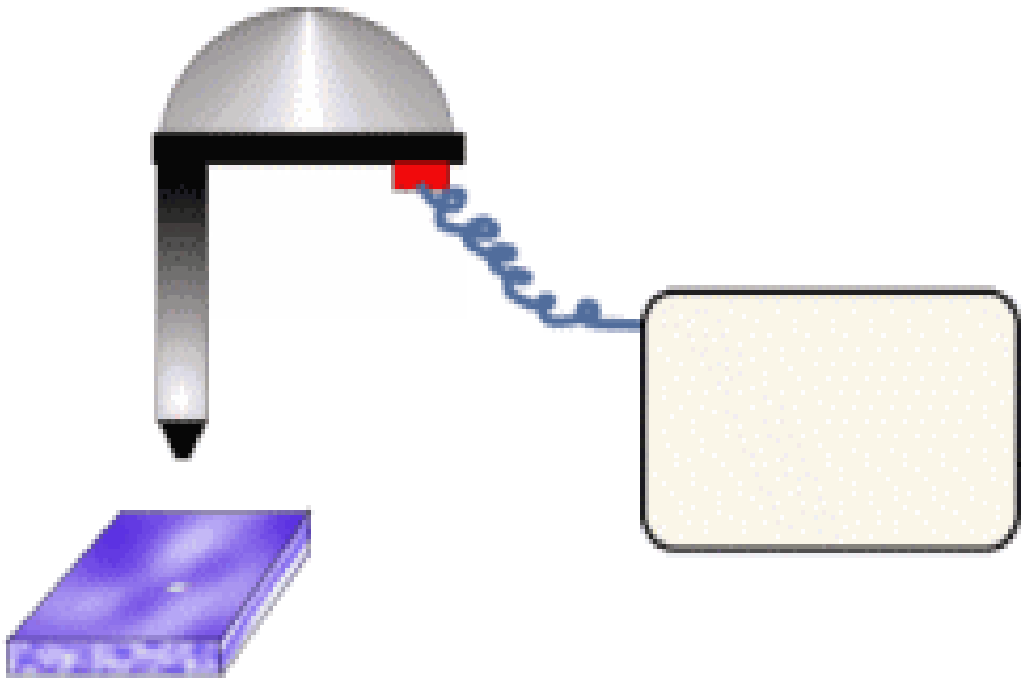

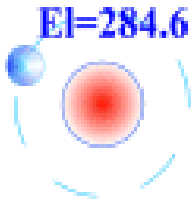

end station

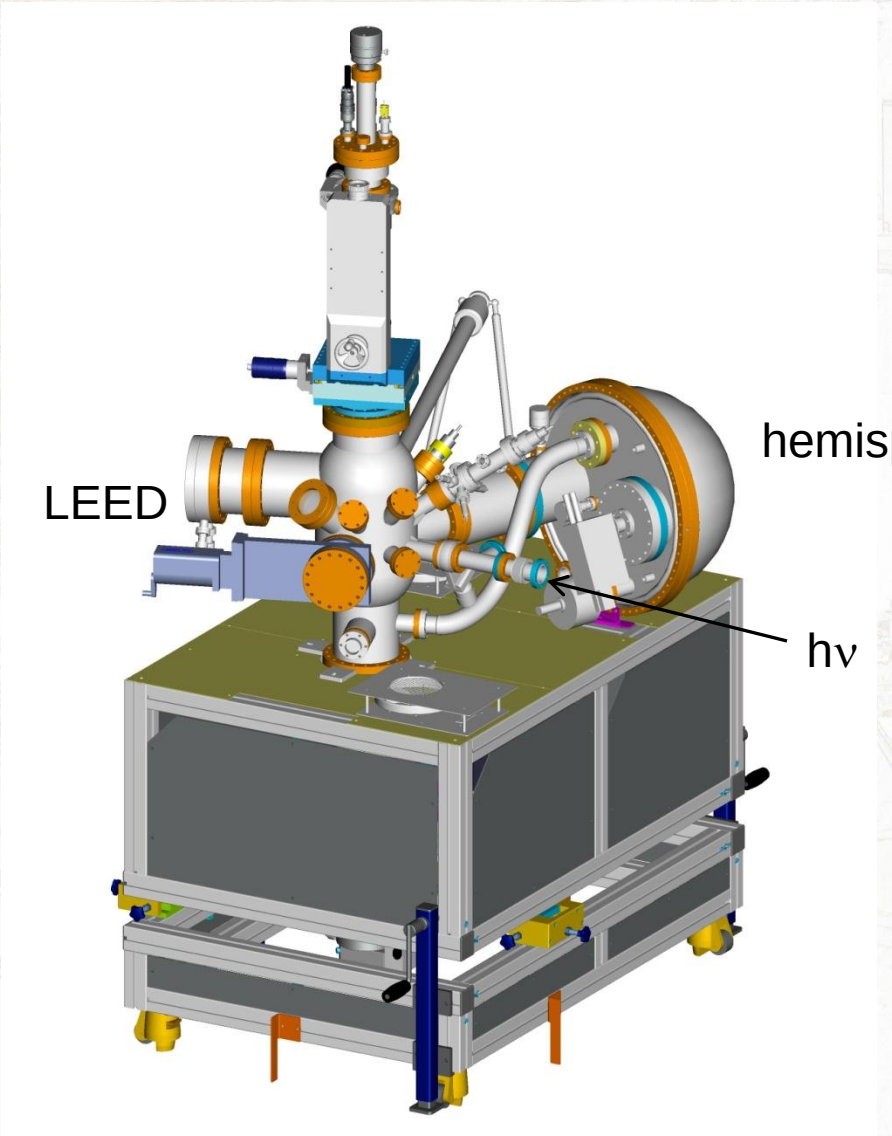

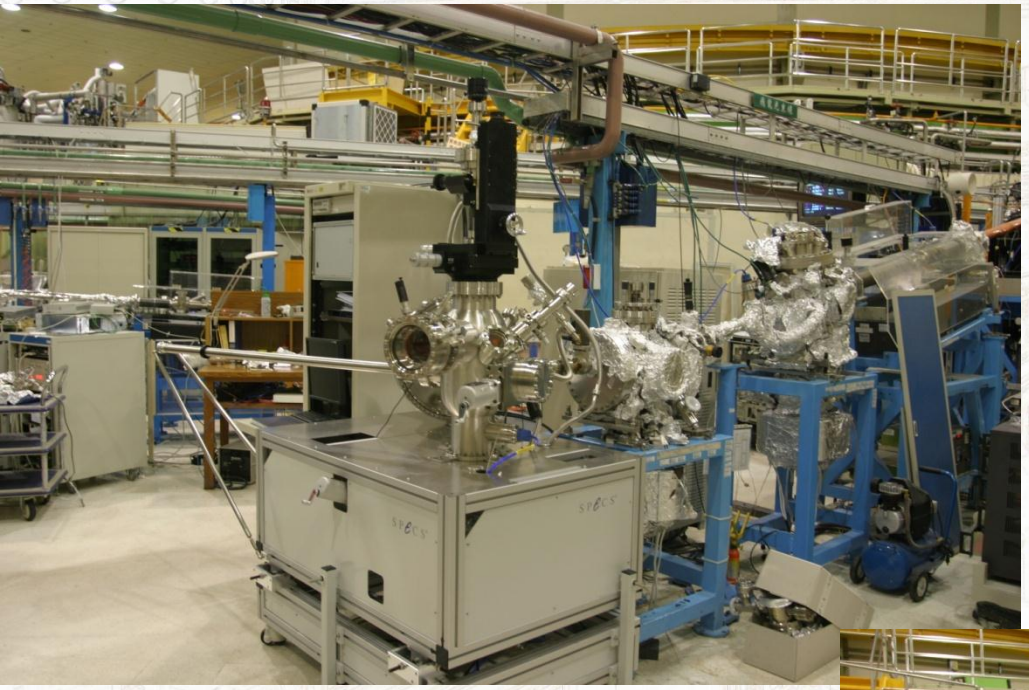


SPECS

λ : (monolayer)

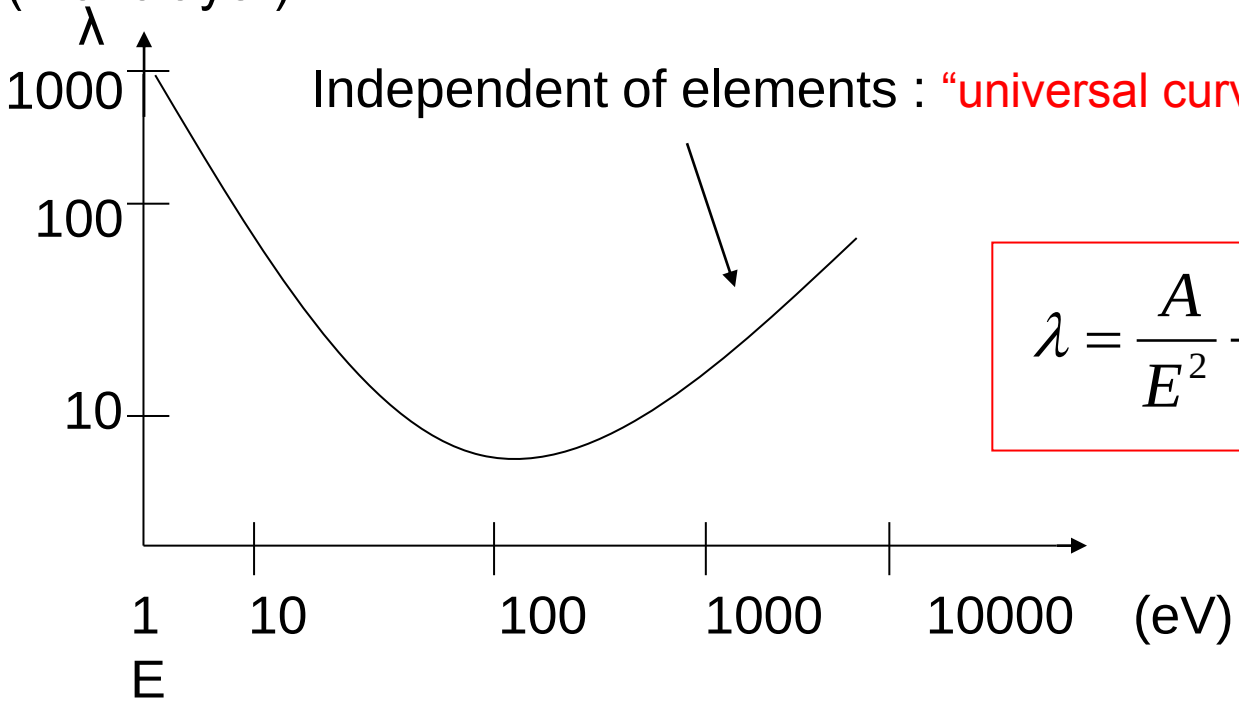

Independent of elements : "universal curve"

$$\lambda = \frac{A}{E^2} + \frac{B}{\sqrt{E}}$$

A = 538
B = 0.210
For elements

"Universal curve" of electron *inelastic mean free path* λ (IMFP) versus KE

IMFP is average distance between inelastic collisions (Å)

Minimum λ = a few Å at 40 ~ 100 eV, *maximum surface sensitivity*

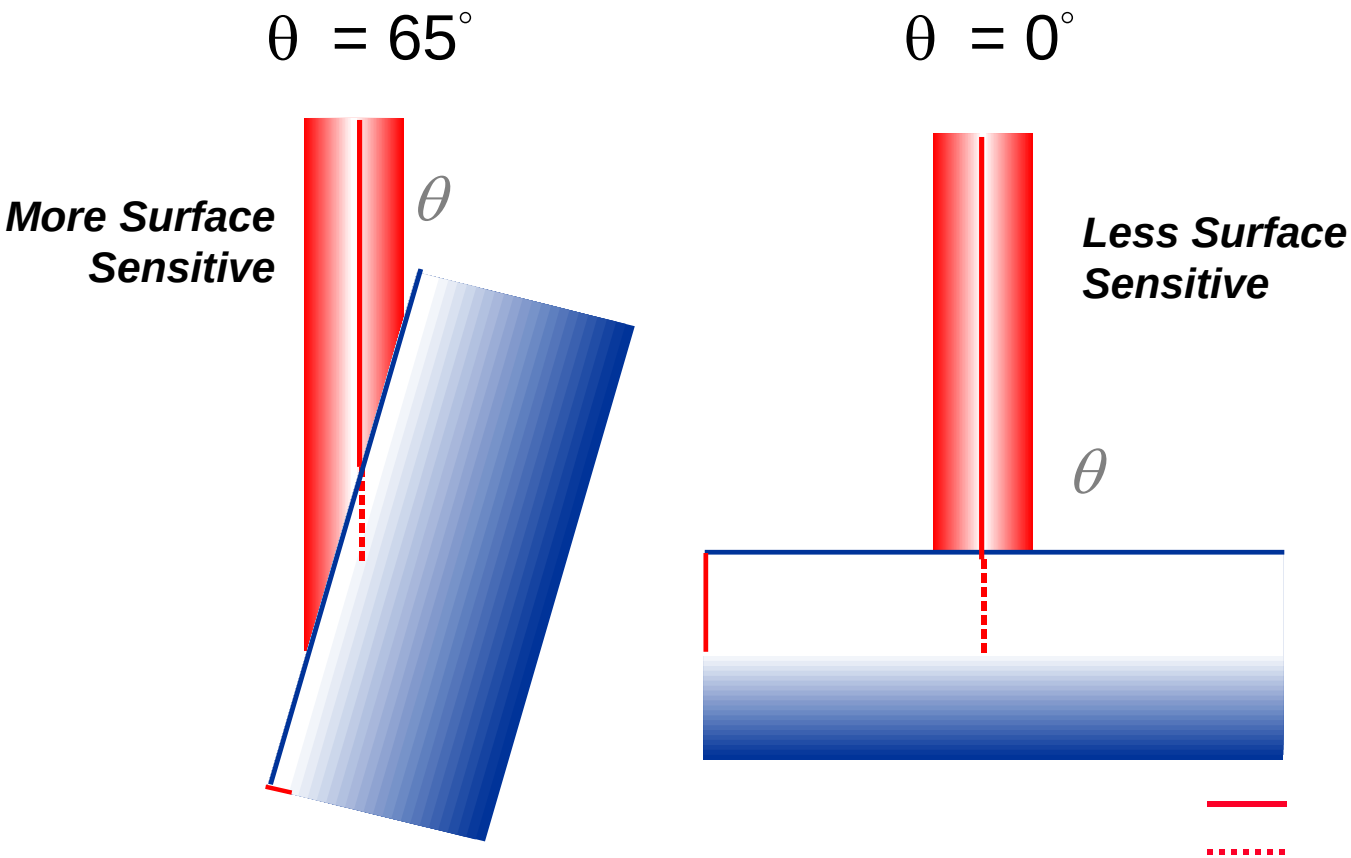

Information depth = dcosθ
d = Escape depth ~ 3λ
θ = Emission angle relative to surface normal
λ = Inelastic Mean Free Path

Surface Core Level Shift

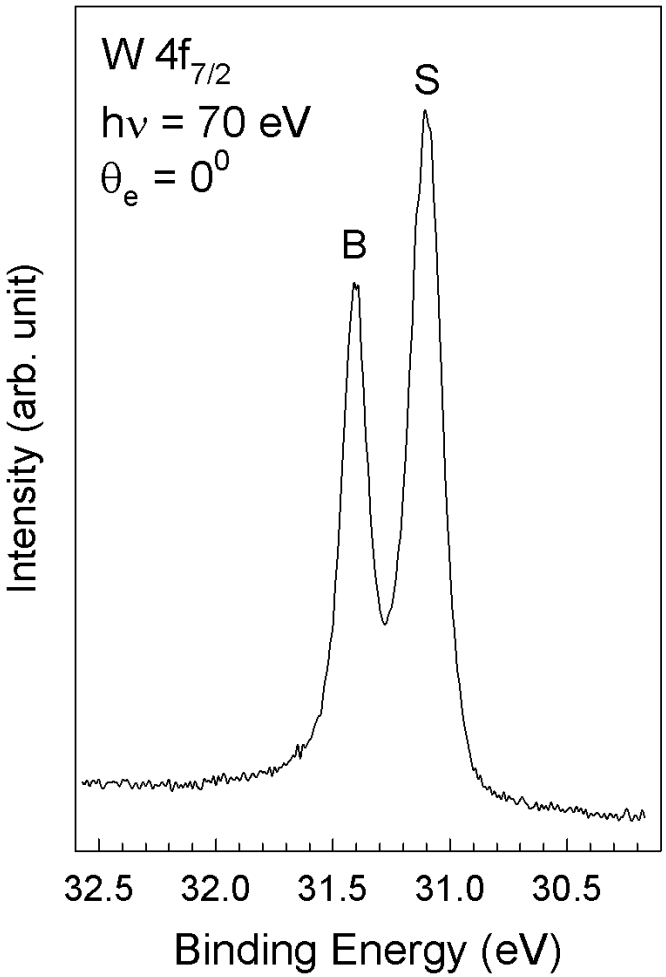

Surface core level shifts (SCLS) are often observed for the transition metals. When the surface is created, the *d*-band is narrowed due to the smaller number of nearest neighbors. Consider the case of more than half filling. A band narrowing would also move the whole band over the Fermi level. This would mean that the surface is charged: it is at a chemical potential different from the bulk. In order to avoid this energy-expensive situation, an electrostatic potential is needed which shifts the whole band up to lower energies. This electrostatic potential does also shift the core level.

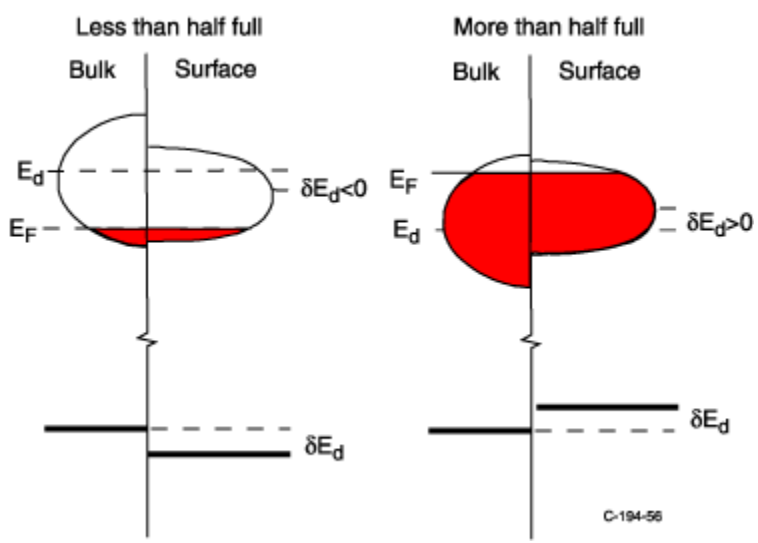

W(110) 0.5 ML Ba on W(110) 1 ML Ba on W(110)

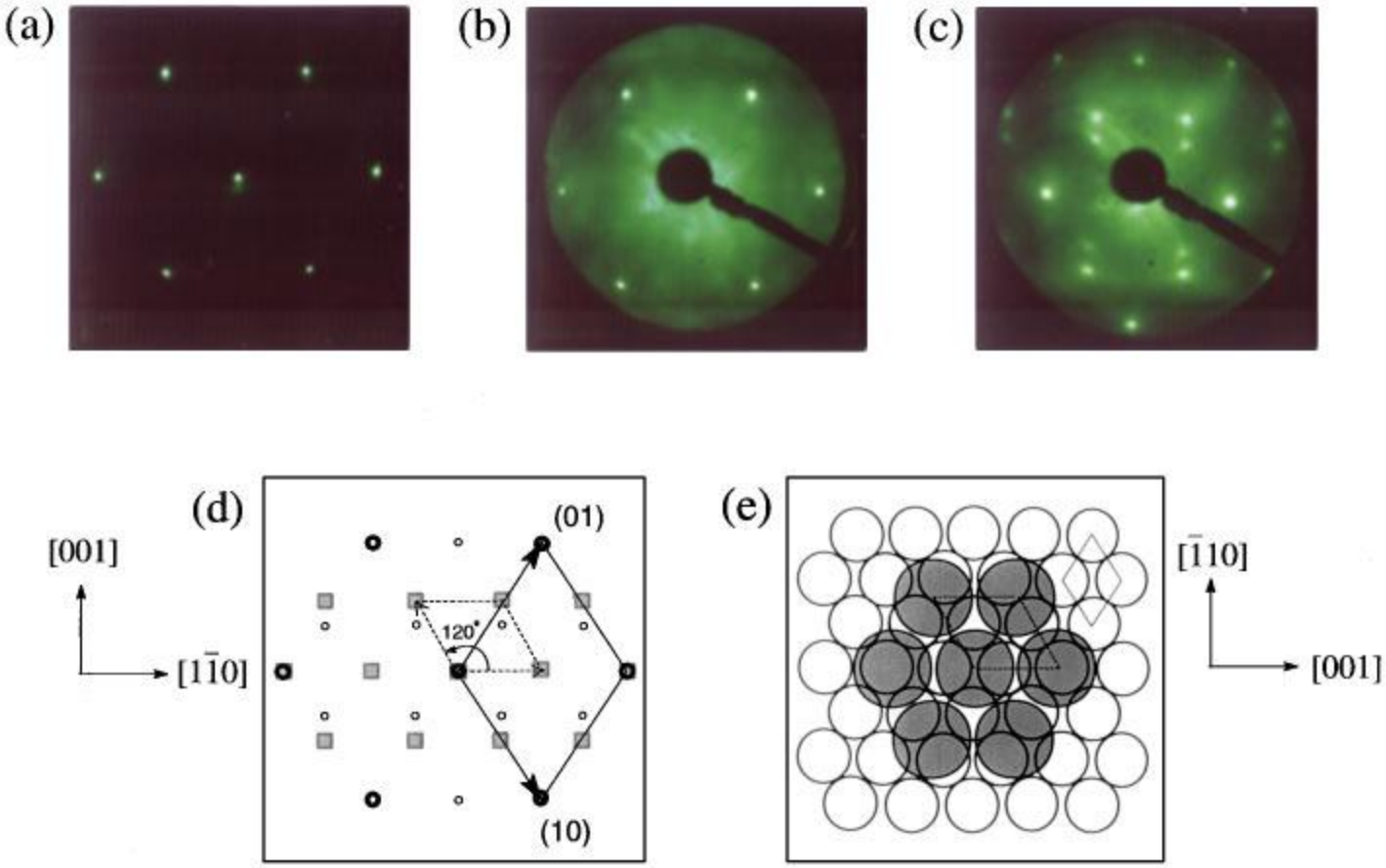

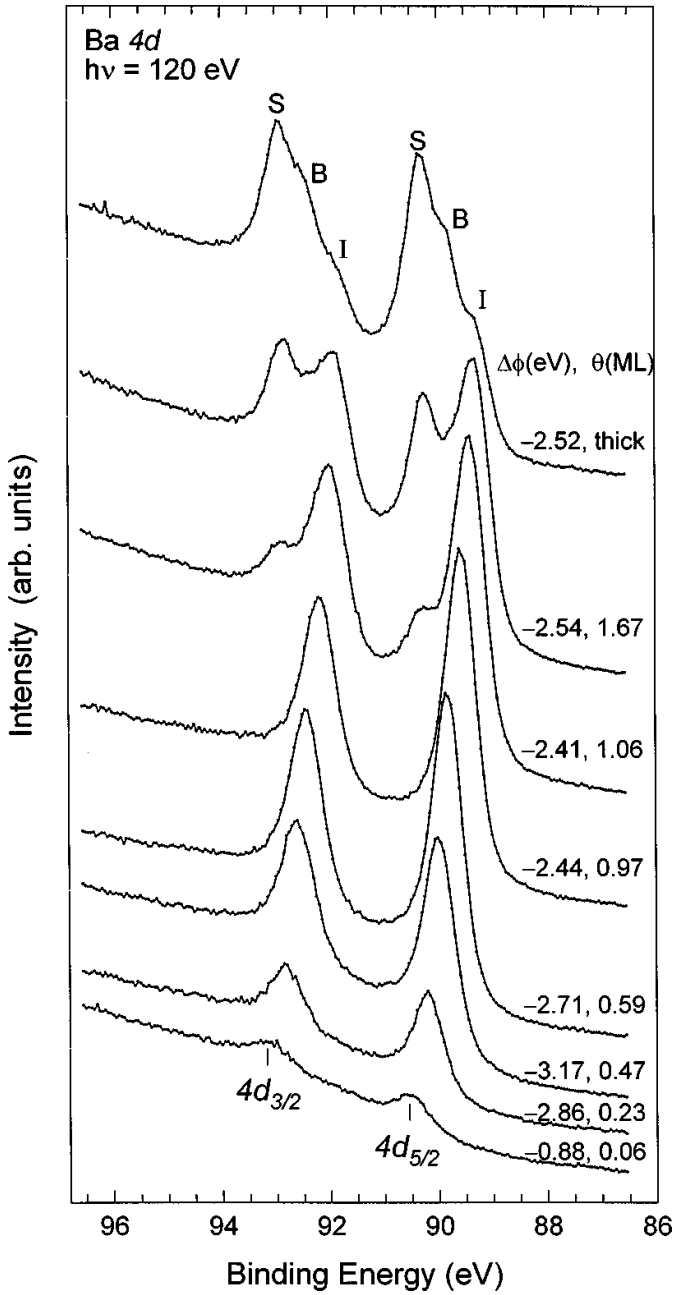
Ba 4d
hν = 120 eV
S
B
I
S
B
I
Δϕ(eV), θ(ML)
−2.52, thick
−2.54, 1.67
−2.41, 1.06
−2.44, 0.97
−2.71, 0.59
−3.17, 0.47
−2.86, 0.23
−0.88, 0.06
4d3/2
4d5/2
Intensity (arb. units)
96
94
92
90
88
86
Binding Energy (eV)

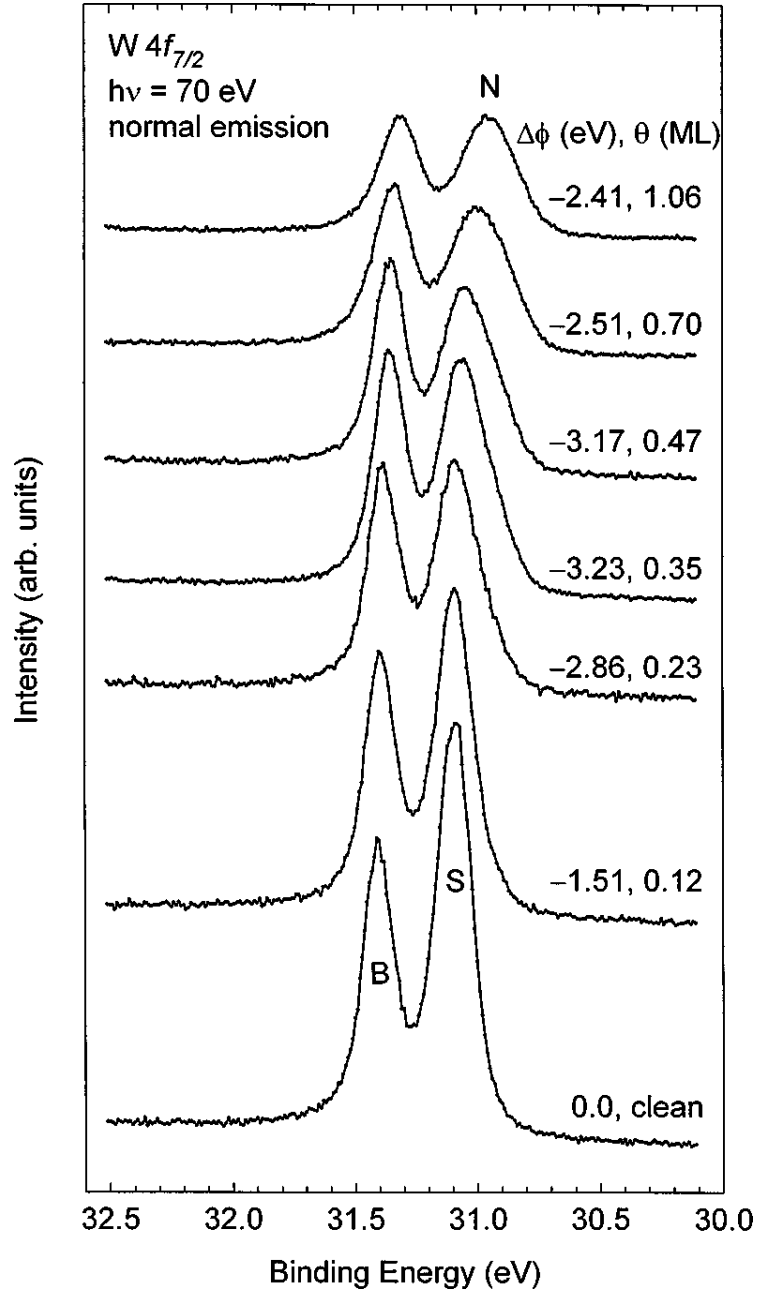
W 4f7/2
hν = 70 eV
normal emission
N
Δϕ (eV), θ (ML)
−2.41, 1.06
−2.51, 0.70
−3.17, 0.47
−3.23, 0.35
−2.86, 0.23
−1.51, 0.12
0.0, clean
S
B
Intensity (arb. units)
32.5
32.0
31.5
31.0
30.5
30.0
Binding Energy (eV)

Ba on clean W(110)

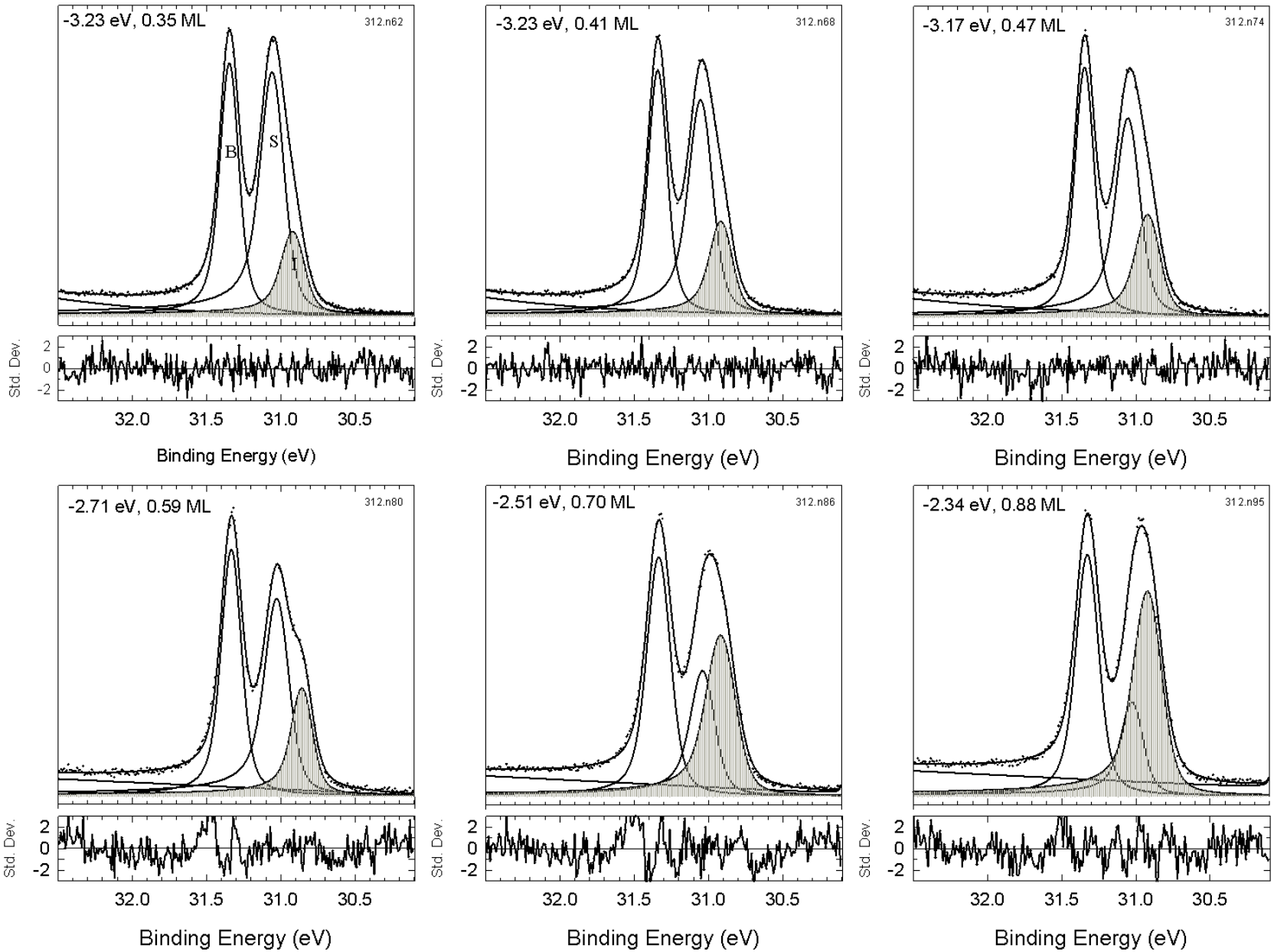

Layerwise growth

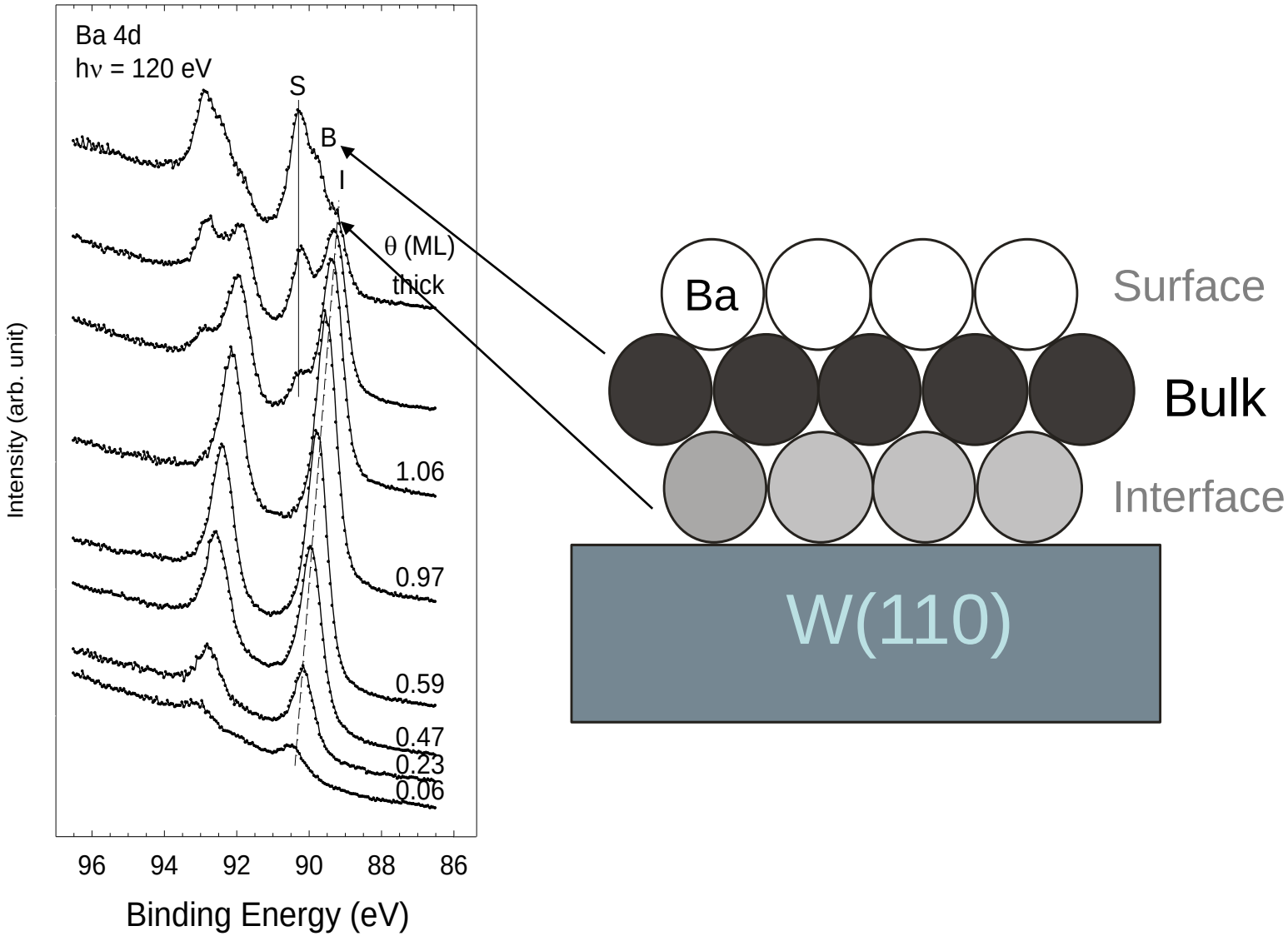

surface core-level shift

W(110)

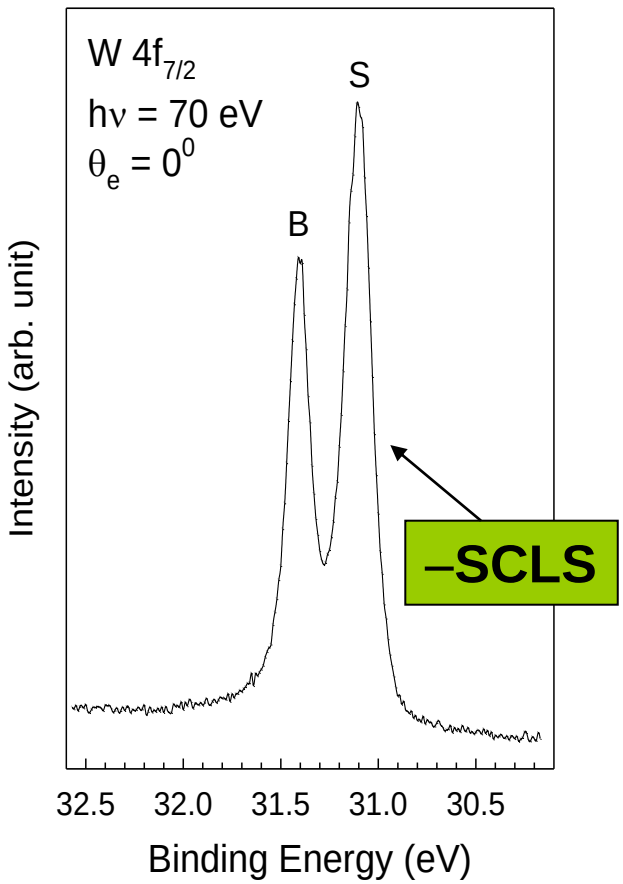

Li

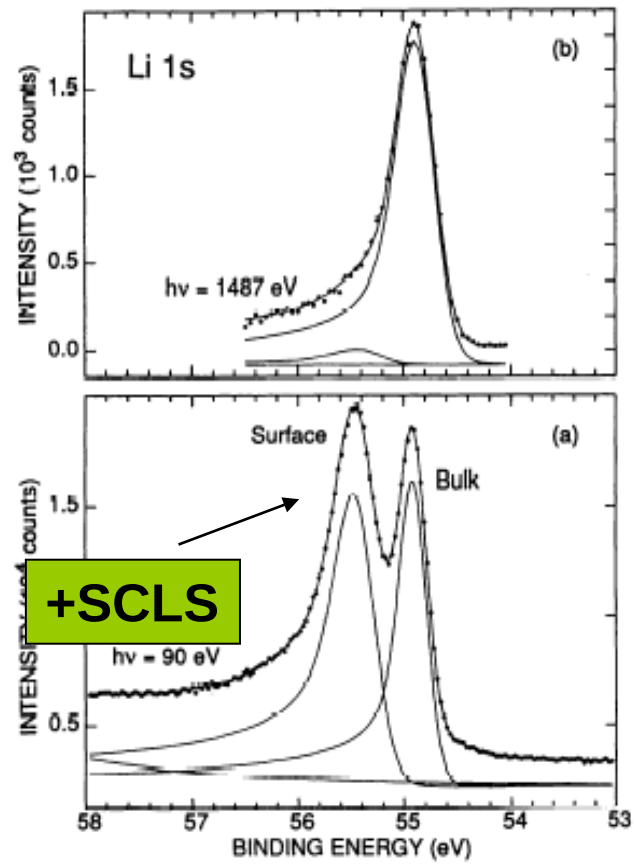

substitutional alloy, Li on Al(001)

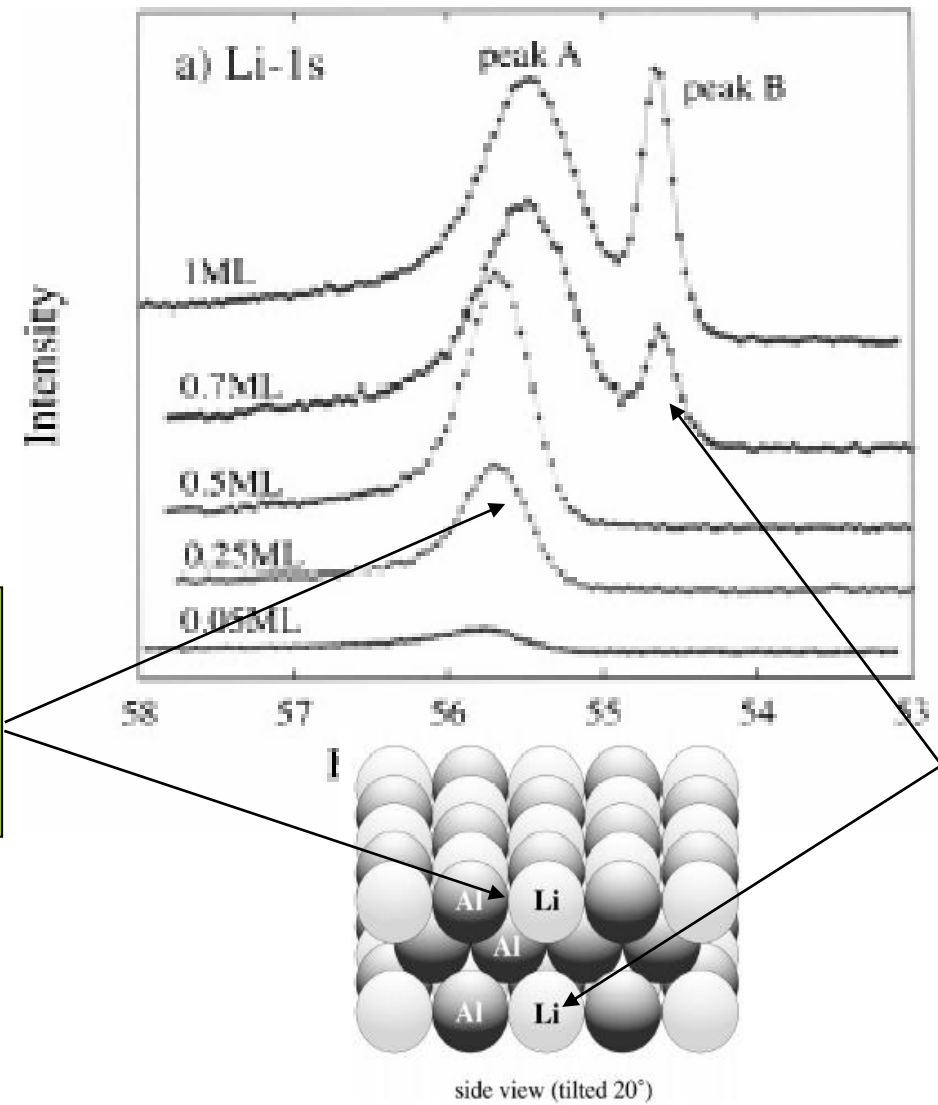

Li in a mixed Al/Li top layer
⇨ **surface-like**

Li in a mixed Al/Li underlayer
⇨ **bulk-like**

supported clusters

Pd on C

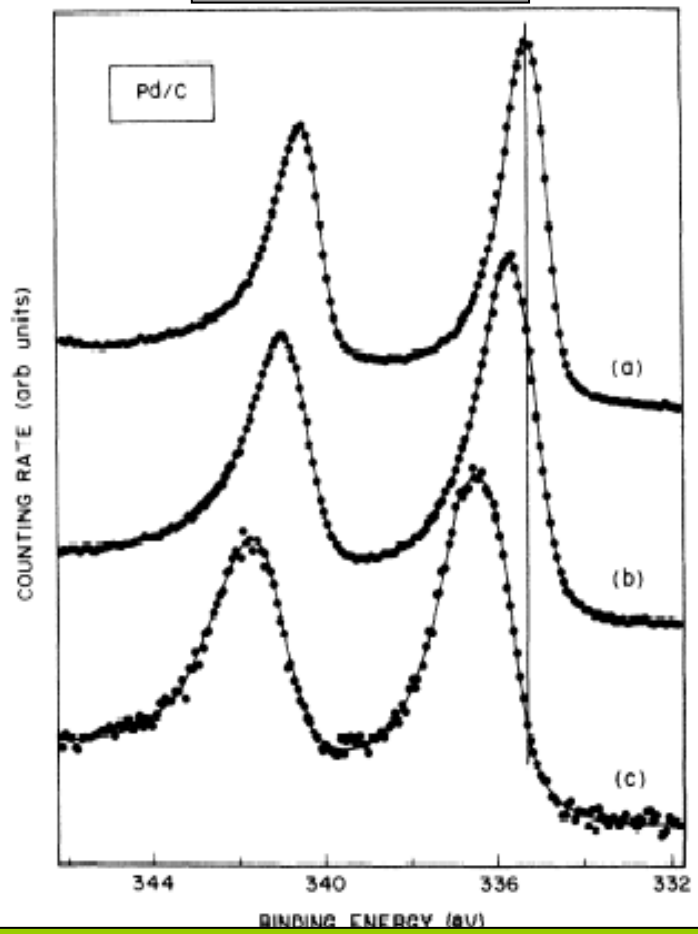

Ag on C

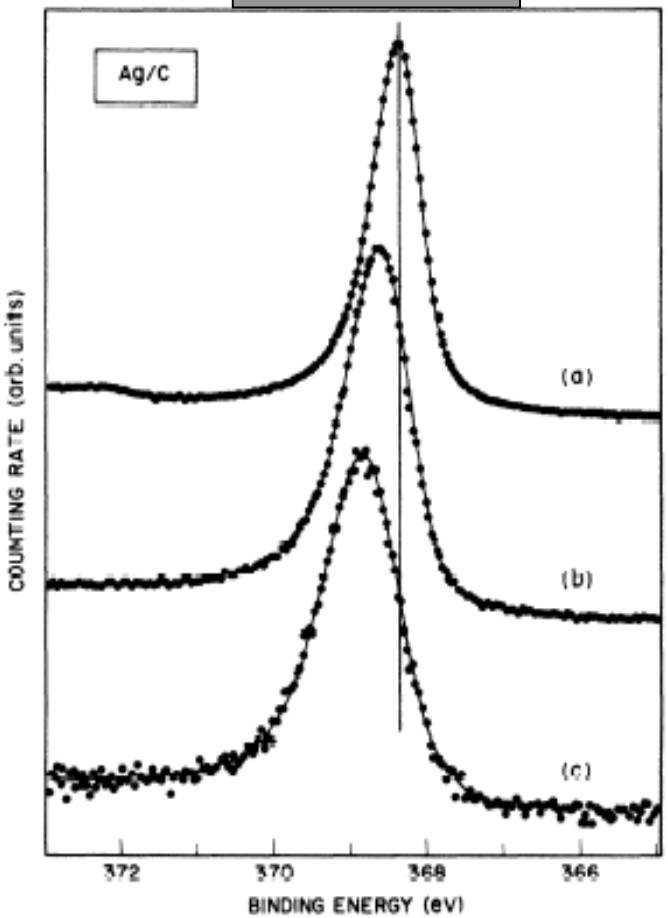

BE increases monotonically with decreasing sizes, a positive shift.

Si(001)-2x1

reconstruction of the Si(001)-2x1 Surface

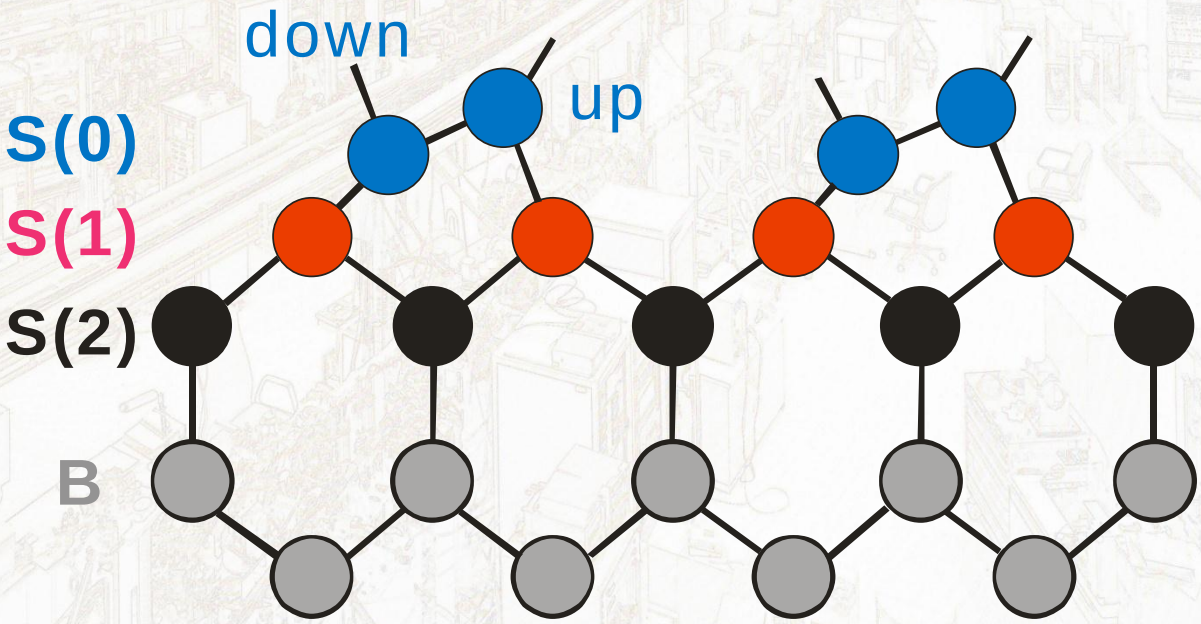

Si 2*p* cores

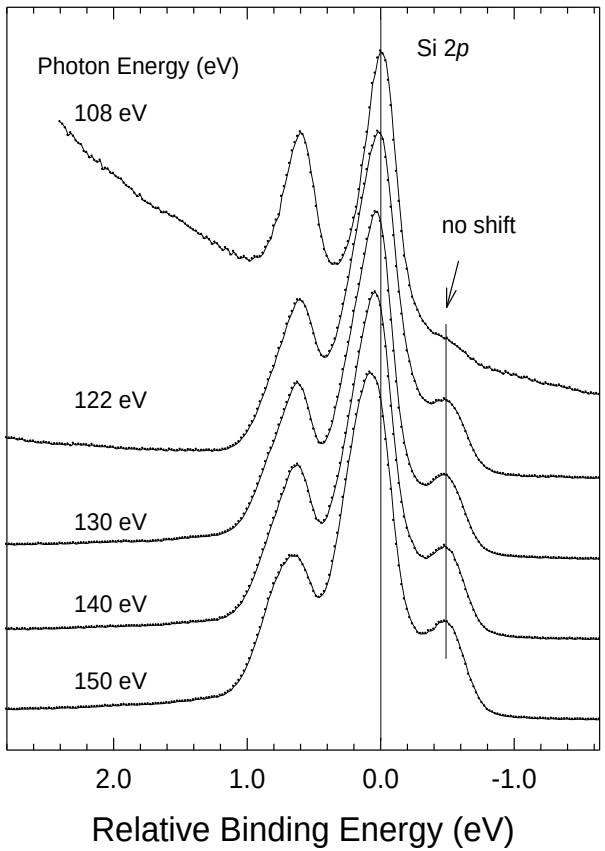
Photon Energy (eV)
Si 2p
108 eV
no shift
122 eV
130 eV
140 eV
150 eV
2.0
1.0
0.0
-1.0
Relative Binding Energy (eV)

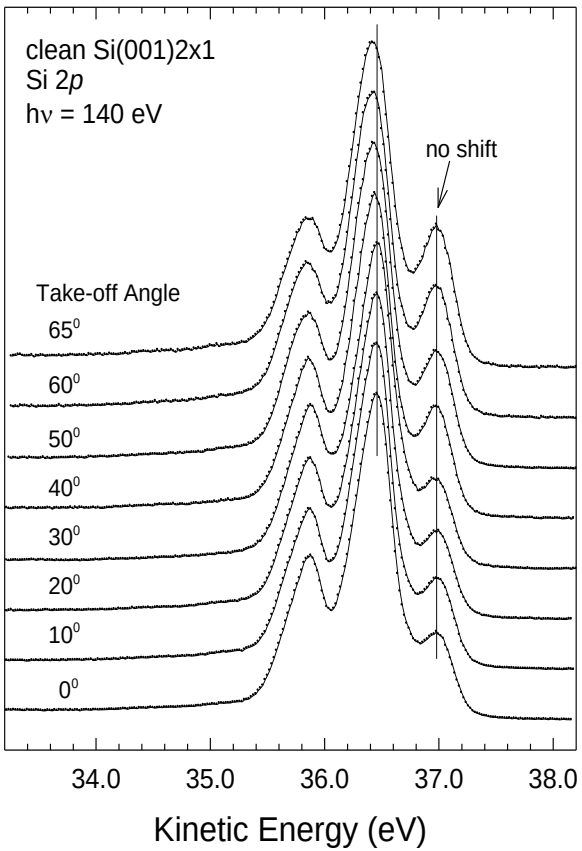
clean Si(001)2x1
Si 2p
hν = 140 eV
no shift
Take-off Angle
65⁰
60⁰
50⁰
40⁰
30⁰
20⁰
10⁰
0⁰
34.0
35.0
36.0
37.0
38.0
Kinetic Energy (eV)

analysis

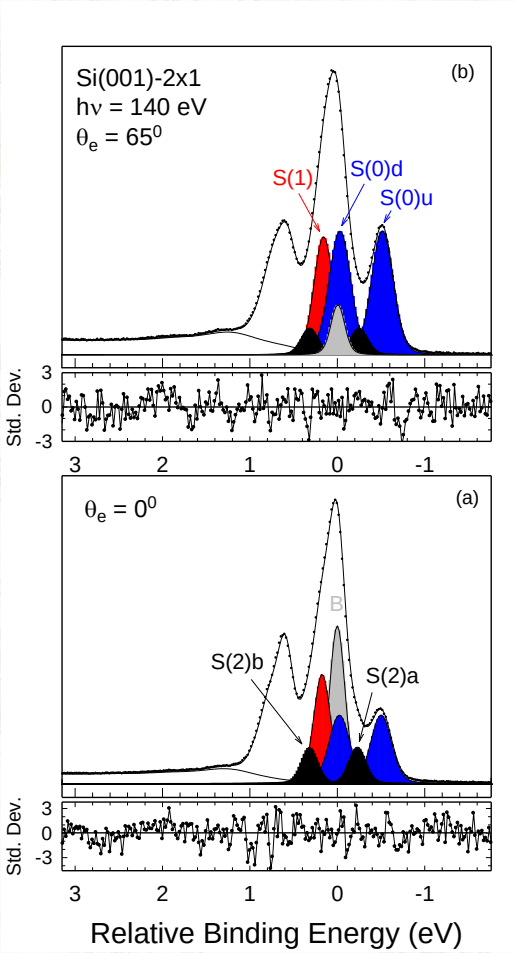

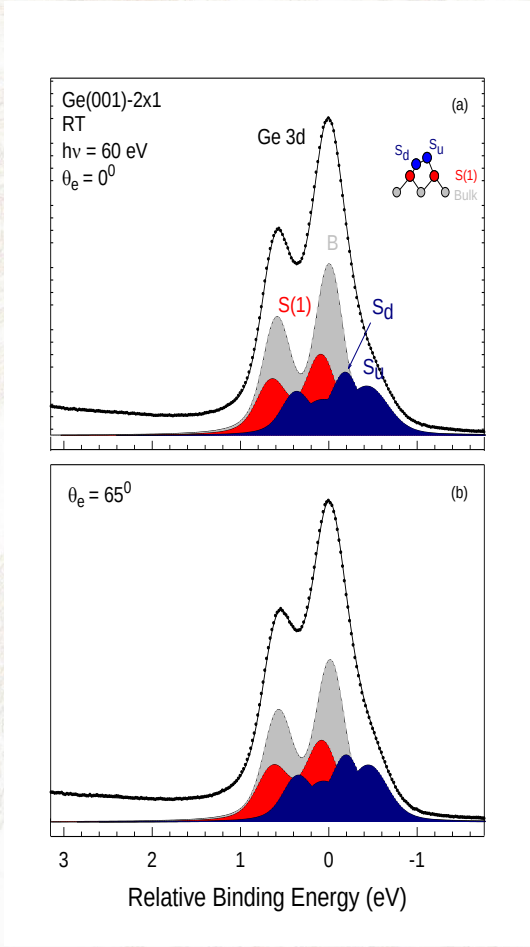

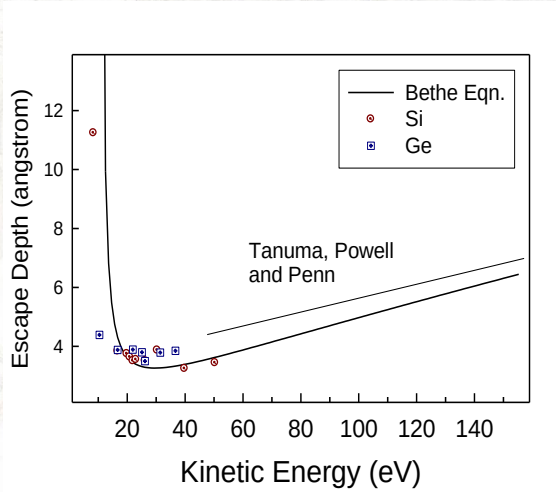

- mean-free-path constrained.
- Support the final-state description, opposite to the case of Si(111)7x7

atomic adsorption

Alkalis

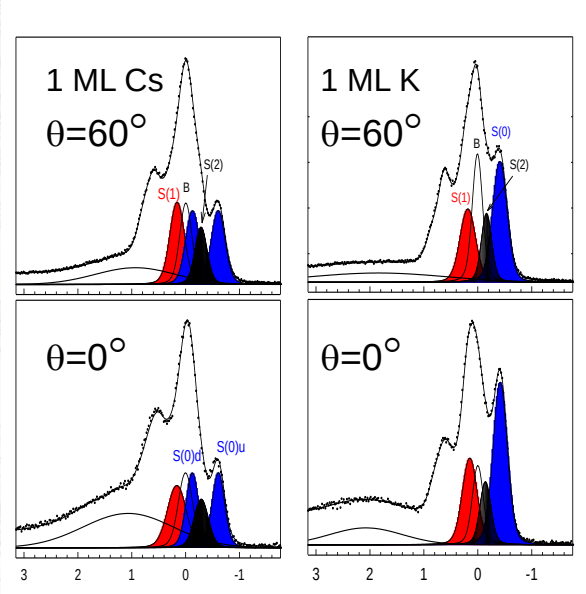

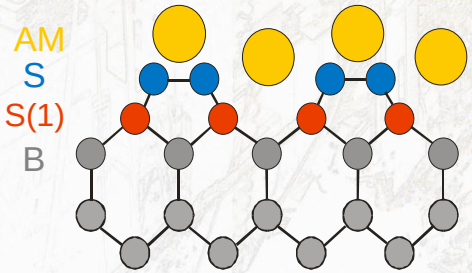

Chlorination

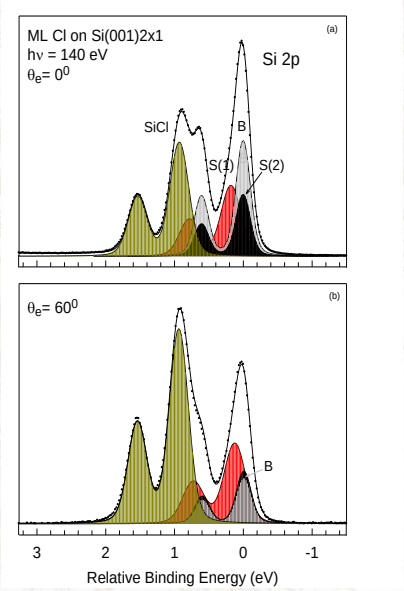

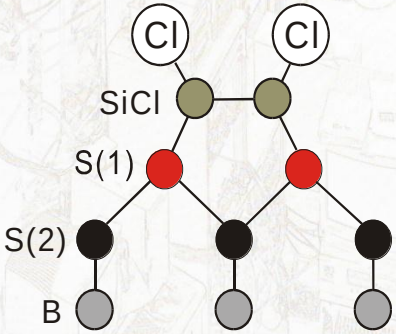

Ge on Si

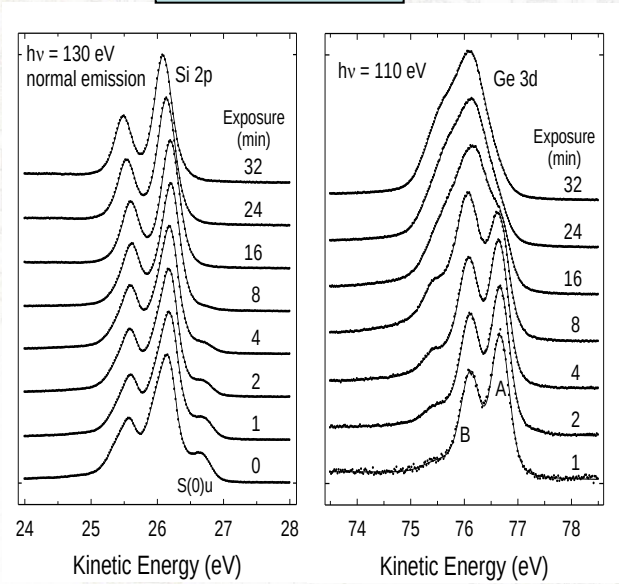

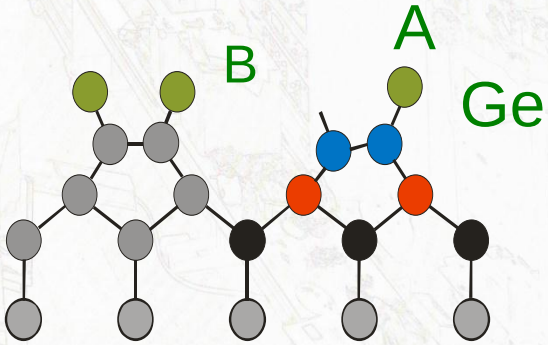

MgB_2 on Si(001)-2x1

$P = 1 \times 10^{-8}$ Torr

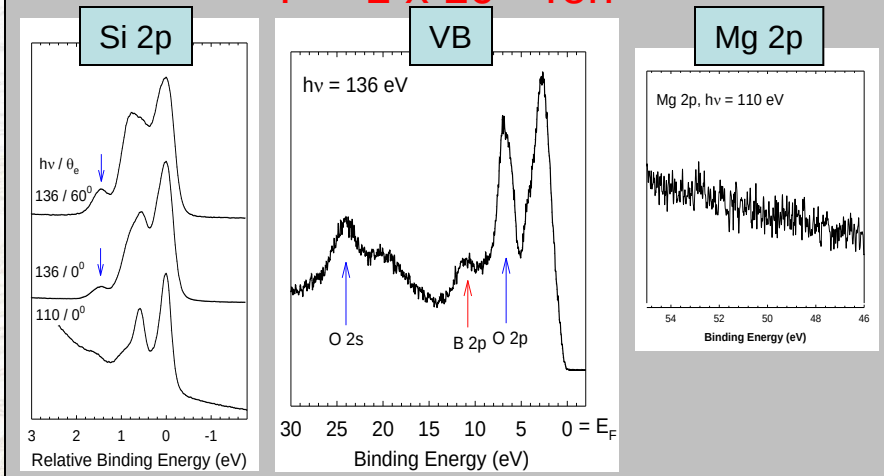

B only, no Mg, with oxygen

$P = 5 \times 10^{-10}$ Torr

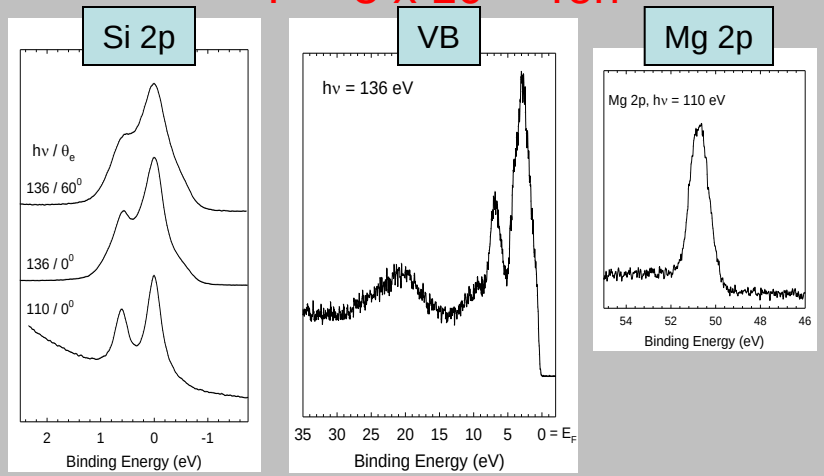

Mg only, no B

$P = 5 \times 10^{-9}$ Torr

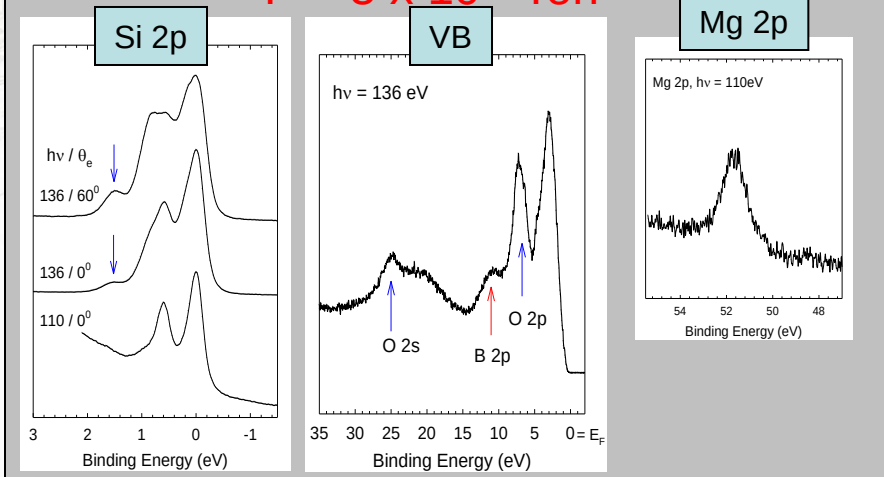

Both Mg and B signals, but with oxygen

$P = 2 \times 10^{-9}$ Torr

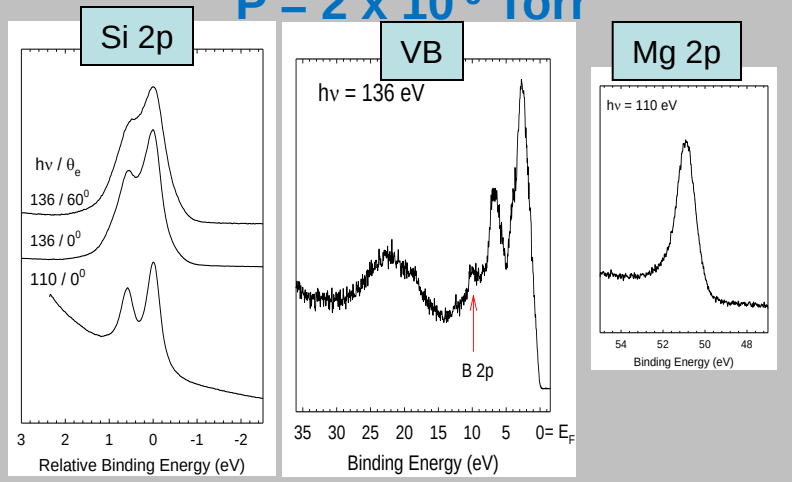

Both Mg and B signals, but without oxygen

Organic Light Emitted Diode (OLED)

Road Maze

Si(001)-2x1

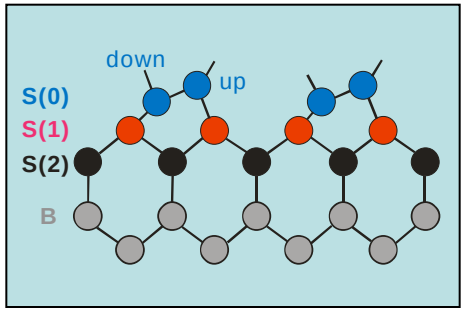

Alq_3

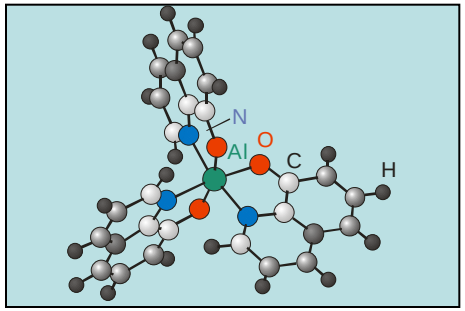

Alq_3 on Si(001)

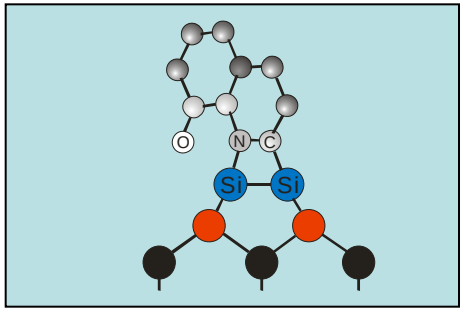

Mg on ML-Alq_3 on Si(001)

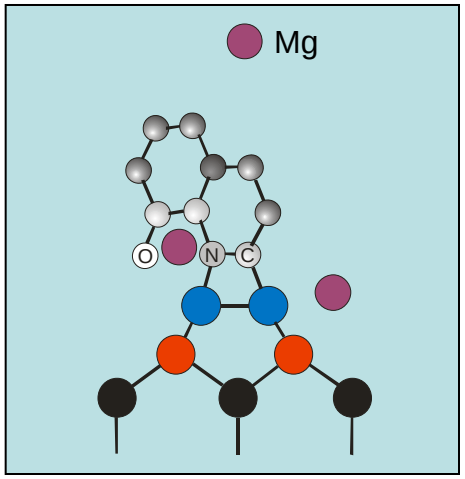

Mg (Ca) on thick Alq_3

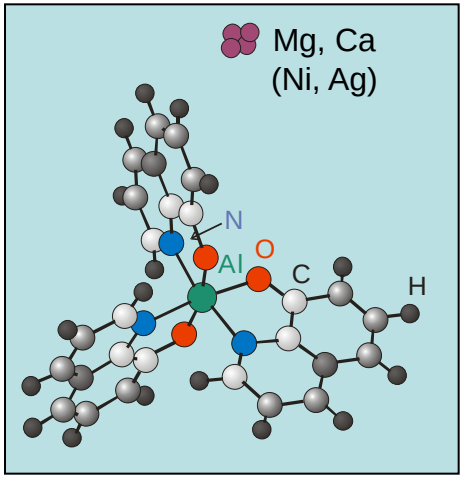

Mg on Ag-doped Alq_3

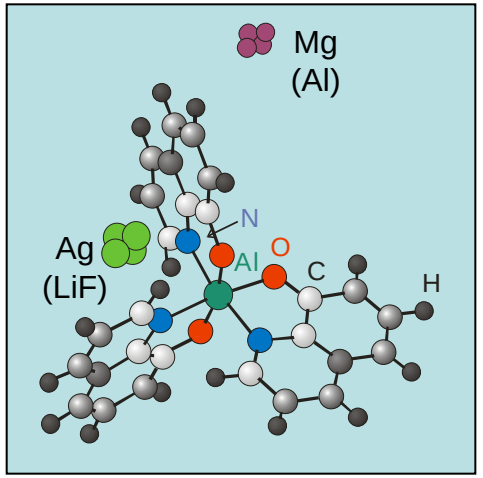

Basic Organic Light Emitting Diode

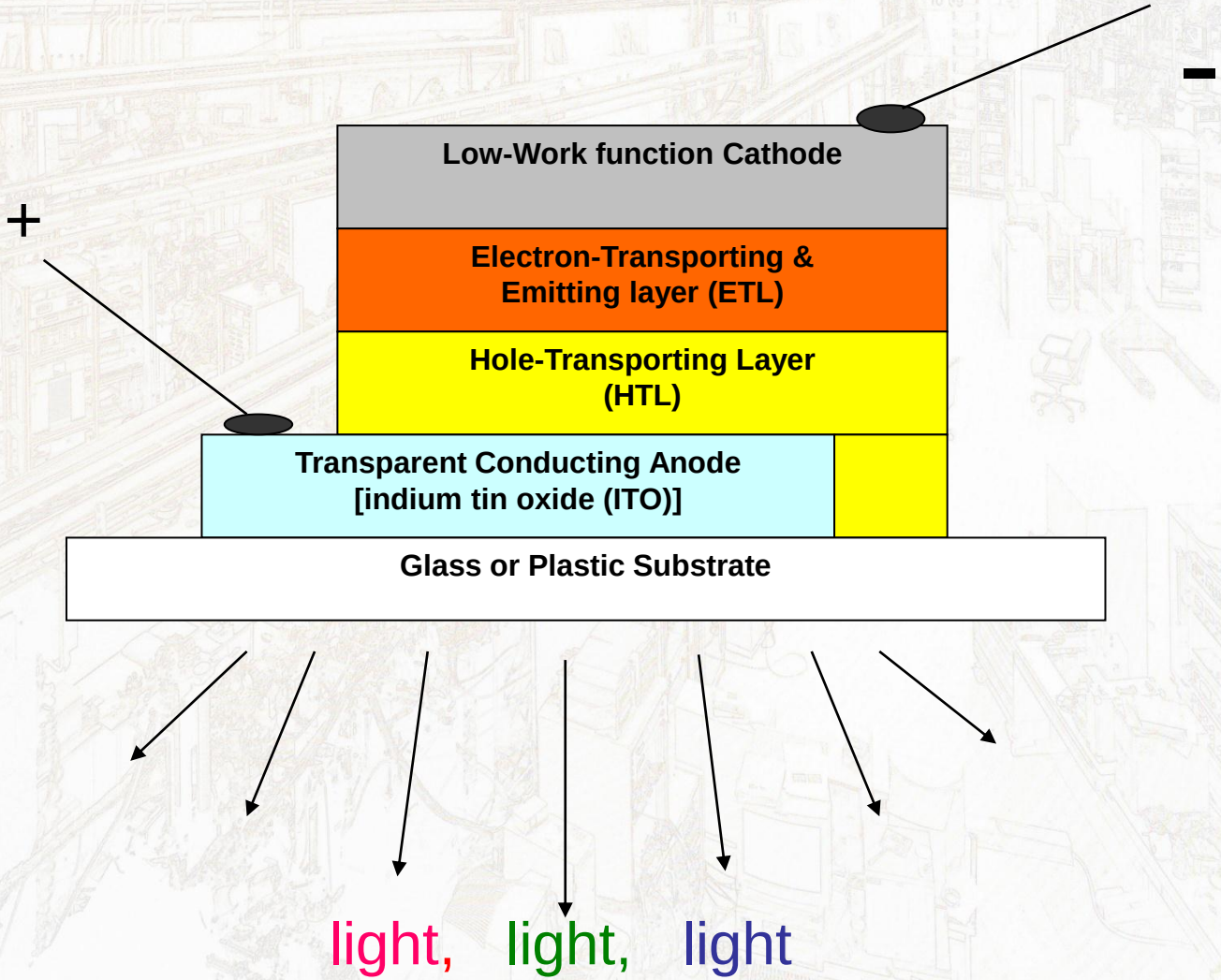

Historical tracks of photoemission study on OLED

- The pioneered work (1987):
  C. W. Tang and S. A. VanSlyke, APL **51**, 913 (1987).
- Energy alignments (1997):
  H. Ishii and K. Seki, IEEE Trans. El. Devices **44**, 1295 (1997).
- Theoretical works (1998):
  A. Curioni *et al.* APL **72**, 1575 (1998) [DFT cal.];
  K. Sugiyama *et al*. JAP **83**, 4928 (1998) [PM3 MO cal.]
- Mg on Alq_3 (2001, in-house line sources):
  C. Shen, A. Kahn, and J. Schwartz, JAP **89**, 449 (2001);
  M. G. Mason *et al*. JAP **89**, 2756 (2001).
- First SR work (2001, K on Alq_3):
  T. Schwieger *et al*. PRB **63**, 165104 (2001).

Tris(8-hydroxyquinolato) aluminum (Alq_3)

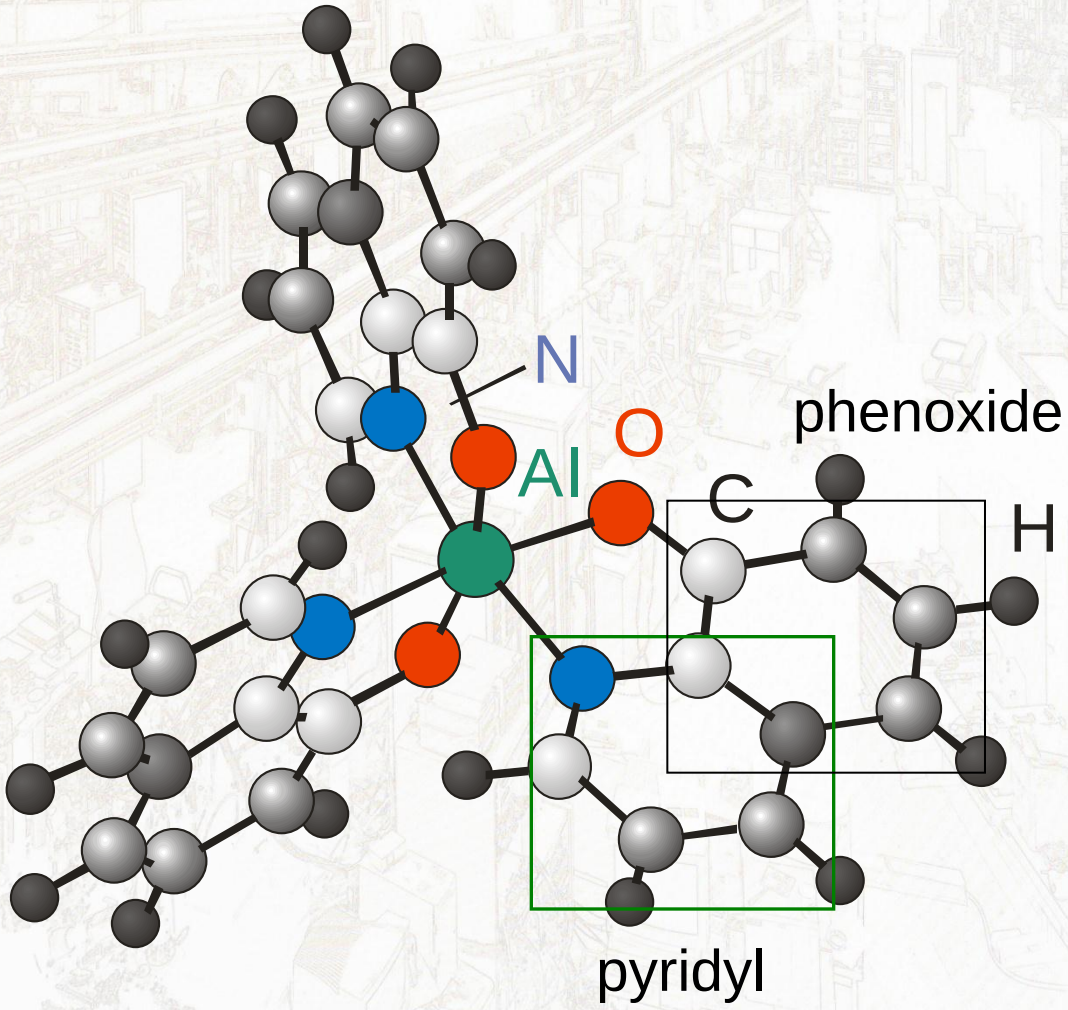

Electronic structure of Alq_3, exp

valence band spectra

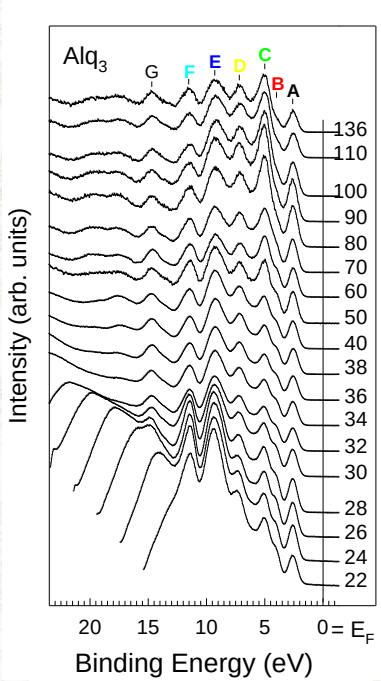

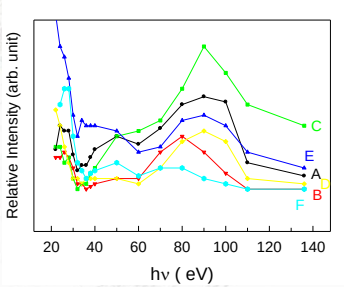

The cross section effect

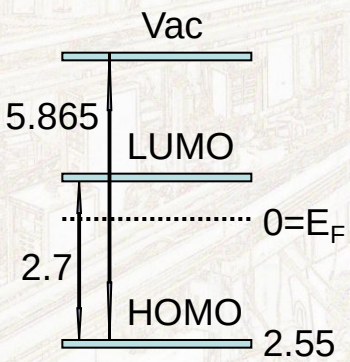

HOMO:
Highest **O**ccupied **M**olecular **O**rbital

LUMO:
Lowest **U**noccupied **M**olecular **O**rbital

core level spectra

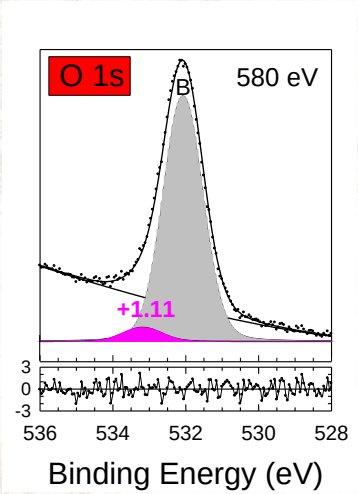

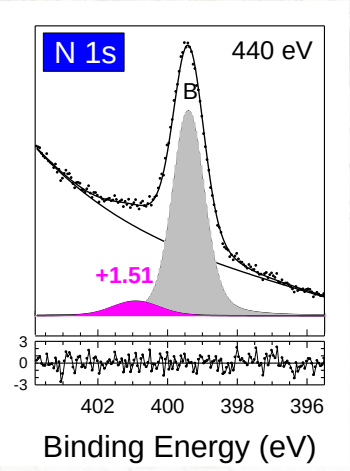

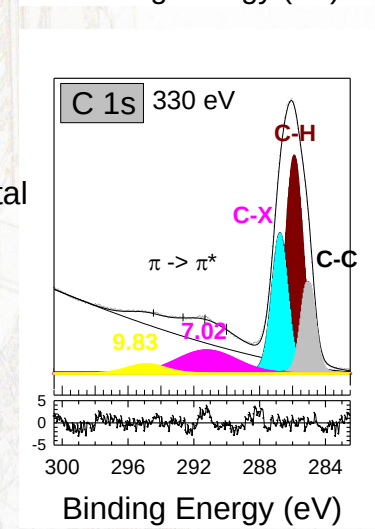

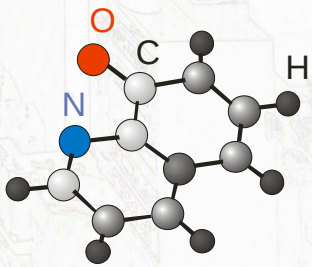

C-C: 285.05 eV (1)
C-H: 285.90 eV (5)
C-X: 286.77 eV (3)

Electronic structure of Alq_3, thy

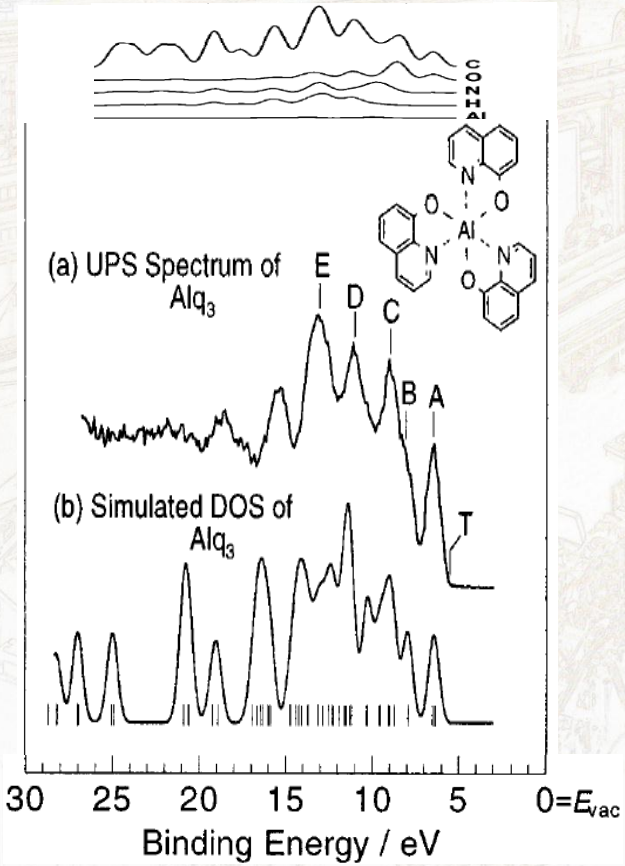

Curioni *et al*. APL **72**, 1575 (98)
Sugiyama *et al*. JAP **83**, 4928 (98)

- The low BE peaks correspond to 2p σ and π orbitials of 8-quinolinol, with no Al^{3+} cation contribution.

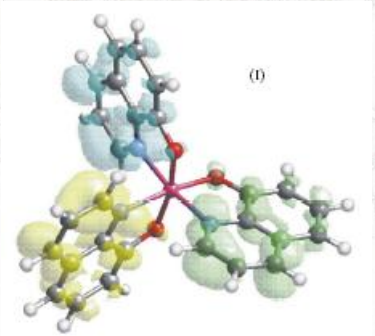

Isodensity surface of LUMO

- The HOMO is localized at the phenoxide side, while the LUMO at the pyridyl ring.

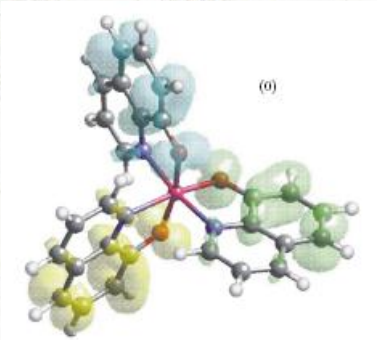

Isodensity surface of HOMO

Organic on Inorganic Surface:

Alq_3 on Si(001)-2x1

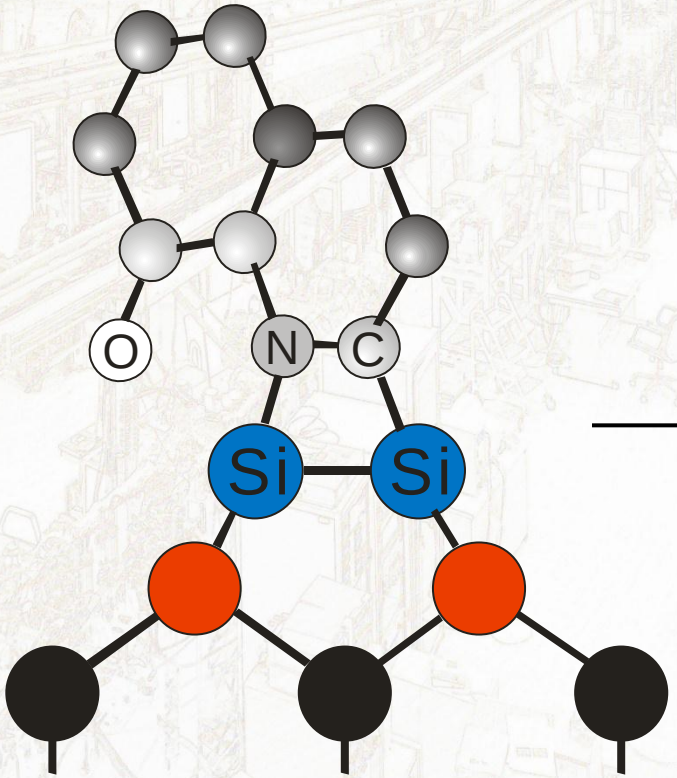

Alq_3 on Si(001)-2x1, VB

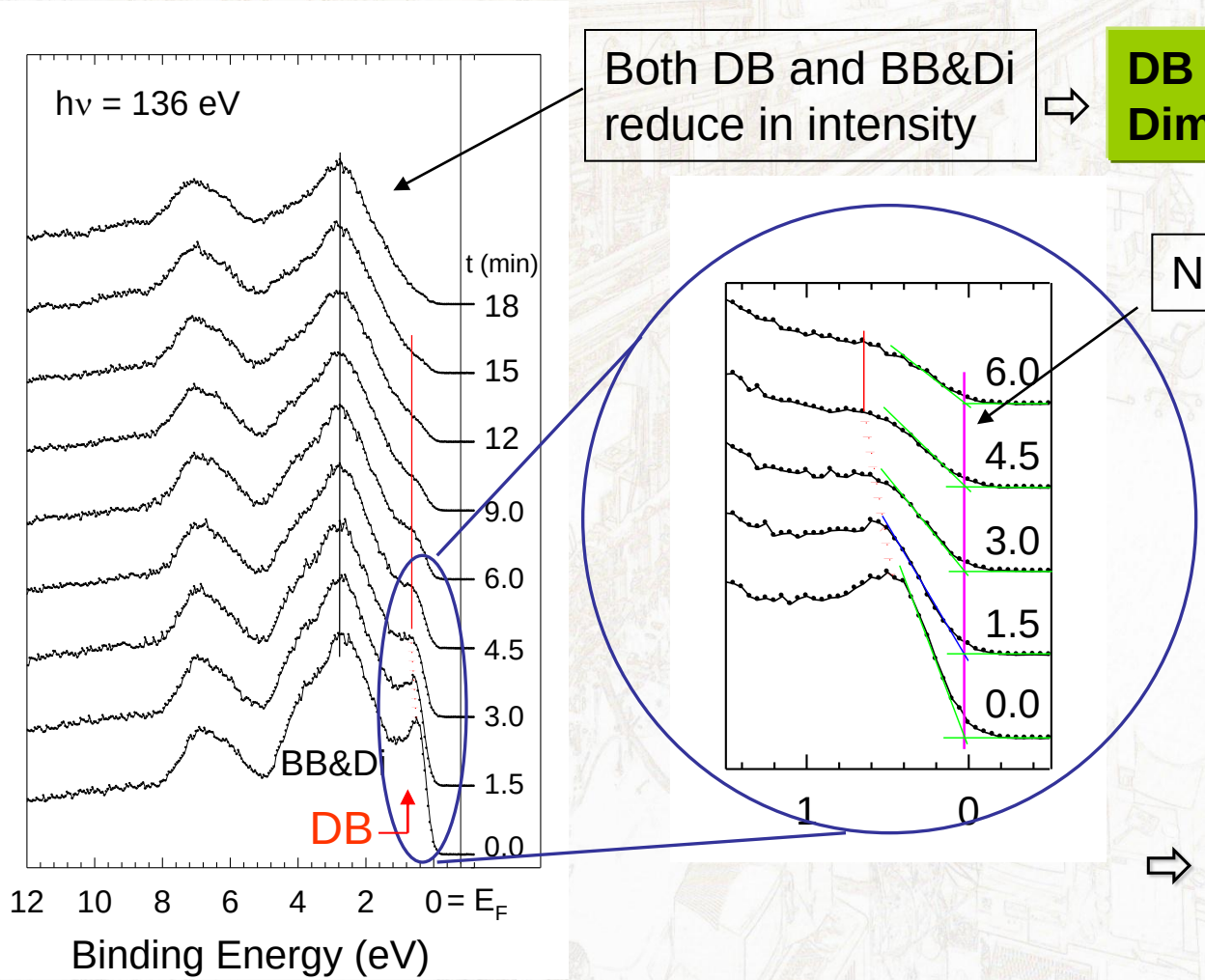

Both DB and BB&Di reduce in intensity ⇨ **DB passivated Dimers broken**

No shift at the intersect

The DB state shifts *monotonically* towards high Eb, while the energy of the BB&Di states remains fixed.

⇨ **No band bending shift**

change of the work function

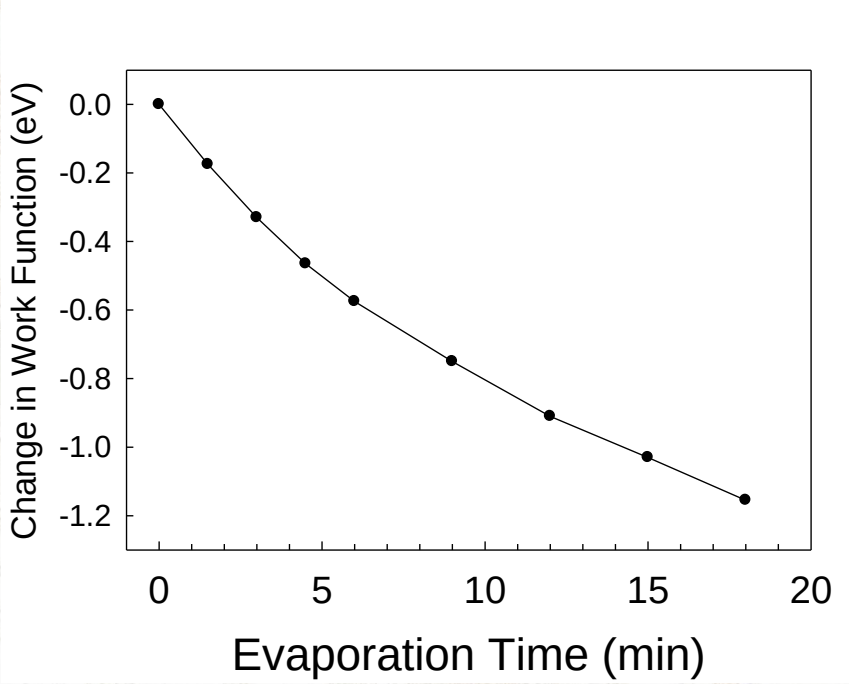

- A –1.31 eV moderate drop, leading to the WF of the Alq_3/Si system 3.29 eV.
- Conventionally, the negative drop indicates that the overlayer donates charge to the supported substrate, as in the case of the alkalis and alkalines adsorption.
- But,… (see the next slide.)

The interfaced cores

the silicon substrate

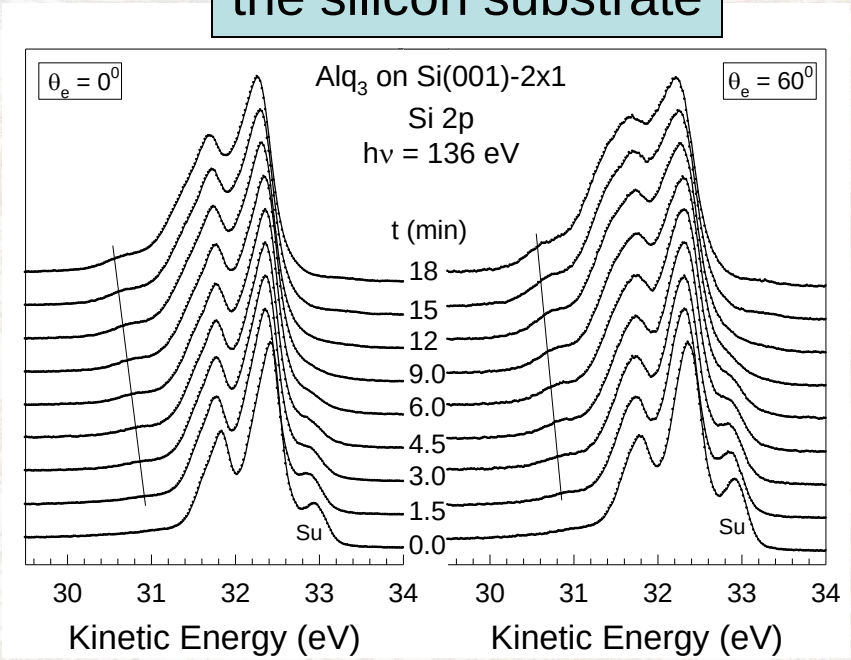

see high Eb component

the Alq adsorbate

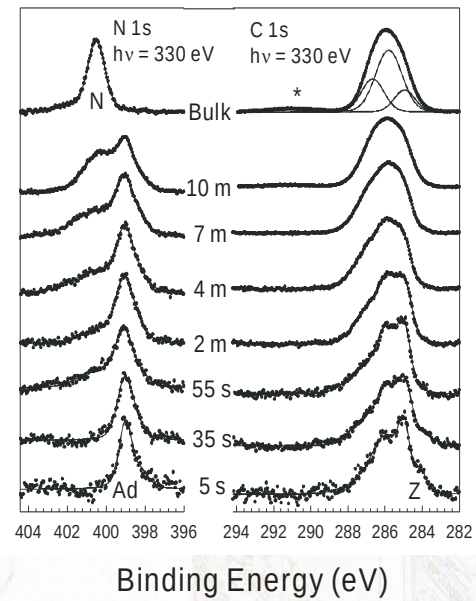

see low Eb components

⇨ Si dimers loss charge to Alq_3 molecules

WHAT HAPPENED: A polarization of surface charge is established between the pyridyl ring of Alq_3 and the dangling bond of the Si(001) surface via an overlapped wave function.

Mg on ML Alq_3 on Si(001)-2x1

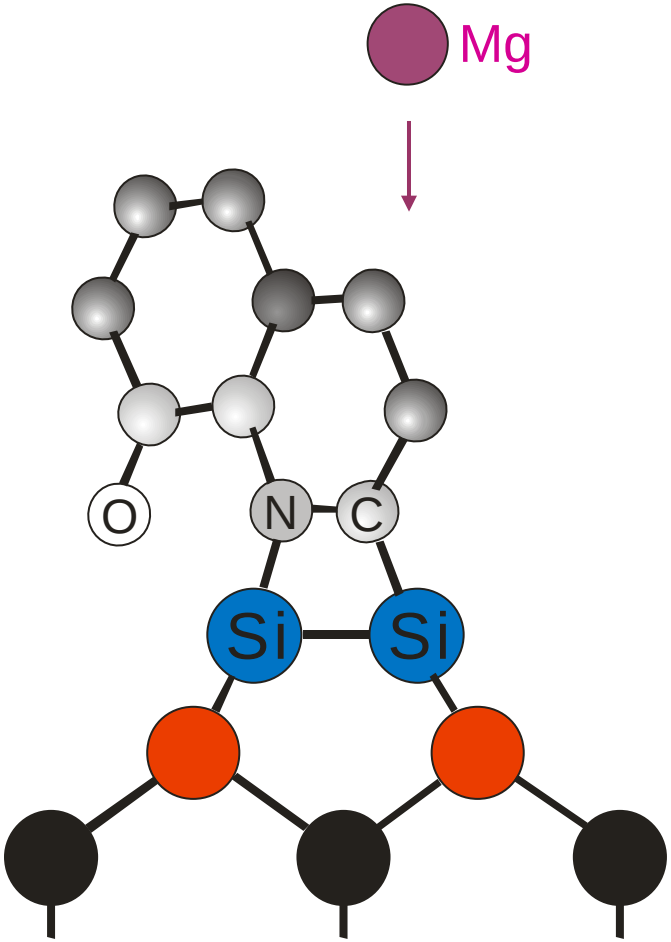

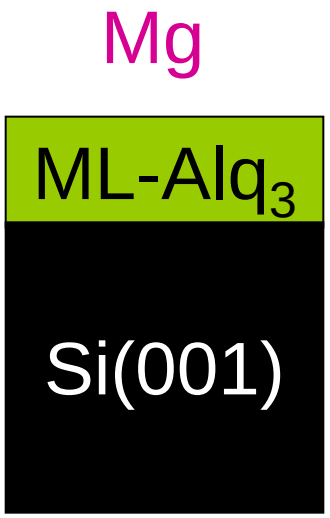

surface reaction (Mg on ML-Alq_3)

PRB**70**, 235346 (05)

response of the Si sub.

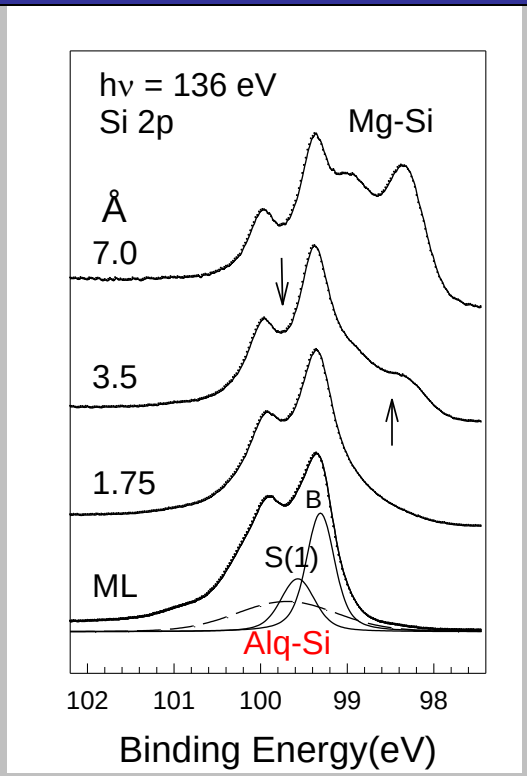

response of the Alq ads.

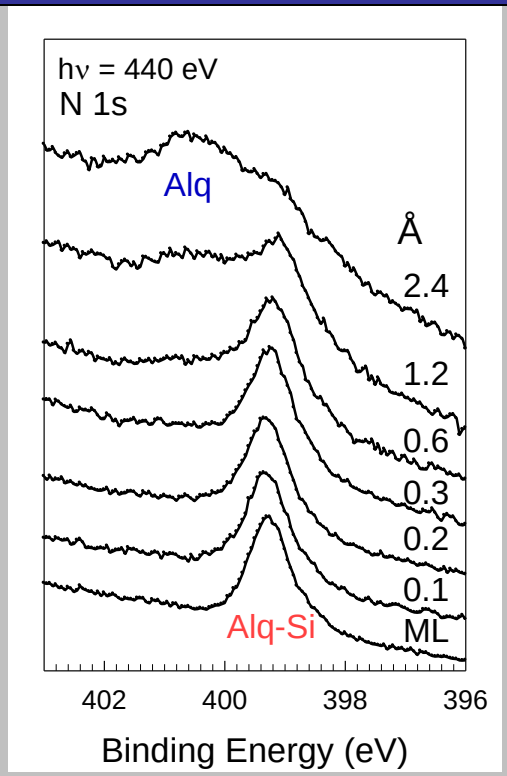

valence band spectra

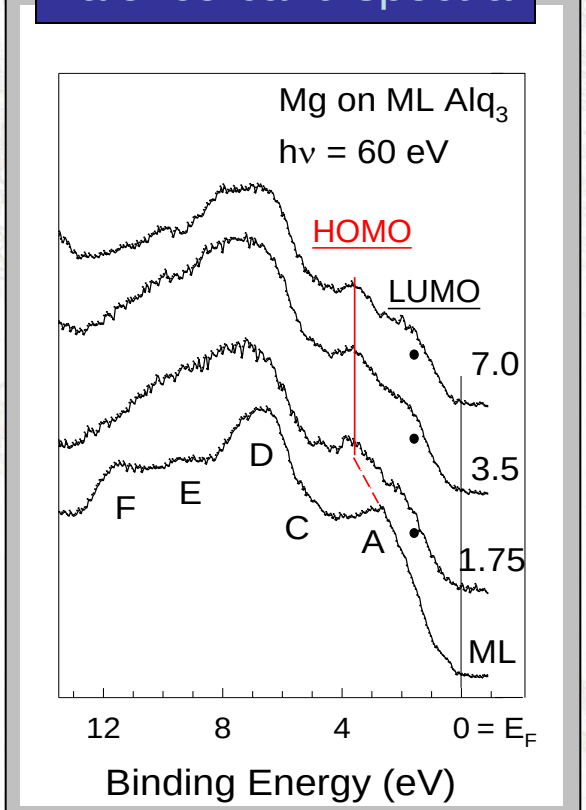

Mg in-diffusion

molecules deterioration

WHAT HAPPENED:

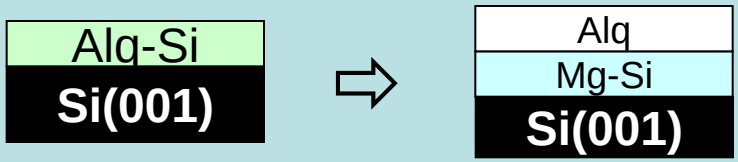

transferred N 1s cores

Alq_3 on Si

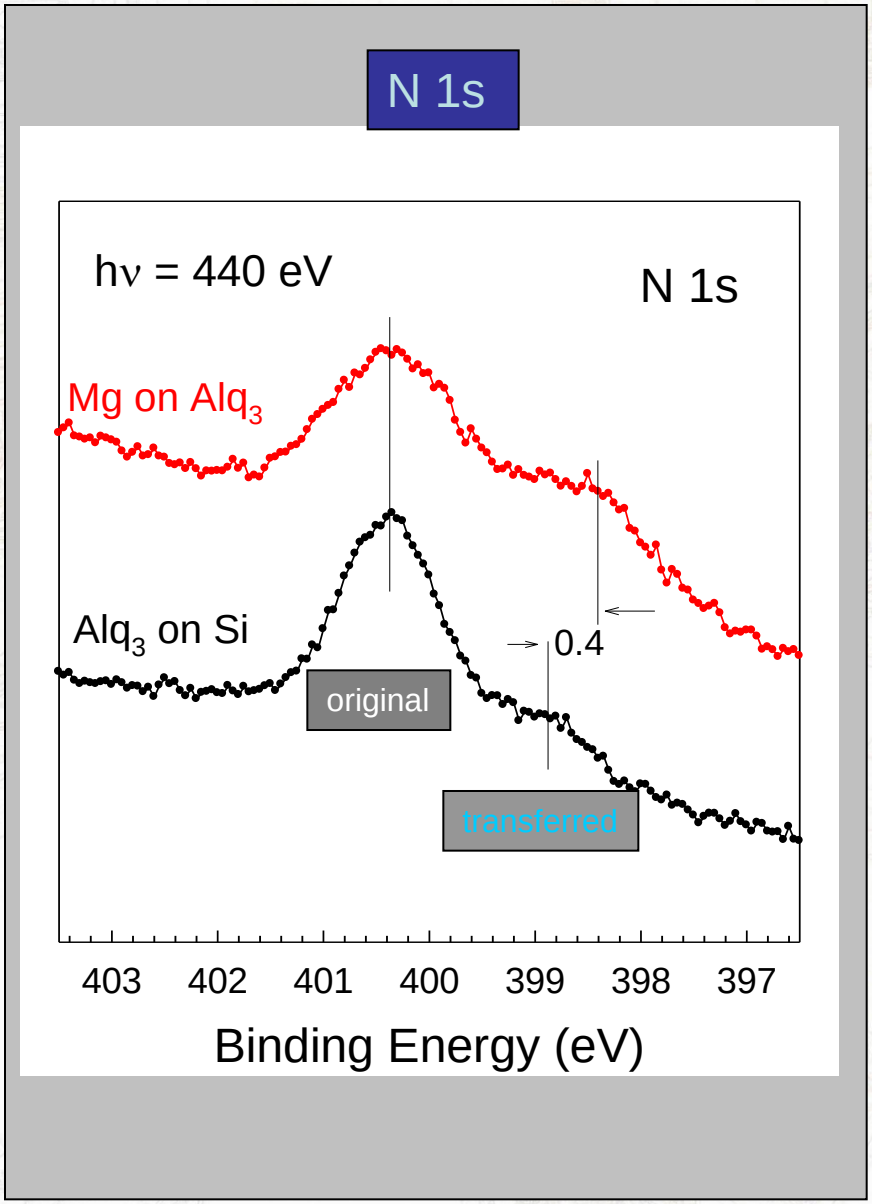

Silicon transfers less charge to Alq_3 than Mg.

Mg on Alq_3

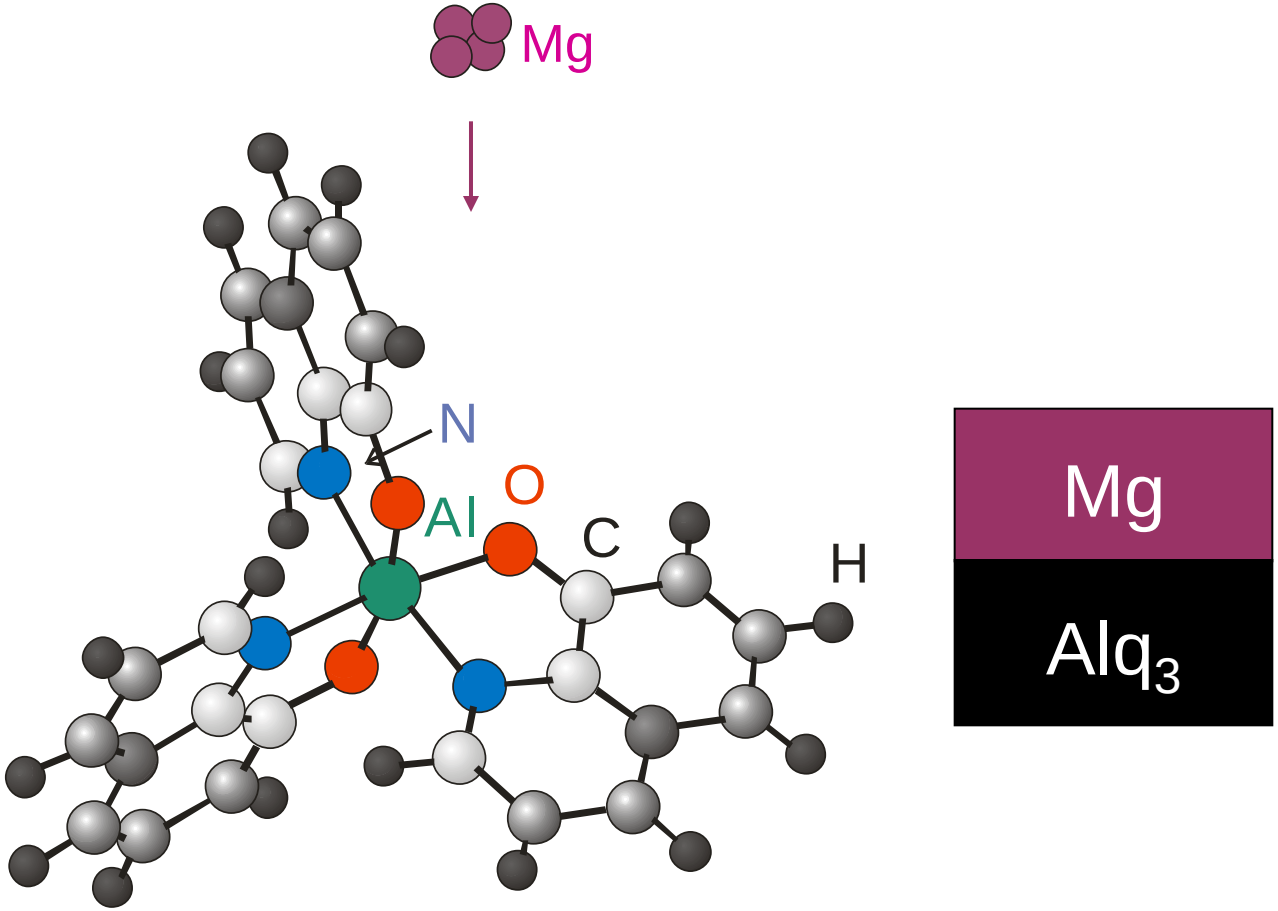

valence band spectra

Mg on Alq_3

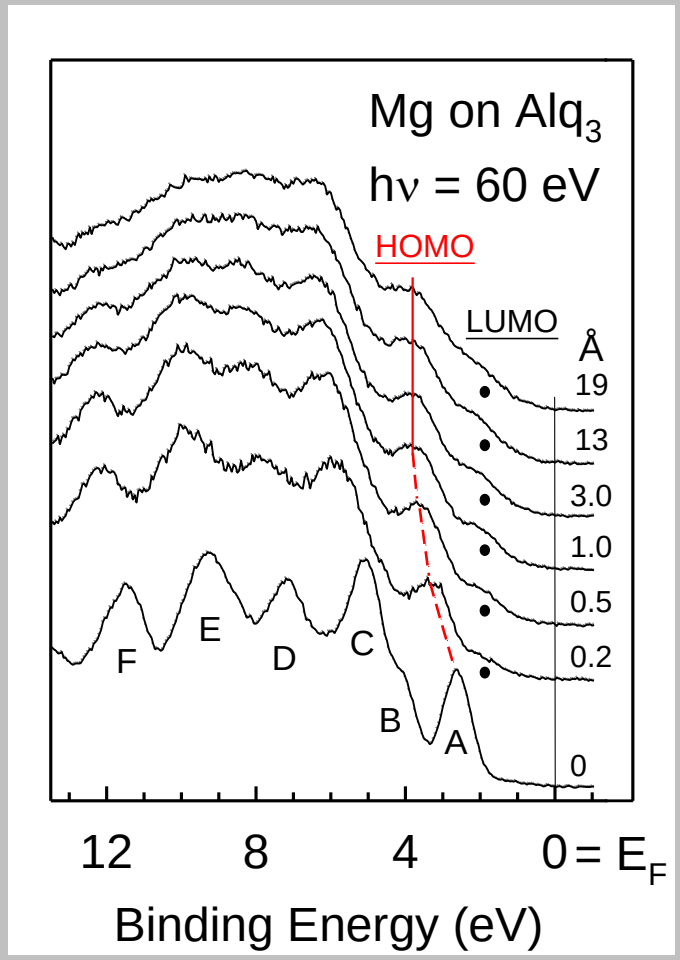

- The HOMO shifts towards high Eb monotonically, and stops at 3.9 eV, while the LUMO remains fixed at 1.8 eV.
- (HOMO-LUMO) < 2.7 eV
- Organomagnesium species dominate the spectra.

➔ Valence band spectra are the same for the surface and the bulk samples.

core-level spectra

Mg on Alq_3

O 1s | N 1s | C 1s

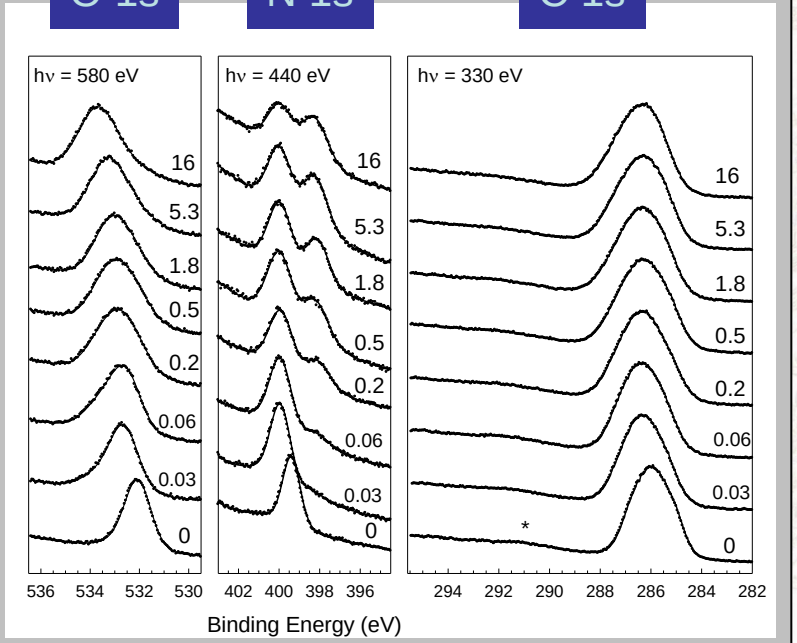

- The C atoms remain unaffected.
- The transferred components in both N and O 1s cores are Mg-dependent.
- The transferred O 1s component appears at +1.09 eV.

a fit

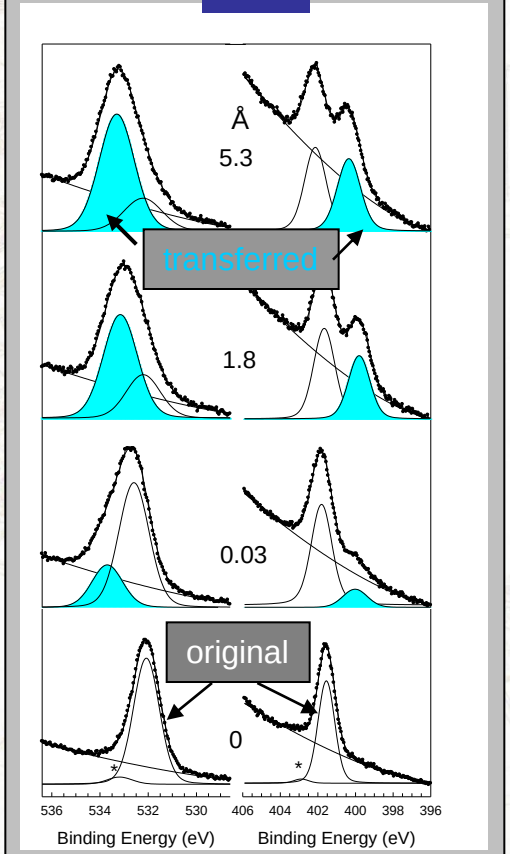

the N 1s cores

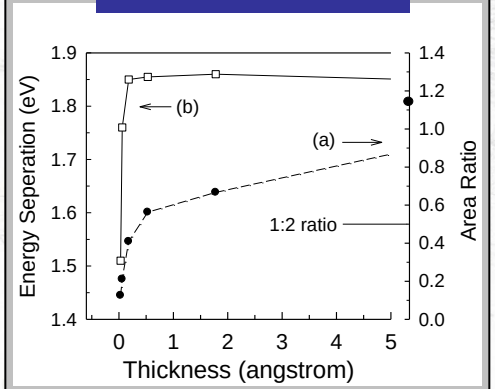

Mg 2p core-level spectra

Mg on Alq_3

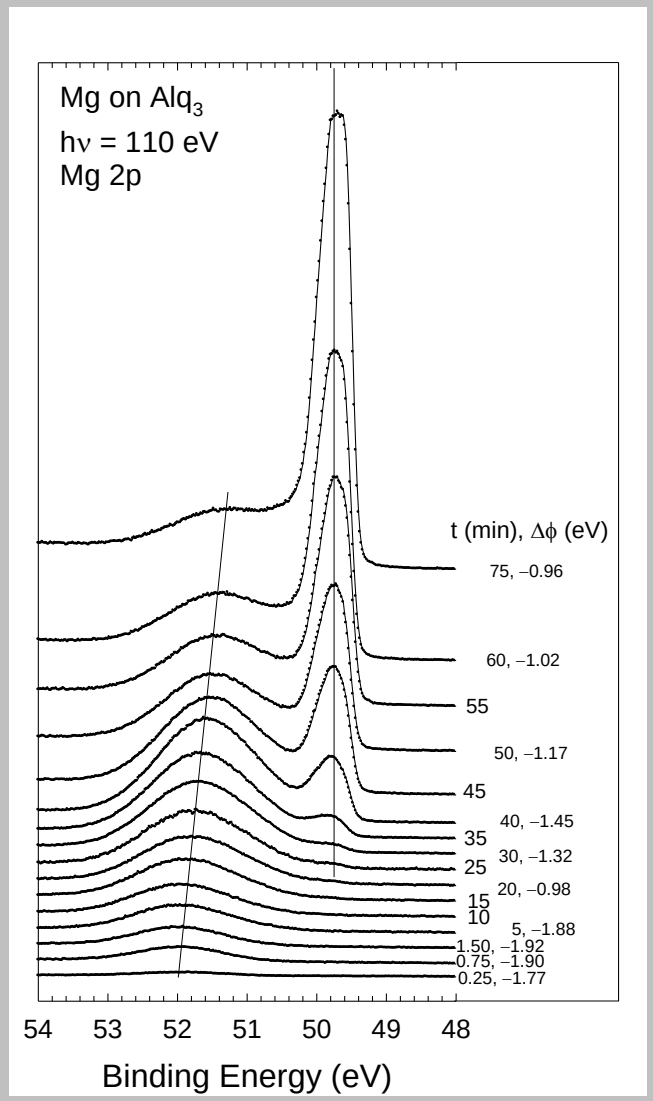

- A high Eb component shifts towards lower binding energy with increasing Mg exposure.
- A metallic component appears after a given Mg thickness.

The proposed model

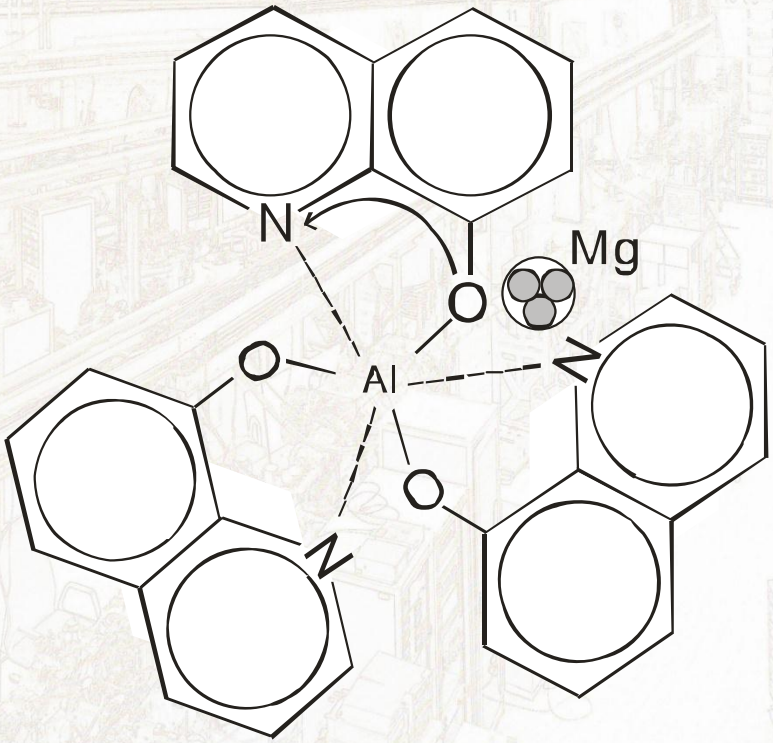

Mg clustering in as well as on top of Alq_3 & charge flowing from O to N

Nano-Mg on Alq_3?

different Alq_3 thickness

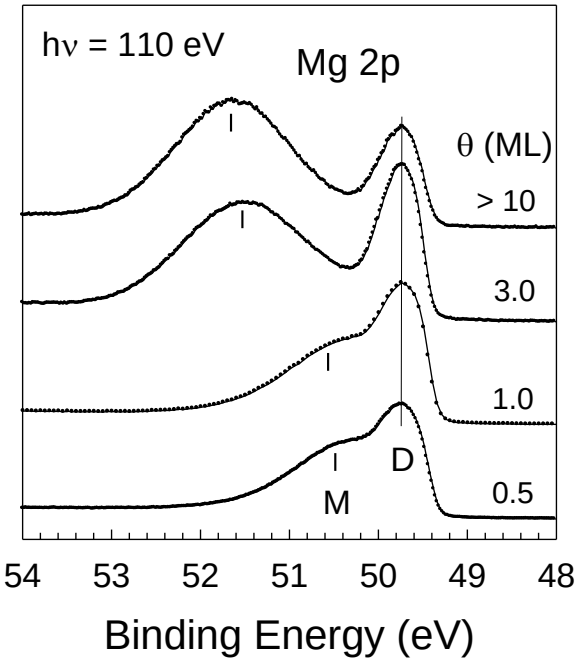

different Mg thickness

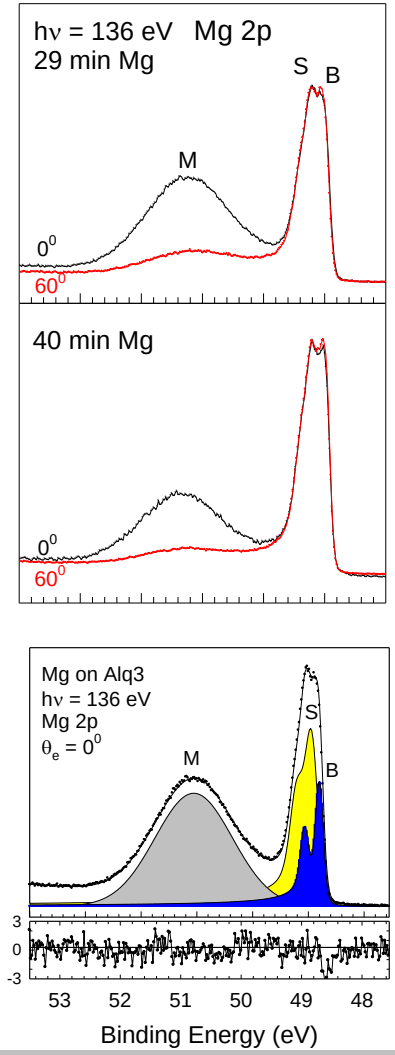

It's possible due to

- Metallic Mg shows up at sub-ML coverage.
- Metallic Mg shows crystallization.
- Metallic Mg is angle-independent.

metallic Mg 2p

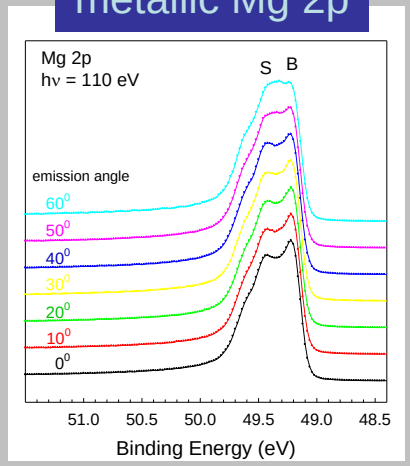

summary of Mg on Alq_3

- Mg actually forms clusters in and on top of Alq_3.
- With the presence of Mg, Alq_3 not only accepts charge from the dopant, but also renders a charge redistribution of the molecule itself.

Ca on Alq_3

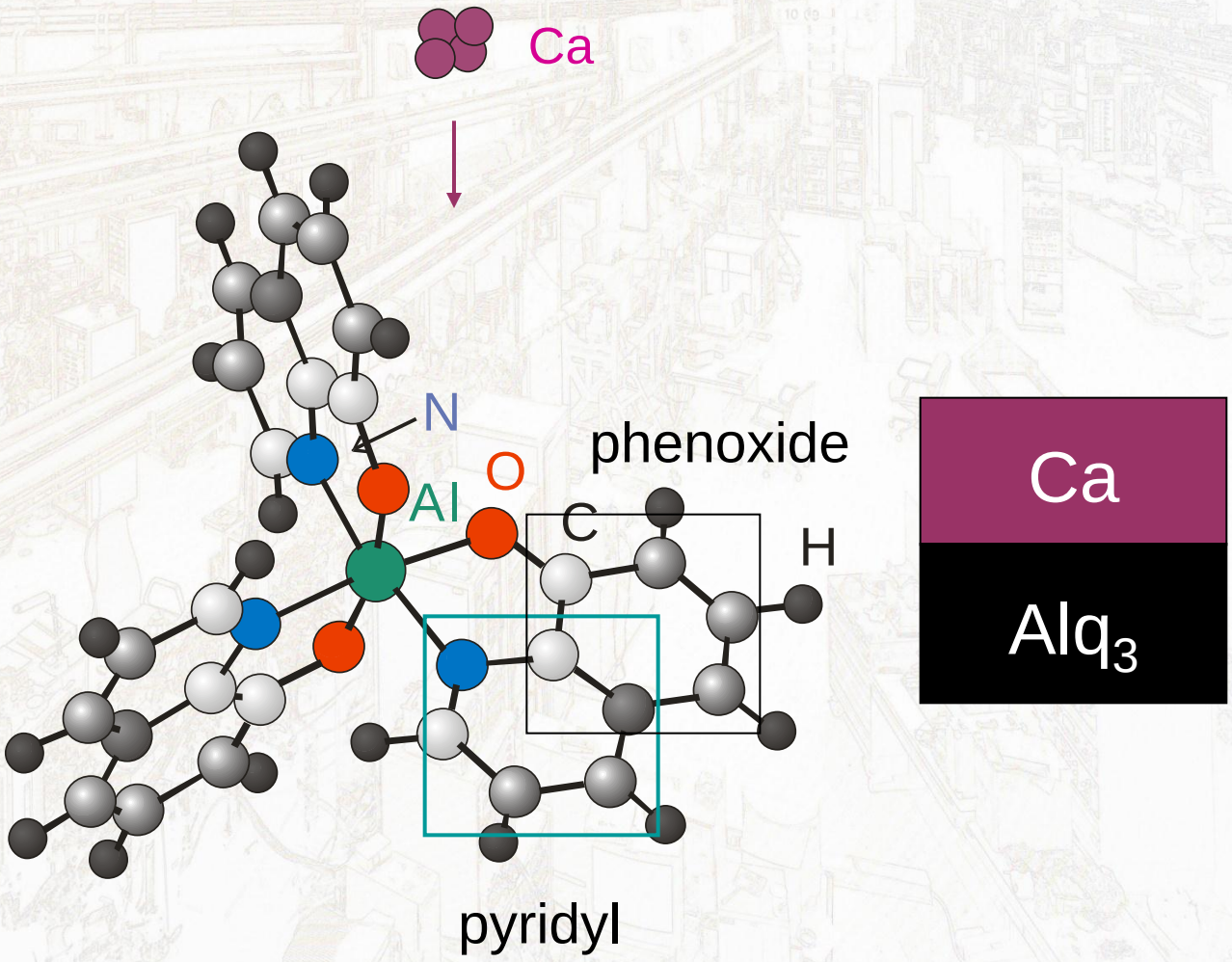

valence band spectra

Mg on Alq_3

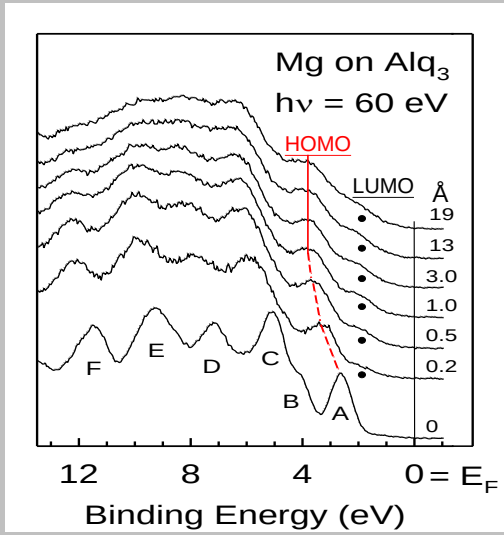

PRB **70**, 235346 (2004)

Ca on Alq_3

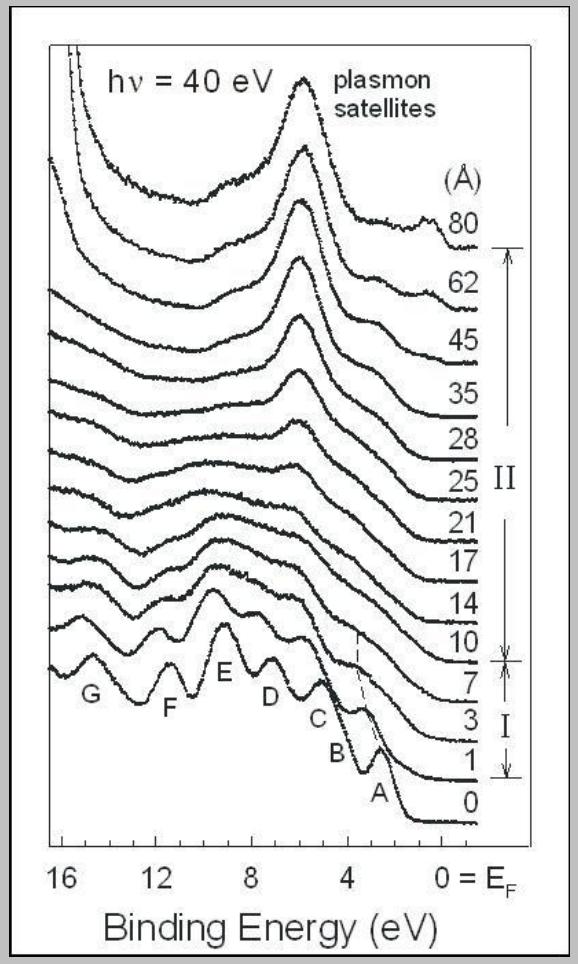

JAP **99**, 123708 (2006)

- The HOMO shifts towards high Eb monotonically, and stops at 3.9 eV, while the LUMO remains fixed at 1.8 eV.
- (HOMO-LUMO) < 2.7 eV
- Organometallic species dominate the spectra.
- Not much differences between Mg/Alq_3 and Ca/Alq_3.

core-level spectra

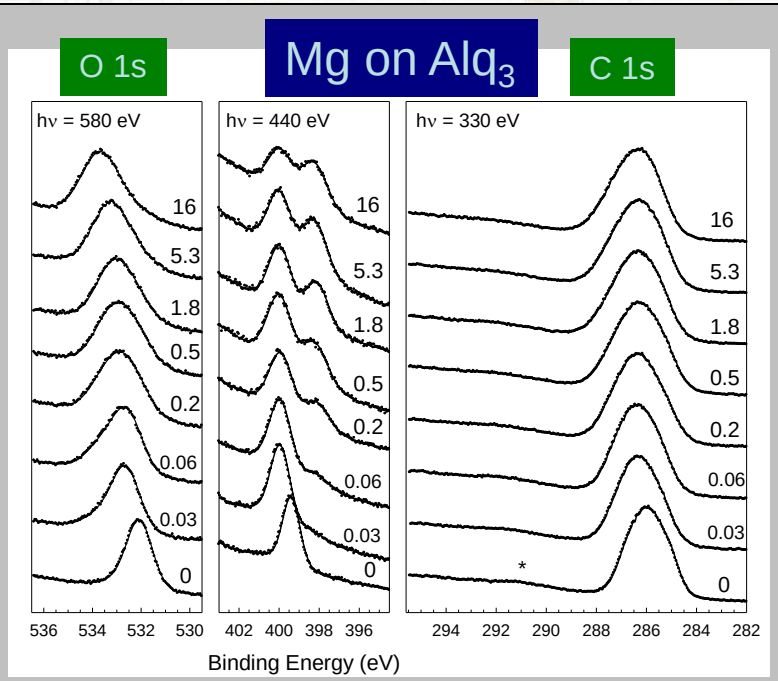

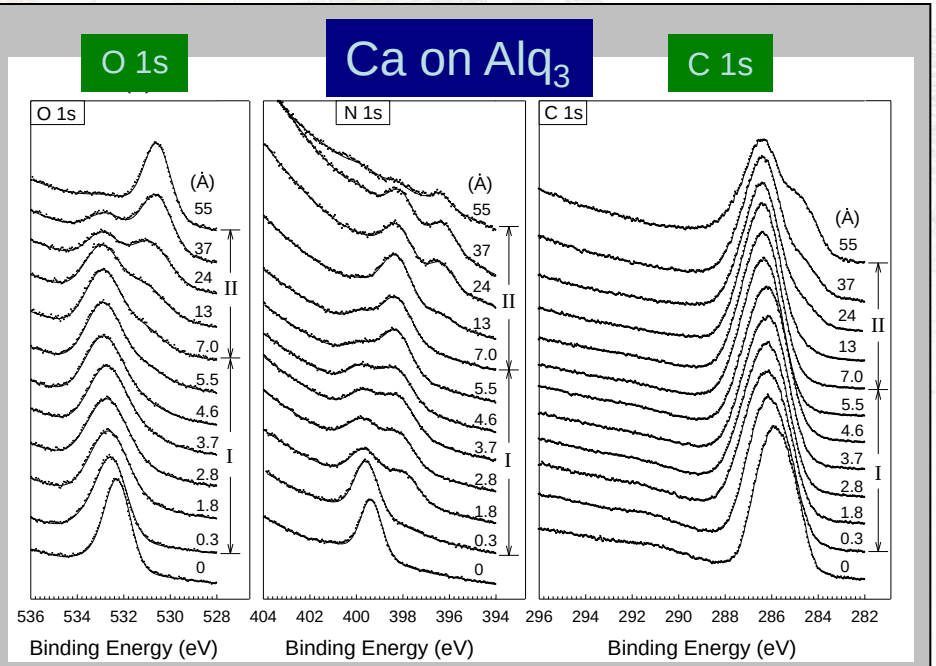

Although being as a member of the alkaline earth metals, Ca and Mg behave dissimilarly upon making contact with the Alq_3 organic layer.

For Ca on Alq_3, two phases of reaction are identified.

Ca 2p & Al 2p cores

Ca on Alq_3

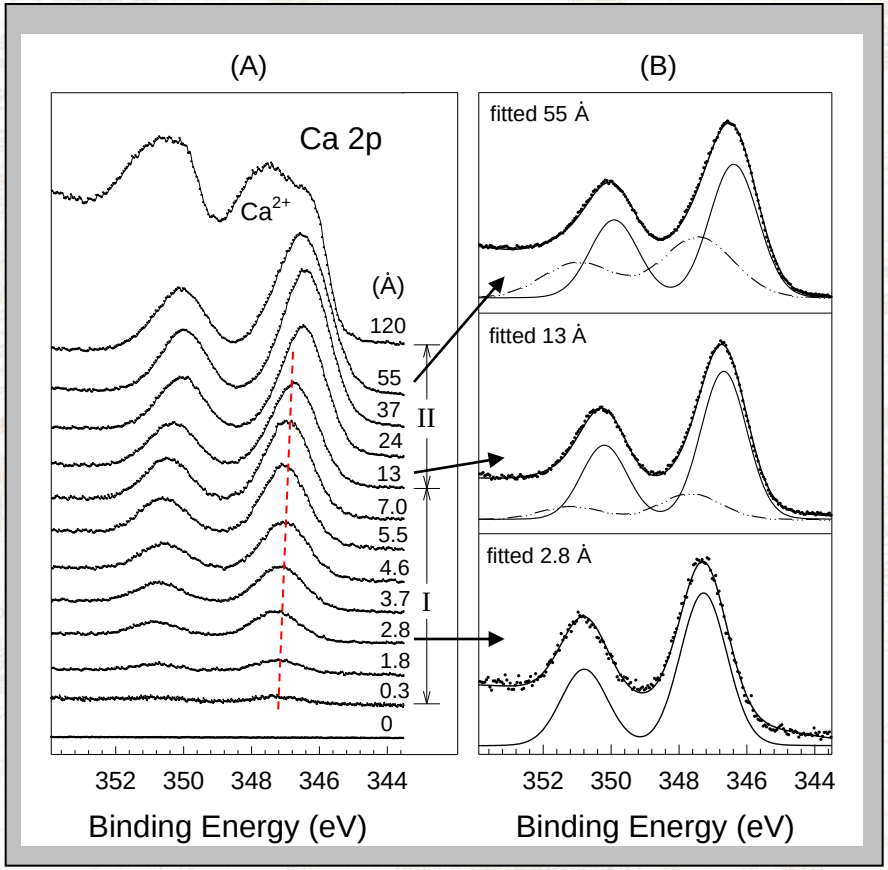

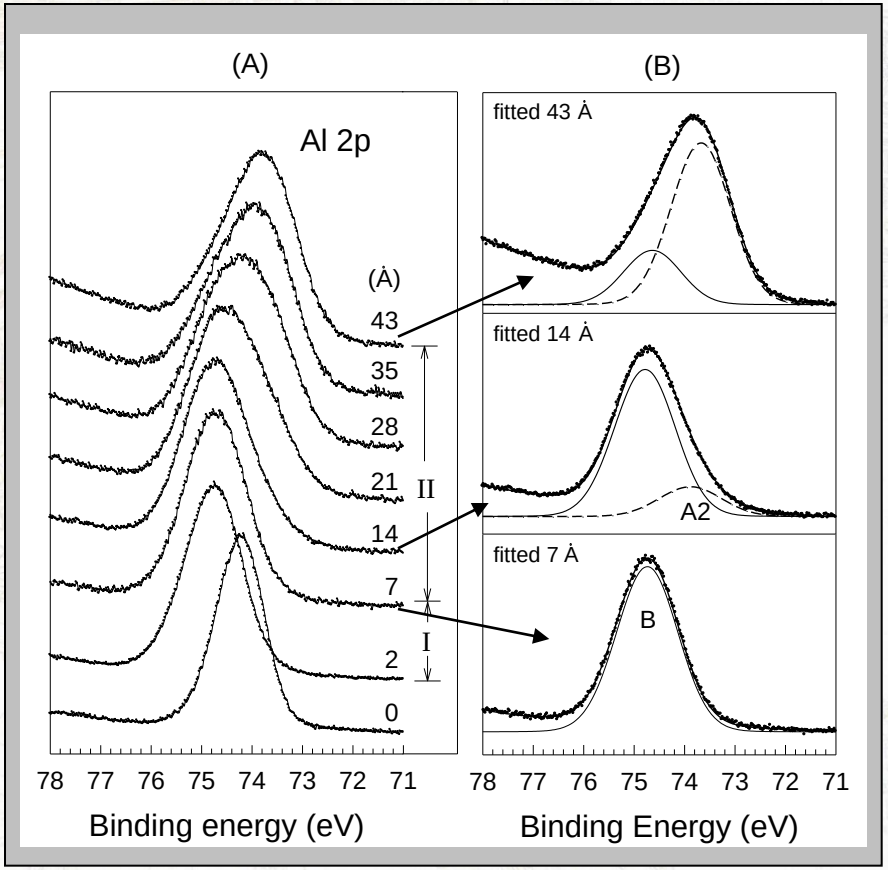

Phase I:

- Charge states of both Al and Ca remain unchanged.
- Ca forms clusters at Alq_3.

Phase II:

- Appearance of Ca^{2+} indicates that the alkaline atoms donate charges to their about.

summary of Ca on Alq_3

- Two phases of reaction are identified.
- The first phase behaves similarly as the case of Mg on Alq_3, Mg clustering and Alq_3 intact.
- The second phase renders Ca charge donation, causing molecule defragmentation.

Mg:Ag on Alq_3

JAP **101**, 043704 (07)

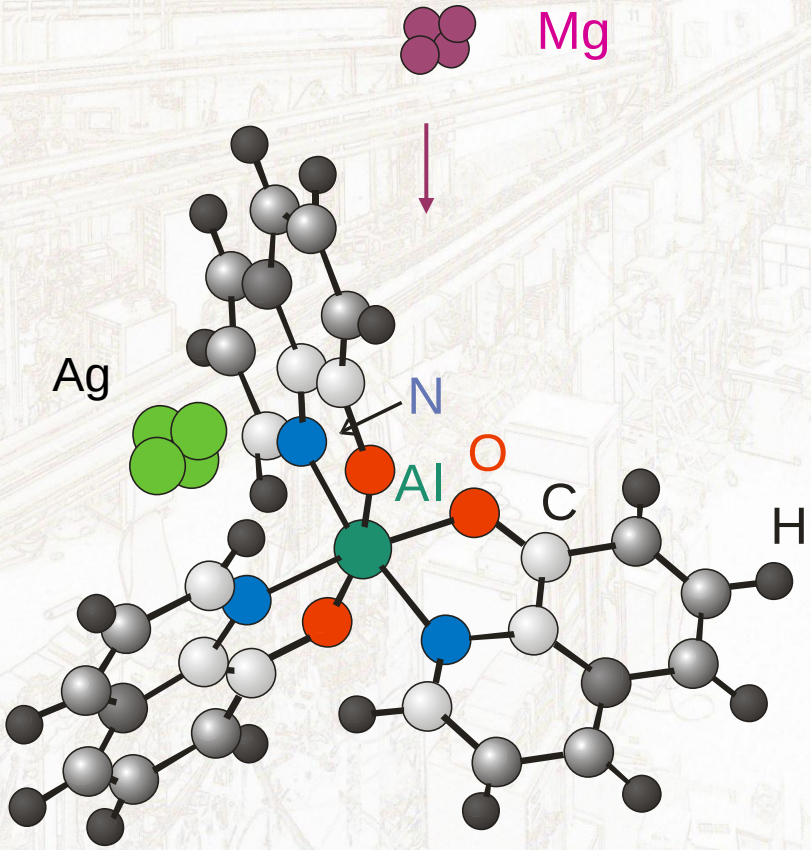

valence band spectra

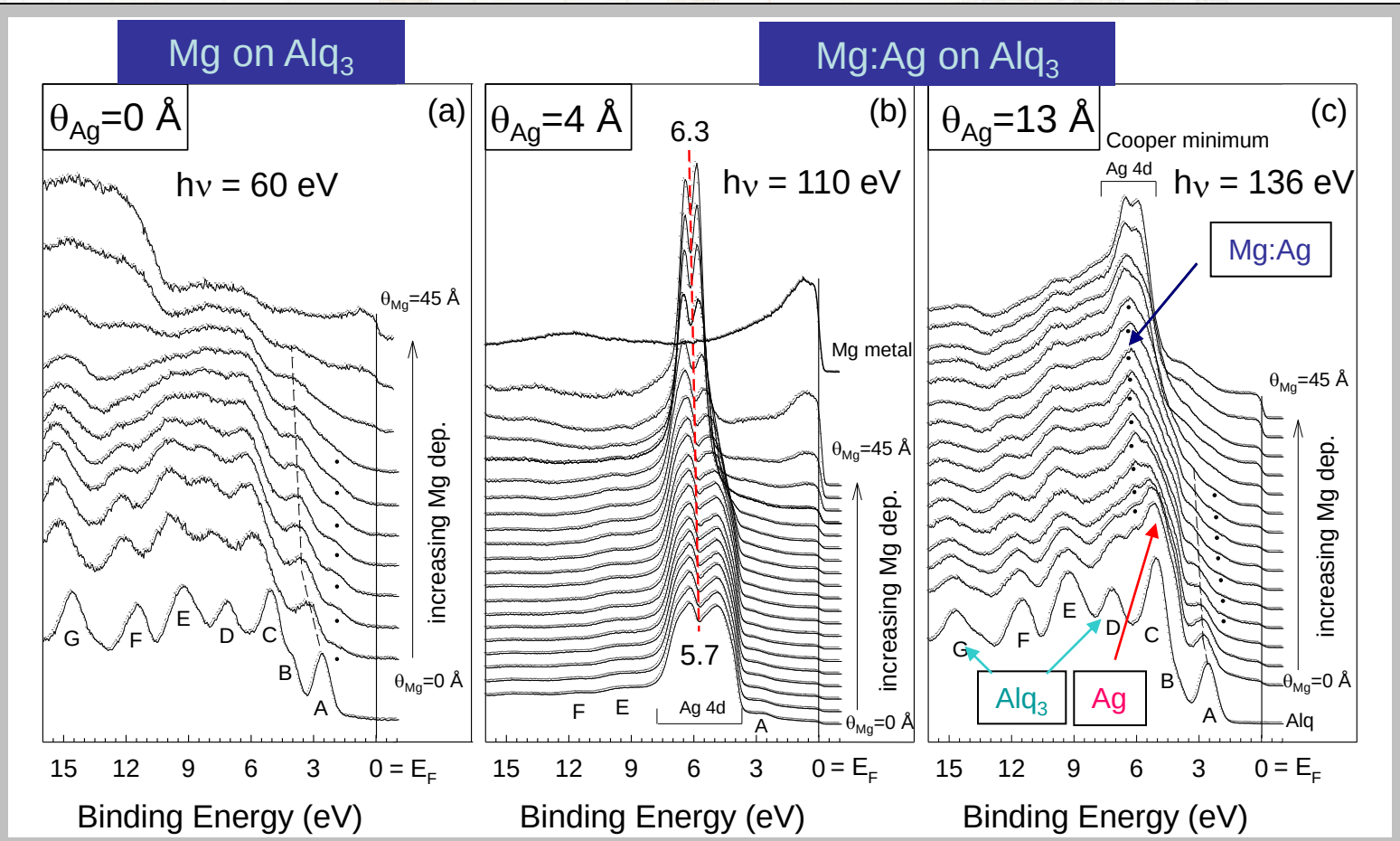

- Ag retains the Alq_3 features.
- The Ag band is narrowed, and its centroid shifts towards high Eb.
- The Ag-, Alq_3-, and Mg:Ag-related features coexists.
- Mg metal grows as a metal on top of the Mg:Ag basin.

Ag 4d orbitals and Fermi emission

Mg:Ag on Alq_3

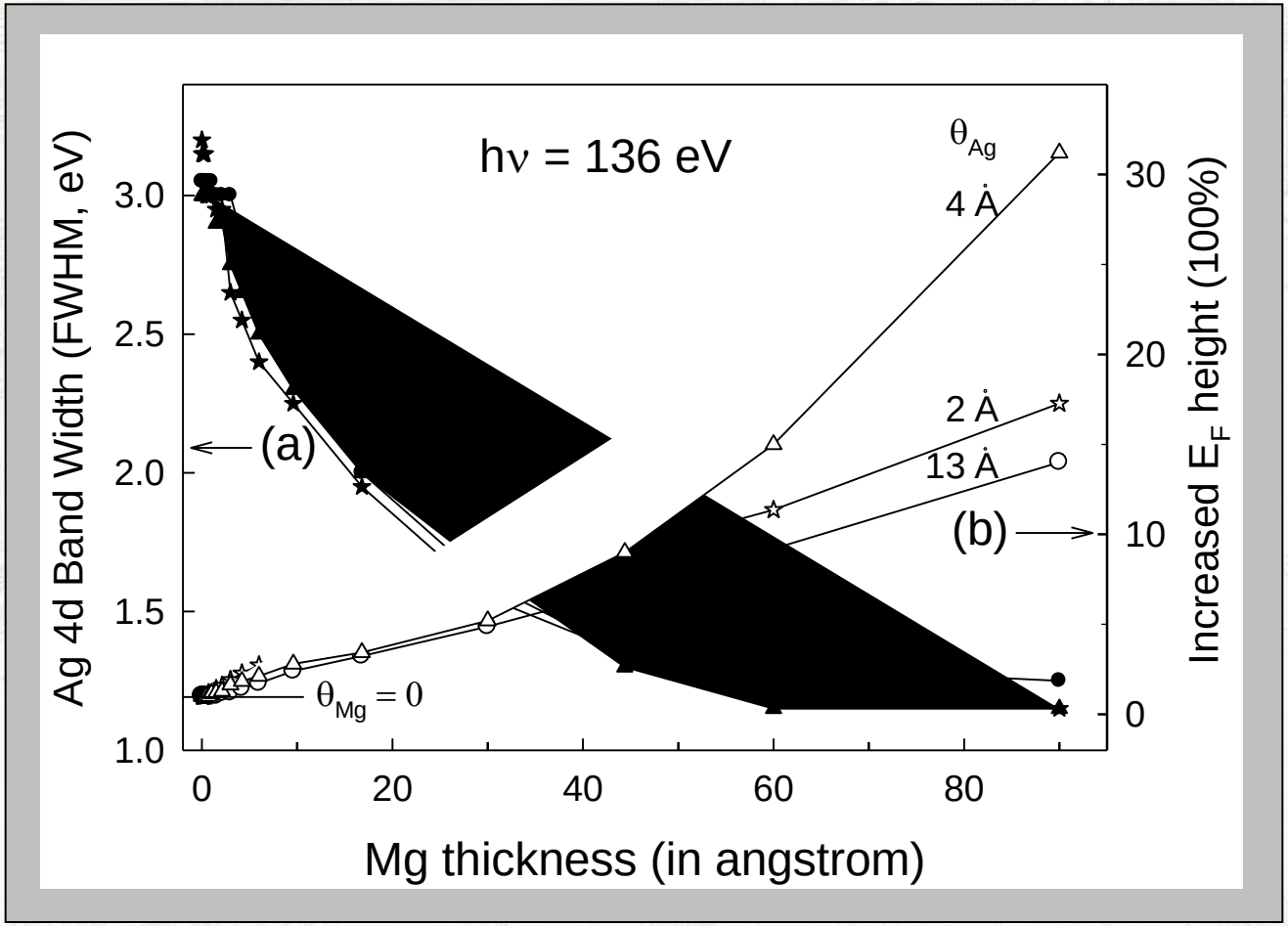

O 1s, N 1s, C 1s, and Ag 4d

Mg on Alq_3

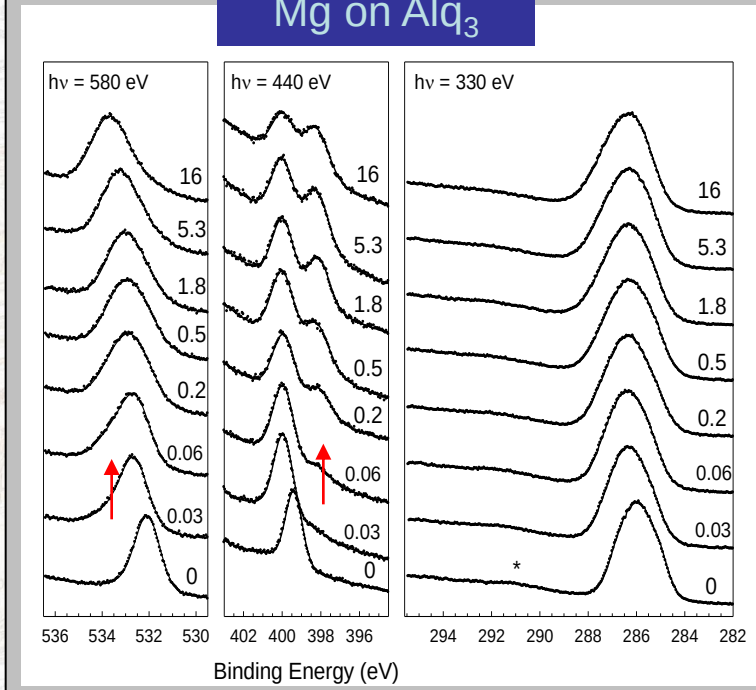

- C: remain unaffected.
- N: negative core-level shift
  O: positive core-level shift
- The strength of the new components are Mg-dependent.

Mg:Ag on Alq_3

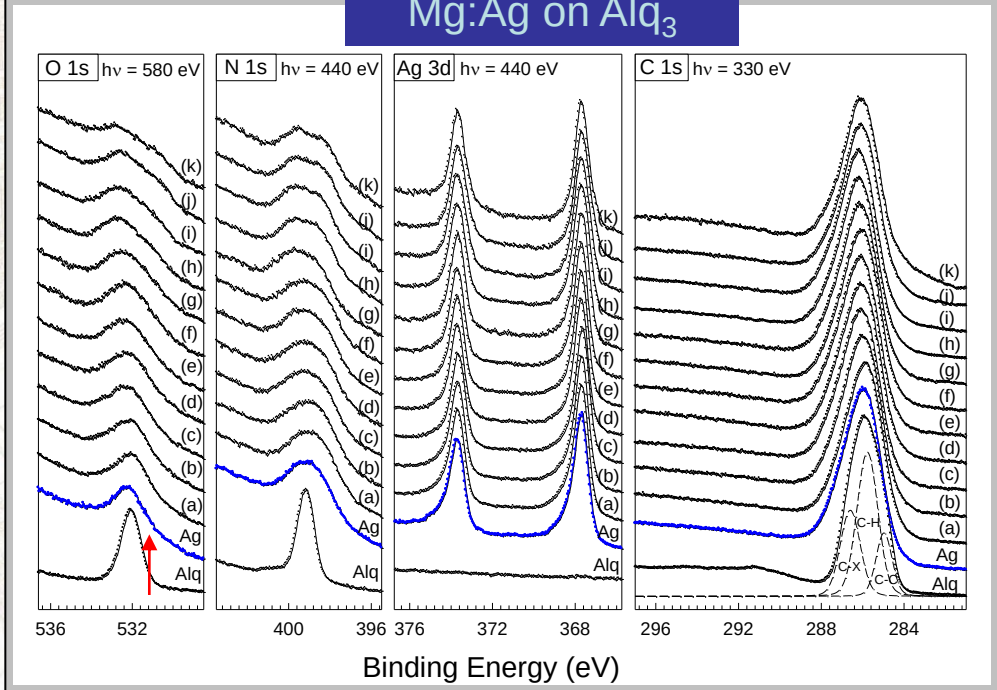

(a) 0.08;(b) 0.25;(c) 0.5;(d) 0.75;(e) 1;(f) 1.5;(g) 2.5;(h) t = 4.0;(i) 5.5;(j) 8.0;(k) 12

- N: remain unaffected.
- O: negative core-level shift

a fit

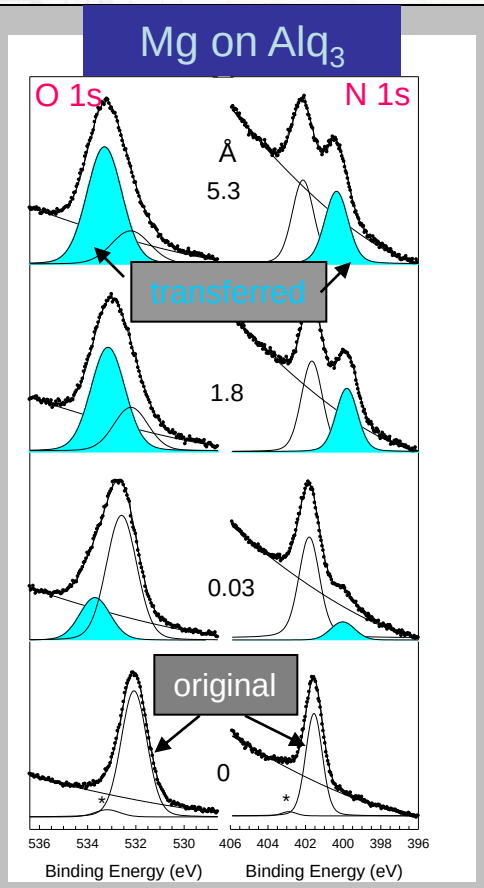

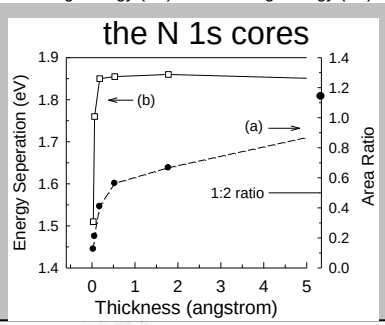

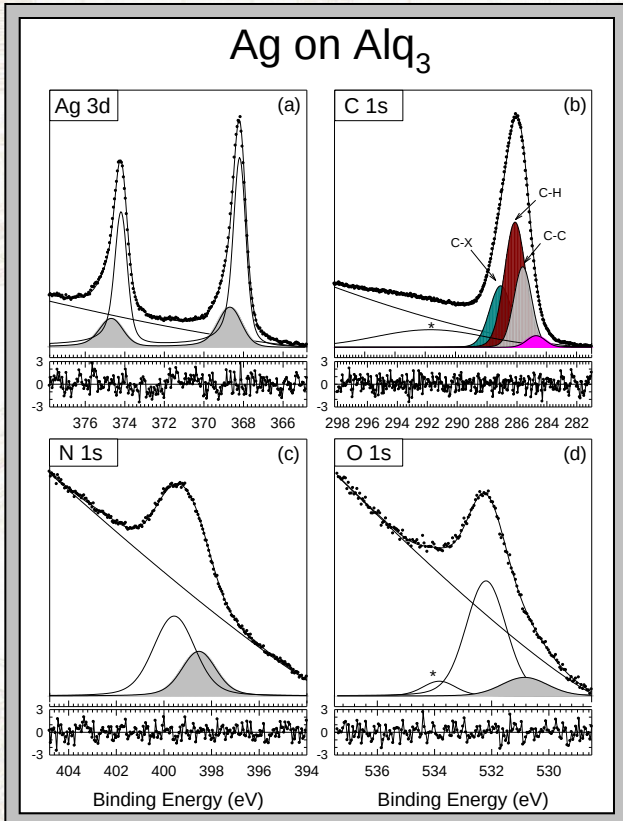

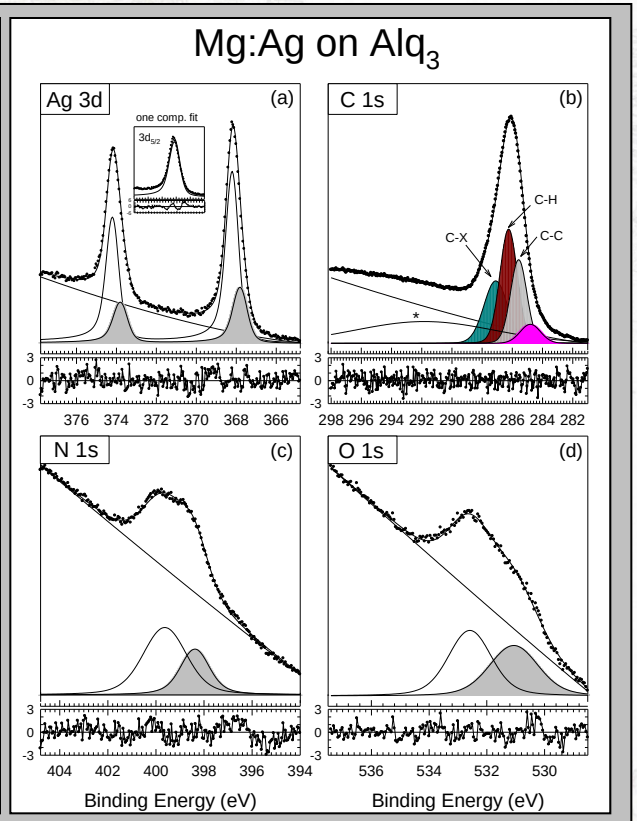

(a) **Ag**: The Ag cluster becomes less screened.
(b) **C**: The C-X component is most affected.
(c) **N**: The N 1s core have the same area ratio in Ag/Alq_3 and $Mg:Ag/Alq_3$.
(d) **O**: Oxygen gains excess charge.

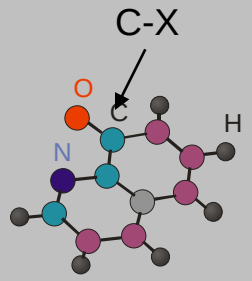

Mg 2p

Mg:Ag on Alq_3

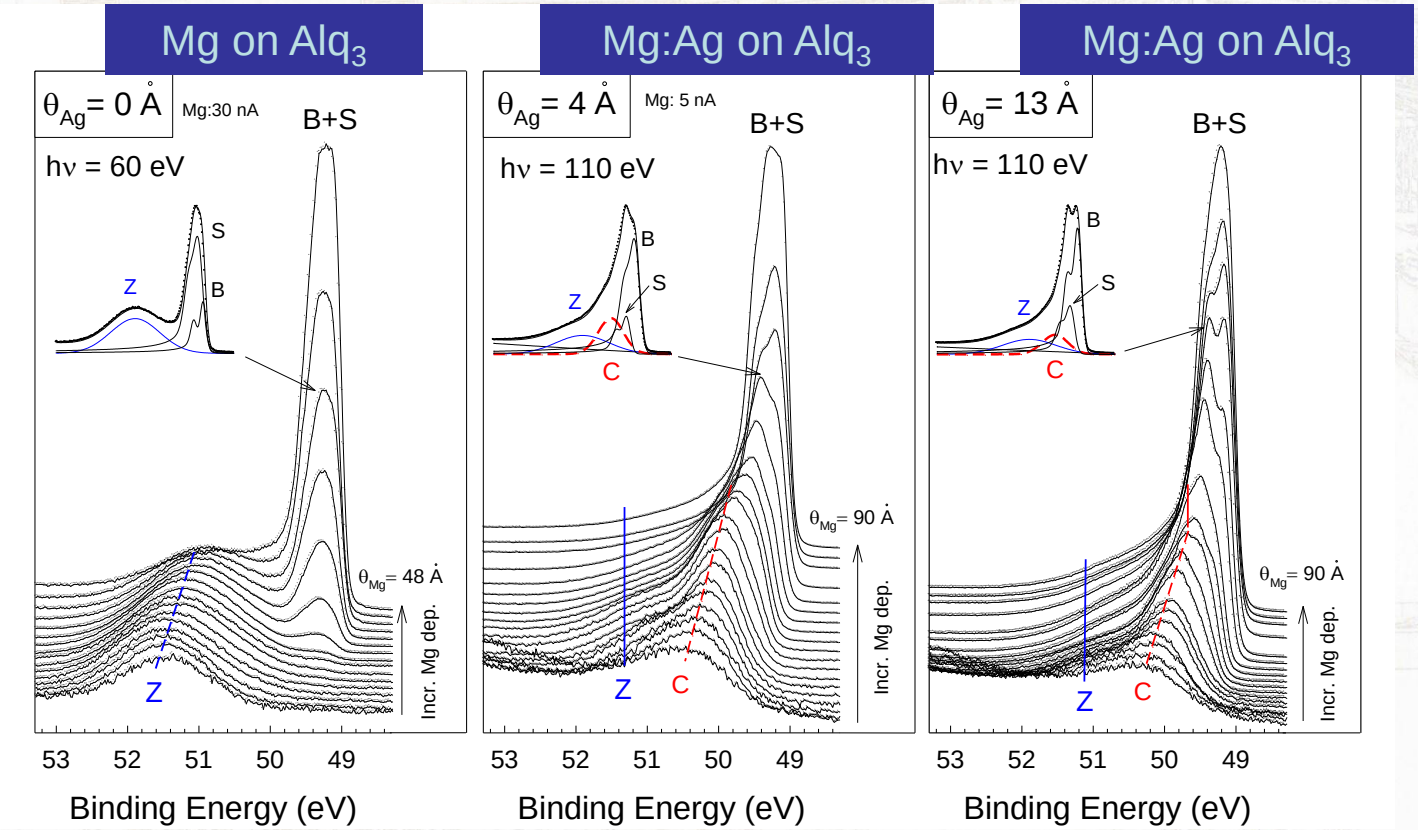

- Mg/Alq_3: Z and S+B; $Mg:Ag/Alq_3$: Z', C, and S+B
- Delayed onset of the metallic S+B components

proposed model

Mg on Alq_3

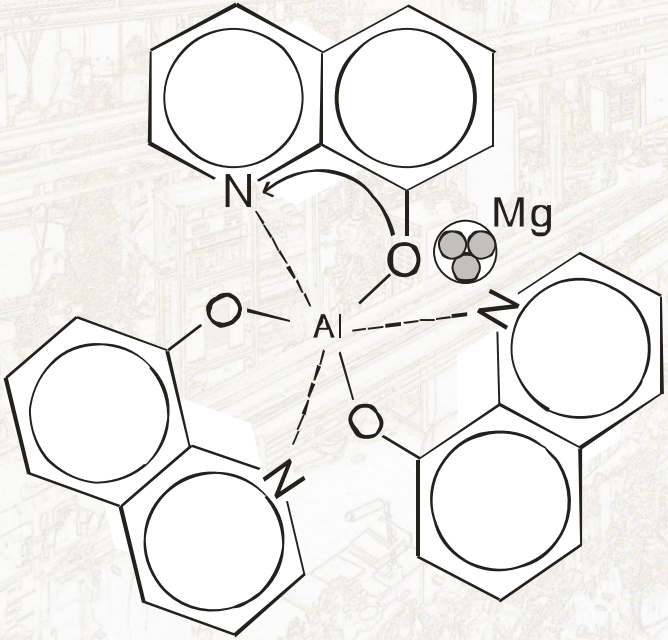

Mg:Ag on Alq_3

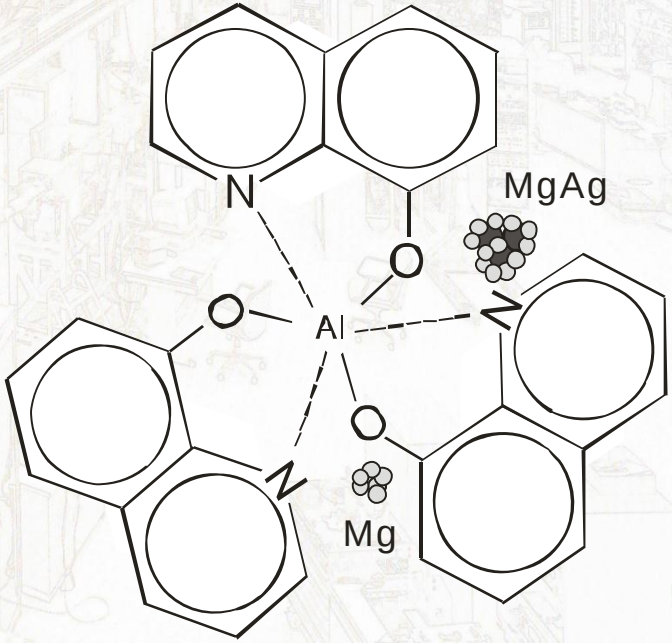

Mg clustering in and on top of Alq_3 & charge flowing from O to N

Mg is mixed with Ag & grouped at the phenoxide ring

Summary

For Mg on Alq_3:

- Mg actually forms clusters in and on top of Alq_3.
- With the presence of Mg, Alq_3 not only accepts charge from the dopant, but also renders a charge redistribution of the molecule itself.

For Mg:Ag on Alq_3:

- Ag blocks effectively Mg from in-diffusion.
- Mg favors to mix with Ag to become Mg_xAg_y complex.
- Mg grows fast as a metal on top of the Mg_xAg_y basin.